

SPATIOTEMPORAL ANALYSIS FOR FIRE FORECASTING USING DEEP LEARNING TECHNIQUES IN GOOGLE EARTH ENGINE – A CASE STUDY FOR THE INDIAN STATE OF UTTARAKHAND

DHANASEKARAN KANAGASABAPATHI
August 2023

SUPERVISORS:
Dr. Kamal Pandey
Mr. Vinay Kumar
Prof. Dr. Ir. Claudio Persello

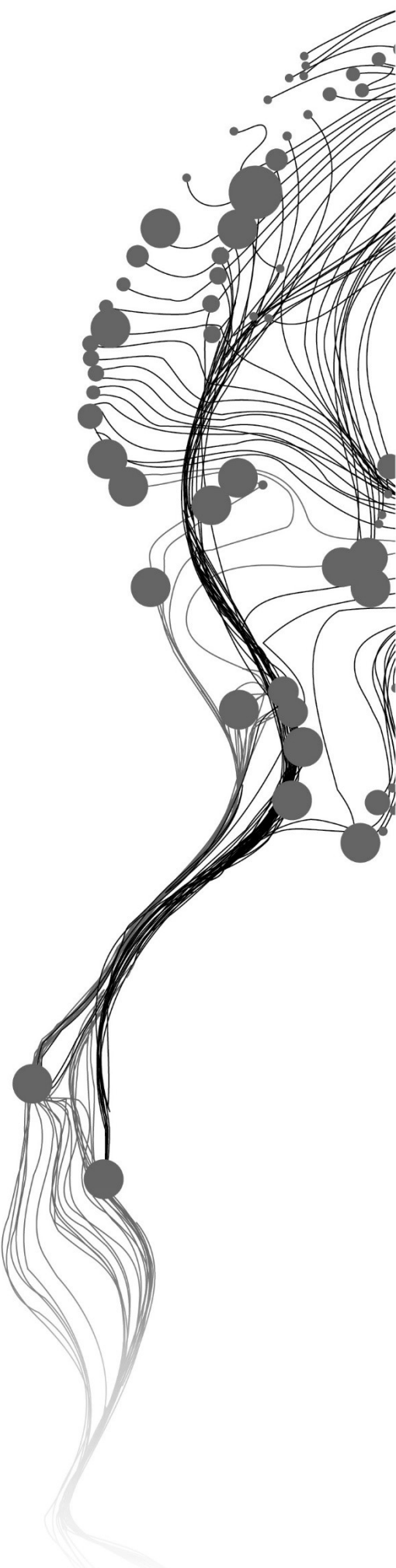


FACULTY OF GEO-INFORMATION
SCIENCE AND EARTH OBSERVATION
UNIVERSITY OF TWENTE
ENSCHEDE, THE NETHERLANDS



INDIAN INSTITUTE OF REMOTE SENSING
Indian Space Research Organisation
Department of Space, Govt. of India





SPATIOTEMPORAL ANALYSIS FOR FIRE FORECASTING USING DEEP LEARNING TECHNIQUES IN GOOGLE EARTH ENGINE – A CASE STUDY FOR THE INDIAN STATE OF UTTARAKHAND

DHANASEKARAN KANAGASABAPATHI
Enschede, The Netherlands, August 2023

Thesis submitted to the Faculty of Geo-Information Science and Earth Observation of the University of Twente in partial fulfilment of the requirements for the degree of Master of Science in Geo-information Science and Earth Observation.

Specialization: Geoinformatics

SUPERVISORS:

Dr. Kamal Pandey, IIRS

Mr. Vinay Kumar, IIRS

Prof. Dr. Ir. Claudio Persello, ITC

THESIS ASSESSMENT BOARD:

Prof. Dr. Ir. Alfred Stein, ITC (The Chair)

Dr. Ashutosh Kumar Bhatt, SAC, Ahmedabad (External Examiner)

DISCLAIMER

This document describes work undertaken as part of a programme of study at the Faculty of Geo-Information Science and Earth Observation of the University of Twente. All views and opinions expressed therein remain the sole responsibility of the author, and do not necessarily represent those of the Faculty.

ABSTRACT

Fire is one of the five important elements for life on earth. Vegetation fires cause great impact on the whole earth system. Forest fires affect the rich flora and fauna of the forest ecosystem. It releases huge amount of carbon dioxide into the atmosphere thereby accentuating the climate of the earth. It also releases pollutants which affect the health of the animals and the people living nearby the forest. Agricultural residue burning also releases large amount of particular matter which affects the health of human beings. Having these consequences, fires cause detrimental impacts to the life on earth. Different factors influence fire in a different magnitude. Dynamic factors such as weather parameters, state of vegetation influence the fire in most of the cases. They follow non-linear relationship between them.

Remote sensing has been used in fire related studies for mitigation, preparedness, response and recovery activities. The variables prepared from remote sensing products can be used to study the fires. Relationship between fire occurrence and different influencing factors in a study area will be helpful to analyse the situation of in an area. This can help to create models to predict fire danger, fire possibility in an area. In this study, the relationship between various fire variables and fire occurrence in the state of Uttarakhand is analysed. Deep Learning, a subset of machine learning has been used to model and forecast fires for the state. Two different approaches were used for fire forecasting. One to forecast with the data of fire-influencing variables of a single day and the other with the data of fire-influencing variables of past five days. A variant of U-Net architecture and Convolutional LSTM are used for the non-temporal dataset and temporal dataset respectively.

Datasets are obtained from Google Earth Engine, and processed for the fire modelling process. In order to reduce the imbalance in proportion of fire and non-fire classes, data is selected from two different patches which represents all the climatic, land use and land cover, and terrain conditions of the state. By this way the imbalance in proportion has been reduced to certain extent. A preliminary analysis of fire distribution on different terrain conditions has been done. It has been found that the terrain conditions have huge impact on the fire situation in the state. In the approach which includes the fire influencing variables of a single day, three different scenarios are performed to analyse whether the fire influencing variable of a single can be used to forecast fire of next day, next two days, and next five days. This has been performed by aggregating the fire labels of next two days and next five days to find the relationship. In the approach which utilized the temporal data of fire influencing variables, last five days of fire influencing variables data is used to model the next day's fire forecast. Hyperparameter tuning is performed by considering the resolution of the data, characteristic of fire in the state and imbalance nature of the dataset. Sensitivity analysis has been performed for different hyperparameters and the results are discussed. The models are built with the selected hyperparameters and the prediction accuracy of the model is found. Fire forecasting is performed for the testing dataset and analysed through different plots. As the time lead increases the recall score of the model increased with the cost of increased false positives. In the temporal approach, the model had high accuracy to predict non-fire locations than the fire-locations. The model built to forecast next two days of fire had high prediction accuracy for both fire and non-fire pixels. The model is selected, and a web application is hosted in local server using python library 'greppo'. It utilizes the advantages of both python and java script to create web application. The application can be hosted in any server after installing the necessary packages. In this way, fire forecasting maps can be disseminated to the users.

Keywords: Fire forecasting, Deep Learning; Fire-influencing variables; U-Net; Convolutional LSTM; Greppo.

ACKNOWLEDGEMENTS

On completion of the research work as part of the M. Sc degree program offered as Joint Education Program by IIRS and ITC, I would like to remember with great gratitude all the fascinating people who made it possible with their relentless support and insightful guidance

This wouldn't have been possible without the solicitous guidance of my supervisors Kamal Pandey sir and Vinay Kumar sir who have been instrumental in shaping the research and guiding me towards the completion of research. They have been helpful in guiding me throughout this journey whenever I needed their support.

I would like to thank my ITC supervisor Claudio Persello for guiding me in formulating the research. His ideas helped me to tackle the problems efficiently. His expertise, dedication, and mentorship have been instrumental in shaping this thesis and my academic growth. I am thankful to John Ray Bergado, lecturer/researcher in ITC for his suggestions during proposal phase and timely help during the research phase.

I would extend my gratitude to the IIRS course coordinator Kapil sir and ITC course coordinator Sander Oude Elberink who act as a bridge between the institutes. I would like to tell my heartfelt thanks to Prof. Alfred Stein for his insightful suggestions during the research proposal phase.

I also take the opportunity to acknowledge the contribution of Dr. Sameer Saran Sir, former Head of Geoinformatics Department and Dr. Vandita Srivastava, Head of Geoinformatics Department for helping me in completing the course.

I would like to thank my batchmates, seniors, PGD batchmates, ITC collegemates, IIRS M. Tech batch mates and juniors who have been the support system for me throughout this journey. They helped me to correct my mistakes and guided me through this journey. I am very happy to share a journey with them.

Last but not the least, the support from my family has been instrumental for me to complete the course. Their hard work and supporting words had inspired me to keep going.

TABLE OF CONTENTS

1	INTRODUCTION	1
1.1	Background	1
1.2	Research Motivation	2
1.2.1	Remote Sensing in Fire Related Studies	2
1.3	Research Identification	3
1.3.1	Research Objectives	3
1.3.2	Sub-Objectives	3
1.3.3	Research Questions	4
1.3.4	Thesis Structure	4
2	LITERATURE REVIEW	5
2.1	Fire-Influencing Parameters	5
2.2	Remote Sensing and GIS-Based Data for Fire-Related Studies	6
2.2.1	Burn Sensitive Spectral Indices	6
2.2.2	Meteorological Parameters	8
2.2.3	Terrain Parameters	9
2.2.4	Anthropogenic Parameters and Landcover Maps	10
2.2.5	Active Fire Data	10
2.3	Remote sensing applications in different fire management elements	11
2.4	Existing systems for pre-fire alerts	11
2.5	Review of Deep Learning Studies	12
2.5.1	Deep Learning application in fire related studies	14
2.5.2	Chosen model and Design experiments	16
2.5.2.1	Image segmentation with non-sequential data	16
2.5.2.2	Image segmentation with sequential data	17
2.6	Class Imbalance problem	17
3	STUDY AREA AND DATASET	19
3.1	Study Area	19
3.1.1	Topography	20
3.1.2	Climate	20
3.1.3	Forests	21
3.1.4	Landcover Statistics	21
3.2	Datasets used	22
3.2.1	Feature dataset	22
3.2.1.1	Global Friction Surface	24

3.2.1.2	Landcover data	25
3.2.1.3	VIIRS Optical Imagery.....	27
3.2.2	Label dataset.....	27
3.3	Platforms used.....	28
4	METHODOLOGY	29
4.1	Preliminary Analysis	30
4.2	Data Preparation.....	30
4.2.1	Data selection.....	30
4.2.1.1	Terrain Dataset	30
4.2.1.2	Meteorological data comparison.....	31
4.2.2	Deriving significant variables for fire-related study	33
4.2.2.1	Spectral indices	33
4.2.2.2	Meteorological Variables.....	34
4.2.3	Data pre-processing.....	34
4.2.4	Data splitting for model.....	35
4.3	Deep learning models	38
4.3.1	Fire forecasting with non-sequential data of fire influencing variables	38
4.3.1.1	Model architecture	38
4.3.2	Fire forecasting with sequential data of fire influencing variables.....	40
4.4	Hyperparameter Tuning	41
4.5	Validating the model.....	42
4.6	Building user interface for fire forecasting.....	44
5	RESULTS AND DISCUSSION	45
5.1	Preliminary Analysis	45
5.1.1	Fire point distribution.....	45
5.1.2	Fire point distribution in different Terrain features.....	46
5.1.2.1	Elevation.....	46
5.1.2.2	Slope.....	47
5.1.2.3	Aspect.....	48
5.2	Meteorological data comparison	48
5.2.1	Correlation analysis.....	50
5.2.2	RMSE Analysis.....	50
5.3	Fire forecasting models.....	51
5.3.1	Model for fire forecasting with single day fire influencing variables.....	51

5.3.1.1	Training and hyperparameter tuning.....	51
5.3.1.1.1	Fire forecasting for next day	52
5.3.1.1.2	Fire forecasting for next two days.....	55
5.3.1.1.3	Fire forecasting for next five days.....	57
5.3.1.2	Quantitative analysis.....	58
5.3.1.3	Qualitative analysis	60
5.3.1.3.1	Next day fire forecasting model output plots.....	60
5.3.1.3.2	Next two days fire forecasting model output plots	61
5.3.1.3.3	Next five days fire forecasting model output plots	63
5.3.2	Model for fire forecasting with sequential data of fire influencing variables	64
5.3.2.1	Training and hyperparameter tuning.....	64
5.3.2.2	Quantitative analysis.....	67
5.3.2.3	Qualitative analysis	67
5.4	User interface for fire forecasting.....	68
6	CONCLUSION AND RECOMMENDATIONS.....	70
6.1	Conclusion	70
6.2	Recommendations	72
	REFERENCES	73

LIST OF FIGURES

Figure 2-1: Spectral signature of Healthy vegetation and burned area.....	7
Figure 2-2: Representation of aspect with corresponding angle.....	10
Figure 2-3: Abstract of a CNN model.....	13
Figure 2-4: Architecture of an LSTM cell.....	14
Figure 2-5: U-Net architecture.....	16
Figure 2-6: Inner structure of ConvLSTM architecture.....	17
Figure 3-1: The Political map of Uttarakhand and its districts. (Inset map - Indian states).....	19
Figure 3-2: Topography map of Uttarakhand. (Inset map – Outline of India and location of Uttarakhand)	20
Figure 3-3: Pie-chart representing different landcover classes in Uttarakhand.....	22
Figure 3-4: Land-based travel time for motorized transport map for the Indian state of Uttarakhand.....	24
Figure 3-5: MODIS LULC classification map of 2021 for the Indian state of Uttarakhand.....	26
Figure 3-6: Year-wise fire pixels count for the study years.....	28
Figure 4-1: Workflow adapted for the research.	29
Figure 4-2: Flowchart of the preliminary analysis.....	30
Figure 4-3: Ground Meteorological stations present in Uttarakhand (as of 31/03/2023).....	31
Figure 4-4: Methodology for comparing meteorological datasets.....	33
Figure 4-5: Patches selected for the study.....	36
Figure 4-6: Fire density map for the state of Uttarakhand and the selected patches for the study.....	37
Figure 4-7: U-Net model architecture for active fire forecasting with non-sequential data.....	38
Figure 4-8: Different scenarios of fire forecasting with non-sequential data.....	40
Figure 4-9: Convolutional LSTM architecture for active fire forecasting with sequential data.....	40
Figure 4-10: Fire forecasting scenario with data of sequential fire-influencing variables.....	41
Figure 4-11: Steps to create fire forecast maps in the web application.....	44
Figure 5-1: MODIS active fire points in Uttarakhand (2016-2023).....	45
Figure 5-2: Fire point density map of Uttarakhand.....	46
Figure 5-3: MODIS Fire points distribution over different elevation ranges.....	46
Figure 5-4: MODIS Fire point distribution in different slope conditions.....	47
Figure 5-5: MODIS fire points distribution on different aspect (slope directions).....	48
Figure 5-6: Interpolated maximum temperature on 07/04/2018 from ground station data.....	49
Figure 5-7: Interpolated maximum temperature on 07/04/2022 from ground station data.....	49
Figure 5-8: Correlation analysis between ERA5 and ground station data for Maximum temperature for 2021.....	50
Figure 5-9: RMSE value of Maximum temperature between ground station data and ERA5 reanalysis data	51

Figure 5-10: The Active fire plot and the corresponding day's forecast plot for 23/04/2022.....	54
Figure 5-11: The active fire plot and fire prediction plots with tuned alpha and neural network architecture	55
Figure 5-12: Aggregated active fire plot of 23/04/2022 and 24/04/2022	56
Figure 5-13: Fire prediction plots for the dates 23/04/2022 and 24/04/2022 for different alpha values..	56
Figure 5-14: Fire forecasting plots for the next five days with different alpha values in focal loss function	58
Figure 5-15: Next day fire forecasting scenario's active fire reference plots and model output plots. Terrain and Land use land cover plots of patch 1. (a) End of Winter, (b) Forest Fire season	60
Figure 5-16: : Next day fire forecasting scenario's active fire reference plots and model output plots; Terrain and Land use land cover plots of patch 2. (a) Forest Fire season (b) Agriculture residue burning season	61
Figure 5-17: Next two days fire forecasting scenario's active fire reference plots and model output plots; Terrain and Land use land cover plots of patch 1. (a) End of Winter (b) Forest Fire season.....	62
Figure 5-18: Next two days fire forecasting scenario's active fire reference plots and model output plots; Terrain and Land use land cover plots of patch 2. (a) Forest Fire season (b) Agriculture residue burning season	62
Figure 5-19: Next five days fire forecasting scenario's active fire reference plots and model output plots; Terrain and Land use land cover plots of patch 1. (a) End of Winter (b) Forest Fire season.....	63
Figure 5-20: Next five days fire forecasting scenario's active fire reference plots and model output plots; Terrain and Land use land cover plots of patch 2. (a) Forest Fire season (b) Agriculture residue burning season	64
Figure 5-21: Reference active fire plot for 23/05/2018 in patch 1 and the corresponding fire forecast plots with different alpha values	66
Figure 5-22: The convolutional LSTM architecture used for fire forecasting.....	66
Figure 5-23: Terrain and Land use land cover plots of patch 1; Active fire reference plots; Fire forecasting output plots. (a) End of Winter, (b) Forest Fire season.....	67
Figure 5-24: Terrain and Land use land cover plots of patch 2; Active fire reference plots; Fire forecasting output plots. (a) Forest Fire season, (b) Agricultural residue burning season	68
Figure 5-25: Fire prediction application hosted in local server and the prediction map of 09/05/2019.....	69

LIST OF TABLES

Table 3.1: Floral species available in different climatic regions	21
Table 3.2: Feature Datasets used and their specifications.	23
Table 3.3: Landcover classes and description for Annual Plant Functional Type classification	25
Table 3.4: VIIRS Moderate-resolution visible and infrared bands and their wavelength ranges	27
Table 4.1: Meteorological variables and their units in Station data and ERA5 data.....	32
Table 4.2: Description of different meteorological datasets	32
Table 4.3: Training and testing data for the study and its significance.....	37
Table 4.4: Hyperparameters considered in the study and their description.....	42
Table 4.5: Confusion matrix for binary classification.....	43
Table 5.1: Patch count and number of fire and non-fire pixels in training and validation set for forecasting fire of next day	52
Table 5.2: Hyperparameters and the experiment values	52
Table 5.3: Hyperparameter search for focal loss function.....	53
Table 5.4: Observations of hyperparameter tuning while changing the network architecture	53
Table 5.5: Hyperparameter tuning observations while changing alpha value and the U-Net network architecture	54
Table 5.6: Patch count and number of fire and non-fire pixels in training and validation set for forecasting fire of next two days	55
Table 5.7: Sensitivity of two days fire forecasting model for different alpha values and accuracy metrics ..	56
Table 5.8: Patch count, number of fire and non-fire pixels in five day forecast training and validation label dataset.....	57
Table 5.9: Sensitivity of five days fire forecasting model and accuracy metrics.....	57
Table 5.10: Number of patches, fire and non-fire pixels in testing dataset	58
Table 5.11: Estimated predictive model accuracy based on sample counts for all the scenarios of fire forecasting models.....	59
Table 5.12: Estimated predictive model accuracy based on recall, specificity, G-mean, CBA for all the scenarios of fire forecasting models.....	59
Table 5.13: Fire and non-fire pixel count for different datasets used for fire forecasting with temporal fire influencing variables' data	64
Table 5.14: Hyperparameter tuning and validation set accuracy metrics for fire forecasting with temporal fire influencing data.....	65
Table 5.15: Hyperparameter tuning experiments performed for different alpha values	65
Table 5.16: Evaluation metrics of next day fire forecasting model with temporal features in testing dataset	67

1 INTRODUCTION

1.1 Background

Fire, land, water, air, and atmosphere are among the five essential elements for life on Earth. Fire can be easily explained with the help of a 'Fire Triangle' where Fuel, Oxygen, and Heat/ignition source forms the parts of the triangle. All three elements are necessary for a fire to sustain. Ignition sources can be lightning, cigarettes, or match sticks in the case of forests; burning of fields voluntarily by farmers in the case of agricultural fields; fires due to reactions between the chemicals or electrical leakages in industrial areas. Forest covers 31 percent of the total land on the Earth. The forest ecosystem is one of the richest biologically diversified landforms in the world (The State of World's Forest 2020, 2020). Fires in the forest directly affect flora and fauna by degrading their habitat and leading to soil erosion in the slopes. Fires in the vegetation release carbon dioxide, a potent Greenhouse gas, along with NH_4 , CO , and SO_2 (Urbanski, 2014). At the same time, forest fire is vital in replenishing the soil's nutrient content and maintaining plant species diversity (Rundel, 1981). However, in the present-day scenario, reducing global atmospheric carbon dioxide emissions is the goal of all the countries to meet net zero emissions (Levin et al., 2023)(The Evidence Is Clear: The Time for Action Is Now. We Can Halve Emissions by 2030, 2022). At the same time, the burning of agricultural residue to prepare the land for the next growing season is also one of the crucial aspects when considering the fire that happens prevalently in the world (Brandt, 1966)(Venkataraman et al., 2006). More than half of the rice straw produced is burnt in India each year, and it causes a severe impact on the atmosphere and the health of living organisms (Dutta et al., 2022). In order to maintain the biodiversity of flora and fauna and reduce the emissions caused by fire, a proper understanding of fire is inevitable.

The native broadleaf trees, such as oak, sal, and deodar, are replaced with pine trees with good economic values (Vatsa, 2022). Chir pine trees (*Pinus roxburghii*) cover approximately 16% of the forest area of the state (from 1000 to 1800 m above mean sea level), whose dry needles are highly inflammable (Negi, 2019). The forests of Uttarakhand are prone to forest fires, and there is a fire season from February to June which peaks in May and June due to scanty rainfall and increased temperature during that period (Jha et al., 2016). The presence of highly inflammable pine needles and the dry season exaggerates the fire in the state. At the same time, anthropogenic activities like clearing forest floor for fresh growth of fodder for cattle, escape of fire from agricultural fields, and the carelessness of tourists, shepherds, etc., results in fire most of the time (Dobriyal & Bijalwan, 2017). The state is home to 3748 faunal species, rare herbs, and shrubs and has the origin of several important rivers of the country. Therefore, the study of fires in the state is significant.

Various factors influence the ignition and spread of fire. Around 95% of fires in India are caused by anthropogenic activities (Ashutosh et al., 2019). At the same time, the availability of dry fuel and scanty rainfall increases the possibility of fires in a forest. Fire is also influenced by the slope and aspect of the terrain, which affects the amount of sunlight falling on a particular location (Chauhan, 2010). These factors are interdependent, which signifies the importance of studying them in detail.

1.2 Research Motivation

1.2.1 Remote Sensing in Fire Related Studies

Ambient conditions for a fire to ignite and spread pose a severe hazard to the communities which depend on forests and nearby areas which are vulnerable to fire. When a fire ignites and spreads uncontrollably, it becomes a disaster destructing the natural habitat and people's livelihood. A Disaster Management plan has four phases: mitigation, preparedness, response, and recovery. For mitigating fire-related disaster, remote sensing can be effectively utilized along with Geographic Information System (GIS) in all the four phases.

- Mitigation – various factors influencing the fire can be studied on a large scale; fire risk maps can be prepared, and mitigation measures can be taken in the areas with high fire risk. Since fuel is a part of the fire triangle, reducing the amount of dry fuel from the ground is one of the effective measures for preventing fires. In forests, the fire lines (clearing trees and dry leaves along a line) reduce the spread of fire from one part of the forest to another. It is an effective plan, but the fire lines must be maintained regularly to effectively control the spread of forest fires (Rawat & Nautiyal, 1999).
- Preparedness – High-risk areas can be selected, and necessary infrastructure can be built for easy access during disaster times. At the same time, pre-fire alerts in the form of maps will be helpful in proper resource allocation. Watch towers installed in fire-prone areas will also be effective.
- Response – Near real-time fire monitoring through satellites will be helpful for identifying the fire in remote locations and timely extinguishing the fire.
- Recovery – Satellite-based burned area mapping and burn severity mapping are efficient methods to plan recovery actions in fire-affected areas.

Therefore, data collected by different satellites and ground-based observation systems can be effectively utilized to manage fires in the forest and agricultural lands.

Recently, Deep Learning, a subset of machine learning, has spearheaded research related to biological image classification, computer vision, and ecological modelling (Christin et al., 2019). The ability of neural networks to extract useful information from the data is valuable for solving problems in various fields. Deep learning implementation in the field of remote sensing includes very high-resolution image classification (Bergado et al., 2018), built-up area extraction from satellite images (Bramhe et al., 2018), slum area detection (Persello & Stein, 2017), and predictive models for solving ecological problems like forest fire prediction (Bergado et al., 2021)(Kondylatos et al., 2022). With the advent of neural networks, the complex non-linear relationship between numerous factors can be modelled, and the knowledge of the processes can be improved. With those advantages, the deep learning approach is analysed for providing pre-fire alerts in the form of forecast maps in this research. This study makes use of various datasets available in Google Earth Engine to build models for forecasting fires. It is a cloud-based platform provided by Google. It is an open forum for exploring various satellite datasets from Landsat, MODIS, Sentinel, and derived datasets like ERA-5, MODIS NDVI, Sentinel - 2 LULC, etc. It leverages Google's cloud computing architecture to handle the processing of larger datasets efficiently and quickly. GEE also provides a python API that allows users to access and analyse the platform's data programmatically and automate workflows. It is a popular option for spatial data analysis, especially for decadal analysis of any

phenomenon on Earth, due to availability of data in the cloud, data processing interfaces, and Python API.

1.3 Research Identification

Causative factors for fire initiation and spreading vary yearly from region to region. Globally, wildfires happen in different regions at different time periods. In the Amazon rainforest, a large number of forest fires are reported because of clearing the forests for cultivation (Amaral & Matsumoto, Marcelo Munroe, 2019). In North America, natural factor lightning is also a primary reason for fire along with anthropogenic activities (Outcalt, 2008). Even the conifer trees in the region need fire to disperse the seeds, and fires play a vital role in the forest ecosystem (Wright & Heinselman, 2014). In Africa, croplands are set to fire in June every year to clear their fields. It is an age-old process called stubble burning (Outcalt, 2008). Likewise, different factors are responsible for the fire in a region. For fire modelling studies, finding and analysing reasonable factors gives more insights into the nature of fire in a region. Therefore, selecting proper variables is also equally important.

The spatial and temporal variation of the factors influencing fire, affects its occurrence and behaviour. Technological development provides us with satellite-based observations and ground-based instruments to record data on the environmental variables influencing fire. Spatio-temporal analysis on these data can be done to find the relationship between the influencing factors and the fires to obtain reliable fire forecasting maps. This kind of study is possible with the help of Deep Learning models, which are good at finding the non-linear relationship between the features (Huot et al., 2020). From the perspective of a fire management authority, it would be beneficial to have fire risk forecasts in advance to mitigate the impact caused by fire. In existing studies, how many days in the future the likelihood of a fire can be projected using data at hand is also not assessed. Additionally, it has never been examined before for a particular study region how many days of historical data on fire-influencing variables are needed to anticipate the chance of a fire. The goals of this study are set to address this criterion.

1.3.1 Research Objectives

The main objective of the research is to generate fire forecast maps by analysing the spatiotemporal dataset of the factors which influence fire using deep learning models for the Indian state of Uttarakhand.

1.3.2 Sub-Objectives

1. To identify the variables required for fire forecasting and preparing the dataset.
2. To develop deep neural network models that capture spatial and spatiotemporal relationships for forecasting fires.
3. To prepare a web application for fire forecasting in the Indian state of Uttarakhand.

1.3.3 Research Questions

The following research questions will be addressed in the research.

Corresponding to Sub-Objective 1:

- What are the influencing factors to be considered for fire in Uttarakhand?

Corresponding to Sub-Objective 2:

- Will multi-temporal data increase the accuracy of fire forecasting?
- For how many days in the future fire can be forecasted accurately?

Corresponding to Sub-Objective 3:

- How to integrate the various datasets and the prepared deep learning model for fire forecasting application?

1.3.4 Thesis Structure

This thesis is documented in six chapters. The background and need for the study, research identification, objectives, and questions are mentioned in Chapter 1. Chapter 2 covers the previous research on fire-related studies, deep learning approaches, and architectures in the form of a Literature review. Chapter 3 covers information about the study area, the dataset, and the platforms used. The methodology followed for the research is mentioned in Chapter 4. The results of the analysis performed and the conclusions and recommendations for further research are mentioned in Chapters 5 and 6 respectively.

2 LITERATURE REVIEW

2.1 Fire-Influencing Parameters

Various factors influence the initiation and spreading of fire. These factors can be well explained with the Fire triangle. As discussed in the Introduction chapter, the components of the Fire triangle include Fuel, Oxygen, and Heat sources for ignition. The fuel acts as the main factor for a fire to sustain. The characteristic of the fuel changes with time. For example, the dry leaf, which acts as the fuel for the fire, will possess less moisture in the summer period. At the same time, it will be moist during the rainy seasons. Natural accumulation of flammable fuel increases the vulnerability of fire in a region like Uttarakhand, where the dry needles (Pirul) from Chir pine trees are prevalent (Negi, 2019). Fuel characteristics change with other factors like weather parameters, terrain characteristics, vegetation types, and anthropogenic influence. Weather parameters like precipitation, temperature, wind speed, direction, and relative humidity are some of them to discuss. The amount and season of precipitation change the biological cycle of vegetation and its characteristics. The number of non-rainfall days also has a direct impact on fire activities. This is well attributed to increased temperature and decreased relative humidity. The latter's combination increases the vulnerability of a region to fire (Dobriyal & Bijalwan, 2017). Increased rainfall in the previous season and increased temperature during the fire season is also a reason for high fire counts. This may sound different from how increased rainfall leads to high fire counts. The point to note is that a good amount of rainfall in the monsoon season results in fresh vegetative growth, resulting in the accumulation of a high volume of flammable fuel. The following high temperature in the fire season makes the situation worse by resulting in high vulnerability for fires (C.S. & Sastry, 2023). The dry winds before the fires remove the moisture content in the air and the vegetation leading to the formation of dry fuel. The behaviour of wind during the fire further leads to the fire's spread, making it difficult for the firefighting measures. Topographical measures like slope and aspect also affect the fuel characteristics and fire behaviour. Terrain features also influence the spread of fire, where the uphill areas catch fire quickly when the downhill vegetation starts to burn (Dobriyal & Bijalwan, 2017). The direction of the slope or the side of the mountain which faces the sun for more time in a day becomes more vulnerable to fire because of falling of increased sunlight, thus resulting in quick drying of vegetation (Chauhan, 2010). Human activity is high in plain regions and near water bodies than on steep slopes, which acts as a proxy for human movement in an area (Sandel & Svenning, 2013). Different species of trees have varying water-storing capacities in their leaves and under the ground. Therefore, the presence of particular species of tree impacts fire. Chir pine trees, because of their highly flammable dry needles, are more vulnerable to fire than any other species. The influence of human beings on land use has an impact on the ecosystem. According to (Cano-Crespo et al., 2015), the burning of forests is high in locations near agricultural pastures.

The second element, the oxygen present in the air, can be regulated by the wind flow. Wind will allow the flow of oxygen from the surroundings. Significant firefighting measures include reducing oxygen supply to the fire-affected region and cooling the fuel. Oxygen supply to fire is reduced by different techniques, including smothering (covering the fire with thick materials like a blanket or sand to stop fuel interaction with air), replacing oxygen with inert gases, etc. (Voelkert, 2015).

For a fire to ignite in a place, various factors are involved. It can be classified either as natural or anthropogenic based on the initiating agent. Natural agents can be lightning or the rolling of stones, which leads to fire ignition in dry fuel (Bergado et al., 2021)(Dobriyal & Bijalwan, 2017). Black kites in Australia are reported to carry fire twigs from one place to another to easily catch their prey which try to escape the fire (Bonta et al., 2017). Human activities like deliberate burning of dry fuel for clearing the forest floor, for collecting the forest produce, to show people agitation or ignorance results in fire in most cases. Various studies suggest and confirm that human-caused fires are the primary reason for fire outbreaks in India and in other parts of the world (Srivatsava, 2020)(*Forest Fires in India*, 2018)(Amaral & Matsumoto, Marcelo Munroe, 2019). Poor management of forests, like forests degraded by logging, deforestation, diseases, or fragmentation of forests due to land use change, also leads to increased fire activities (Cano-Crespo et al., 2015)(Maeda et al., 2009).

The various factors discussed in this section are interdependent and act unpredictably, which makes the problem complex to understand and make decisions. Therefore, these factors and proxies for these factors are to be considered in this study to build a model for forecasting fires.

2.2 Remote Sensing and GIS-Based Data for Fire-Related Studies

The advent of satellites has paved the way for imaging and understanding various phenomena happening on Earth through remote sensing techniques. It has reduced the time to study a phenomenon, reduced the efforts required to collect data, and provided us with a snapshot of a large area in a single frame. Based on the type of energy they capture, satellite sensors are classified as active and passive. Active sensors emit their own pulses and record the backscattered pulses. At the same time, passive sensors record the amount of electromagnetic radiation reflected from the earth's surface. They will not generate their own source of light. They rely on the sun's radiation or any other light source to reflect or emit from an area. Passive sensors majorly record the EMR from visible and Infrared regions. Vegetation has some characteristic signatures in this wavelength range. Several spectral indices can act as proxies to find the state of vegetation, water content in the vegetation, etc. Some of the sensitive spectral indices for assessing the vegetation characteristics and burned areas are reviewed from the literature.

2.2.1 Burn Sensitive Spectral Indices

NDVI - Normalized Difference Vegetation Index

Healthy vegetation has significant reflectance in Near Infrared wavelength and high absorption in the Red wavelength of EMR. This characteristic of vegetation is due to chlorophyll present in the leaf. Based on this characteristic, an index is formulated to analyse the greenness and density of vegetation in a region.

$$NDVI = \frac{\rho_{NIR} - \rho_{RED}}{\rho_{NIR} + \rho_{RED}} \quad (2.1)$$

ρ_{NIR} is the reflectance in NIR wavelength (0.8 - 1.1 μ m), and ρ_{RED} is the reflectance in Red wavelength (0.6 - 0.7 μ m). This index is originally formulated using Band 5 - Red (0.6 - 0.7 μ m) and Band 7 NIR (0.8 -

1.1 μm) of MSS (Multispectral Scanner) sensor in Landsat satellites (Rouse, J. W. et al., 1974). The index value ranges from -1 to +1. Where healthy and dense green vegetation has a value above 0.6 and sparse and dry vegetation has a value between 0.1 to 0.4. A value less than or equal to zero indicates a lack of vegetation, barren land, and water. The chlorophyll structure changes during the dry and wet season. Therefore, this index acts as a proxy for the nature of vegetation (Lillesand et al., 2015).

NBR - Normalized Burn Ratio

The NBR index can be used to understand the leaf's water content and vegetation condition. Healthy vegetation has high reflectance in the NIR region because of the chlorophyll presence and significant absorption in the SWIR region because of the water content present in the leaves. Since a burned area or vegetation at risk of burning will be dry and have less water content, this particular characteristic is being utilized in formulating this index. It is a normalized index calculated with NIR and SWIR bands.

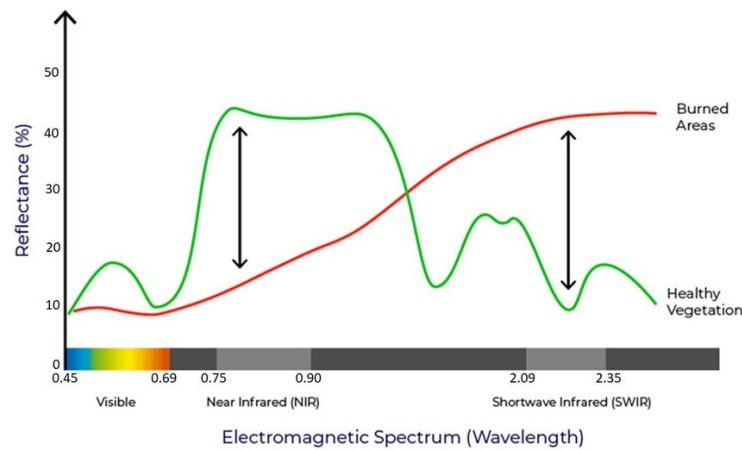


Figure 2-1: Spectral signature of Healthy vegetation and burned area.

(Source: USDA Forest Service)

$$NBR = \frac{\rho_{NIR} - \rho_{SWIR}}{\rho_{NIR} + \rho_{SWIR}} \quad (2.2)$$

ρ_{NIR} is the reflectance in NIR wavelength (0.77 – 0.90 μm), and ρ_{SWIR} is the reflectance in SWIR wavelength (2.08 – 2.35 μm). A severely affected burned area will have a distinct change in reflectance in NIR and SWIR bands (García & Caselles, 1991). The value ranges from -1 to +1. The healthy vegetation will have a higher NBR value than dry and burnt vegetation. This aids in discriminating burnt areas from healthy vegetation. The index is also used for assessing the burn severity of an area. A differential index of pre-fire NBR and post-fire NBR is also utilized for fire-related studies (*Normalized Burn Ratio (NBR)*, n.d.).

PMI - Perpendicular Moisture Index

The moisture content in the vegetation is one of the essential characteristics to determine whether a particular vegetation is prone to fire danger. That can be defined with LFMC (Live Fuel Moisture Content). LFMC is the ratio of the mass of water content present in a fresh leaf to the mass of a completely dry leaf. It has a good relationship with PMI. A study performed over three different areas of the Mediterranean region found that PMI value changes with the change in vegetation characteristics during the fire season. It is also found that the PMI correlates well with the average number of fires and the rate of fire spread (Maffei et al., 2014).

$$PMI = -0.73[(\rho_{1.230-1.250\mu m}) - 0.94(\rho_{0.841-0.876\mu m}) - 0.028] \quad (2.3)$$

In the above equation, ρ refers to reflectance. PMI value is higher for vegetation with high moisture content than dry vegetation. In another study (Maffei & Menenti, 2019), it was found that with decreasing PMI value, the probability of extreme fire events increased.

MNDFI – Modified Normalized Difference Fire Index

The reflectance nature of chlorophyll in the NIR region and the water absorption characteristic of healthy vegetation in the SWIR region are used to analyse the vegetation condition in this index as per figure 2.1.

$$MNDFI = \frac{\rho_{2.105-2.155\mu m} - \rho_{0.841-0.876\mu m} - 0.05}{\rho_{2.105-2.155\mu m} + \rho_{0.841-0.876\mu m} - 0.05} \quad (2.4)$$

In the above equation, ρ refers to reflectance. This spectral index is calculated for MODIS imagery (Pandey et al., 2022) for utilization in fire risk modelling. As this index considers vegetation's greenness and radiative nature, it will provide helpful information in fire-related studies. The probability of the fire incidences can also be found with this index (Pandey et al., 2022).

2.2.2 Meteorological Parameters

As we have discussed the fire triangle and its components, the meteorological parameters influence the fire components significantly. The extreme temperature and less precipitation in the late winter and during summer make the forests of Uttarakhand vulnerable to fire (Dobriyal & Bijalwan, 2017). Some operational systems for rating the danger of forest fire consider only the meteorological parameters for their models. They are empirical models which develop indices using meteorological parameters for different aspects of fire like fire moisture code, fire behaviour index in the case of Canadian fire weather index and burning index, spread component, and ignition component in the US National Fire Danger Rating System (NFDRS). Different sub-models are generated in McArthur's Forest Fire Danger Rating System, like Fine fuel availability, Surface fine fuel moisture, rate of spread, and difficulty of suppression. All these indices and sub-models are generated with meteorological variables as inputs. The variables which are commonly used are,

1. Temperature
2. Relative Humidity
3. Wind speed and direction
4. Precipitation
5. Dew point temperature

All these parameters are measured from ground station points and made available for usage in the models. It is logical also to use these variables as they influence the nature and behaviour of the fire. Along with the values of these variables for a single day, fire danger is also calculated by aggregating them temporally to get a picture of the weather in the past. The temporal aggregation can be either a week, 10 days, or a month before the day of consideration.

2.2.3 Terrain Parameters

Digital Elevation Model (DEM) image products are derived using various methods, which is a digital representation of the elevation of a surface. In the early days, contour lines were drawn in topographic maps to represent the elevation of a location in a two-dimensional plane surface. Preparing ground-based contour maps is laborious and time-consuming. With the advent of satellite-based remote sensing techniques, it is found that images of the same place taken at slightly different angles can produce relief of objects in the overlapping region. This concept of obtaining overlapping images is called stereo photography and is utilized to prepare the elevation of a region. From then, elevation information is made available as DEM imagery. DEM preparation has evolved with techniques such as Radar Interferometry and LiDAR (Light Detection and Ranging) imaging. With advanced methods, more accurate elevation information is obtained.

DEM imagery of the earth represents the elevation of a unit area in the earth from a common datum using grid cells. The unit of elevation is generally in meters or feet. This elevation data is used further to calculate the terrain's slope and aspect (slope direction). Elevation, along with slope and aspect, is a critical input for the various environmental processes. They have numerous applications as they represent the characteristics of terrain. Some of them are flood-related models (Thakur et al., 2020), fire simulation models (Zheng et al., 2017), and landslide hazard mapping (Zheng et al., 2017). The change in elevation of a surface with respect to its surroundings is referred to as slope. In three-dimensional surfaces, there are different methods to calculate slope, four nearest approach and third order infinite approach (*How Slope Works?*, n.d.). The slope is denoted as degrees or percentages. The direction of the steepest downslope is referred to as aspect. The direction is calculated by considering North as 0° in the clockwise direction. It is denoted as degrees.

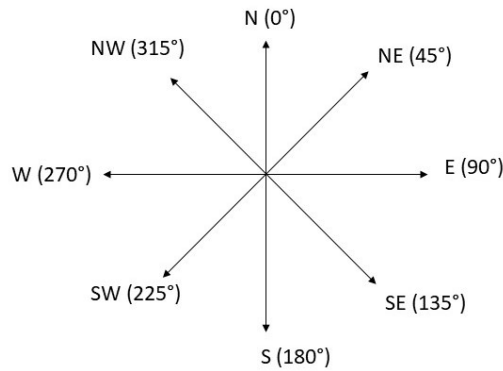


Figure 2-2: Representation of aspect with corresponding angle

Figure reference - (Abd El-Hady et al., 2015)

2.2.4 Anthropogenic Parameters and Landcover Maps

95% of the fires in India are primarily caused by human activities (Ashutosh et al., 2019). Therefore, considering parameters that can well define human presence in an area is necessary for this study. Human activities can be mapped efficiently with GIS. GIS-based mapping of roads, settlements, recreational locations, and land use mappings can be used to represent human activities in a location. It can be well understood from each land use class the impact it could make on forests based on its nature. Distance from those parameters can be well attributed to the accessibility or influence of humans in a specific location. Proxies like the distance of a location from the nearest city can also act as a proxy for human influence in an area (Weiss et al., 2018). Land cover maps of an area demarcate the various types of vegetation, the nature of the land like barren, waterbodies, and the presence of snow or ice in a region. This gives information about the nature of vegetation in the area.

2.2.5 Active Fire Data

Near real-time monitoring of fire is also being operationalized with the advent of satellite remote sensing. It is the first step in finding the location of forest fires and the fires that are about to spread from one forest patch to another or from agricultural land to forests. It is also helpful to take response measures to control the fire and share the resources appropriately from a fire management perspective. Remote sensing through satellites is an evident tool for those applications (Coskuner, 2022). By using the thermal wavelength of the electromagnetic spectrum (4 μm and 11 μm) in sensors such as MODIS (Moderate Resolution Imaging Spectroradiometer) in Aqua and Terra satellites and VIIRS (Visible Infrared Imaging Radiometer Suite) in SNPP (Suomi National Polar-Orbiting Partnership) spacecraft the thermal anomaly in any part of the earth is identified (with revisits over exact location more than once a day), and it is delivered as active fire points (Giglio et al., 2016; Schroeder et al., 2014). These datasets are used to detect active fires present in any location with the help of satellites.

2.3 Remote sensing applications in different fire management elements

As discussed earlier in the Introduction chapter, remote sensing and GIS is utilized in all four phases of disaster management. Fire susceptibility maps help demarcate the regions based on their vulnerability to fires, which helps in mitigation efforts. They can be prepared by considering various factors which influence fire in a region. Then the different factors can be given different weights based on their importance or influence on fire based on the locality's characteristics. Various methodologies are followed for assigning the weights, such as Analytical Hierarchy Process (AHP) (Lamat et al., 2021), Frequency Ratio (Tiwari et al., 2021), and Fuzzy Modelling Techniques (Tiwari et al., 2021). Machine Learning (ML) and Deep Learning (DL) based fire susceptibility mapping studies are also performed (G. Zhang et al., 2021). These fire susceptibility maps prepared using various techniques are utilized by various forest departments and planning authorities to mitigate fires before fire season (Ashutosh et al., 2019).

GIS-based suitability analysis is performed to find suitable locations to build a fire station in a city (Wahab, 2014). This kind of study helps to identify the infrastructure facilities needed in particular locations by considering previous fire incidents and the accessibility to the high-fire vulnerable locations. Pre-fire alert maps for the near future are also inevitable for resource allocation and planning practical firefighting activities. Predicting the burned area probability (Bergado et al., 2021)(Gray et al., 2018), forest fire spread modelling using deep learning techniques (Huot et al., 2022)(Zheng et al., 2017), wildfire prediction (Huot et al., 2020) are different forms of studies performed to generate pre-fire alerts for the next day and at maximum for the next week. Operational forest fire danger forecasting systems also provide fire danger ratings based on the station-wise meteorological data and interpolate them to deliver in the form of maps (Chowdhury & Hassan, 2015).

Near real-time monitoring of forest fires help in identifying the locations where the fires are active (Giglio et al., 2016). The availability of active fire data twice a day for each satellite (MODIS – AQUA, TERRA; VIIRS – NOAA-20, SNPP) makes it possible to observe the fire spread direction. Recovery activities in a fire disaster include afforestation and restoring the ecosystem, thereby restoring people's livelihood. These activities can be performed by identifying the burned locations and finding the severity of fires in different locations. Both of them can be performed with remote sensing data. The information collected by satellites in visible and infrared wavelengths of Electro Magnetic Radiation (EMR) is utilized along with specific burn-sensitive indices to map burned areas and the severity of fire (Bar et al., 2020)(Giglio et al., 2018)(Chuvieco et al., 2018)(Roteta et al., 2019). Fire regime studies are also performed with the vast collection of active fire data collected over the past two decades to understand and analyse the trend of fires in different regions (Lafon & Quiring, 2012)(Kumar & Kumar, 2022). These studies illuminate our understanding of the areas where fires happen frequently. This gives the fire managers an idea about the locations that must be given importance for fire-resilient infrastructure development.

2.4 Existing systems for pre-fire alerts

Pre-fire alerts/fire forecasts in the form of maps deliver the possibility of fire in a particular location for a given time in the future. They are an evident tool for efficiently planning fire mitigation and management activities in the near future. There are empirical systems such as the Rothermel fire spread model (Andrews, 2018), the Canadian Fire Weather Index system (Van Wagner & Pickett, 1985), McArthur Mk5 Forest Fire Danger Index for Australia (McArthur, 1967), which are in practice in different parts of the world providing pre-fire alerts. These models depend only on weather parameters to come up with fire

risk. Predicted fire danger maps are produced and circulated to the head of the forest management officials (*India State of Forest Report 2021*, 2021). These danger maps are used for resource allocation during forest fire season in India. Nevertheless, these danger maps are produced from interpolation techniques in coarse resolution. This may not provide sufficient information in places where there are undulating terrains or change in climate within small distances. That makes the usage of these fire danger maps impractical on the ground (Chowdhury & Hassan, 2015).

2.5 Review of Deep Learning Studies

Deep Learning (DL), which comes under the umbrella of Artificial Intelligence (AI), has become the spotlight of research in the last decade. Even though the research in Neural networks started in the 1940s (Jaspreet, 2016), its journey to its popularity had numerous ups and downs. Some of the recent developments in the computing facility in the last two decades and the availability of enormous data are notable for deep learning's achievements. Various architectures of deep neural networks can potentially find complex relationships and patterns in the dataset. This is the primary reason that it has been used in specific fields like object identification (He et al., 2016), sentiment analysis (Liu, 2012)(Ismail Fawaz et al., 2019), ecological studies (Christin et al., 2019), medical sciences (Ronneberger et al., 2015), fire management studies (Jain et al., 2020) and many more.

Major breakthroughs have occurred in image analysis, like object recognition, with the advent of Convolutional Neural Networks (CNN) (LeCun et al., 2015). Their ability to learn low-level to high-level features and patterns from the data makes them successful. They are also useful in identifying non-linear relationships between features. Basic CNN has three primary operations being performed in it; 1. Convolution filters, 2. Pixel-wise Activation, 3. Max pooling. The convolution filters possess learnable weights and bias. The filters convolve over the image to learn the features from the images, i.e., patterns from the values present in the various bands of the image by considering the neighbourhood pixels as well. This makes the CNNs learn the spatial context of the images. The pixel-wise activation functions activate only the pixels with the necessary information to pass on to the subsequent layers based on the activation function. In order to reduce the dimensionality of the images and take into consideration the translational and scale invariance, maxpooling is used. In fully connected neural networks, a series of these layers constitute the architecture and connect with a dense, fully connected layer to result in the output layer. In a fully convolutional network – the series of convolution, activation, and max-pooling layers provide output with a final layer, also as a convolutional layer, thereby reducing the dense connections. The Backpropagation technique allows the model to learn the weights and bias of filters to fit the model to the training data. A diagrammatic representation of various operations performed in a Fully connected CNN model is shown in Figure 2-3.

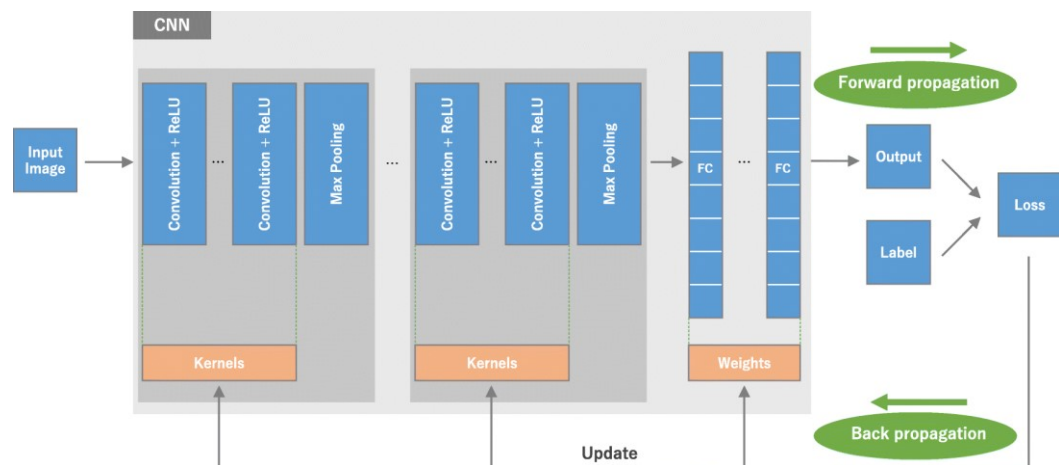


Figure 2-3: Abstract of a CNN model

Source: (Yamashita et al., 2018)

Recurrent neural networks (RNN) are another type of neural network design that can be taught to address issues when it is necessary to process the data as a series. These networks learn information from sequential data. They have memories of past information and transmit it to the subsequent levels of the network as needed. They can offer answers to problems involving sequential data in this way. RNNs are effectively used in speech recognition (Graves et al., 2013), image-to-text formation, audio and text translation, and many more tasks involving sequential data (Yu et al., 2019). An improved version of RNN is LSTM (Long Short-Term Memory) networks developed by (Hochreiter & Schmidhuber, 1997). Practically, RNNs are better at handling information of shorter time sequences rather than longer ones (Olah, 2015). This is because of the vanishing gradient problem, which mitigates the network to pass on the information for a longer duration (Pascanu, 2013). This makes it challenging to use it when dealing with long-term sequential data. The variant of RNN, LSTM has resolved this.

LSTM networks are structured to handle long-term dependencies in the data. The basic structure of the network is called an LSTM cell which regulates the transfer of information from both short-term and long-term data through gates. There are three different gates in an LSTM cell: forget gate, input gate, and output gate. The forget gate regulates the amount of information to be restored from the cell state (long-term memory). It takes input as the previous hidden state (short-term memory) (H_{t-1}) and Input state (X_t), and a sigmoid function is performed on them to result in a value between 0 and 1. A value of 0 denotes that no information from the cell state should be passed, and 1 represents a complete flow of information. This is performed by a matrix multiplication. In the input gate, the information to be stored in the cell state is calculated with Input state (X_t) and hidden state (H_{t-1}) by performing sigmoid and tanh operations. The obtained output is updated with the cell state's value. The output gate calculates the value of the particular cell's hidden state (H_t). The diagrammatic representation of an LSTM cell and its operations are in Figure 2-4.

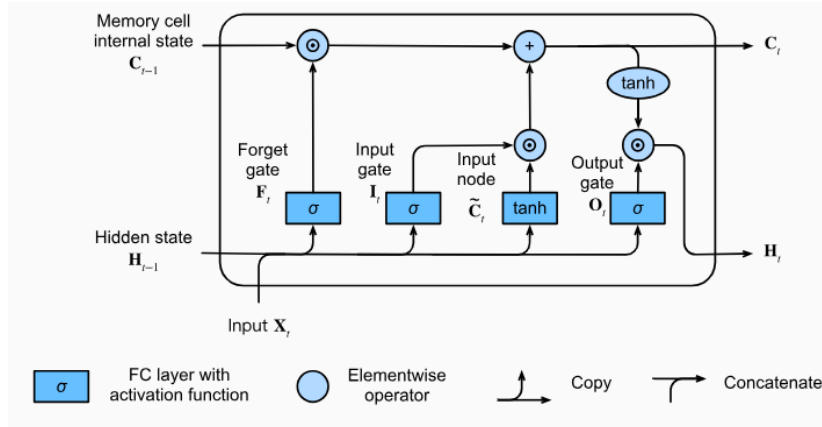


Figure 2-4: Architecture of an LSTM cell

Source: (A. Zhang et al., 2021)

LSTM has also been analysed for its usage in weather forecasting (Shi et al., 2015) and air quality forecasting (Alléon et al., 2020).

2.5.1 Deep Learning application in fire related studies

Some of the works done in the field of fire sciences with DL are discussed in this section. A Deep Learning based forest fire susceptibility modelling using Convolutional Neural Network was carried out by considering spatio-temporal fire influencing factors data from 2002 to 2010 (G. Zhang et al., 2019). This study uses the temporally varying dataset from those study periods and produces a static fire susceptibility map. The technique with CNN yielded higher accuracy than the machine learning models Random Forest (RF), Support Vector Machine (SVM), Kernel Logistic Regression, and Multi-Layer Perceptron (MLP). The significant advantage of CNN is its efficiency in learning spatial features from the different influencing factors of fire. There are various parameters in deep learning architectures whose values must be optimized by considering the dataset and application. Patch size, one of the hyperparameters in DL, is considered as 25X25 in this study, considering the nature of fire in the study area. DL-based active fire detection is performed with the Landsat dataset globally by (de Almeida Pereira et al., 2021). Different variations of U-Net were used for semantic segmentation. Three different fire masks are produced using three different active fire detection conditions, which are used for model building. The results were also compared with test sets of manually annotated Landsat images. The U-Net light version (a smaller number of input features and filters in convolution layers) also produced significant results. This shows the advantage of the U-Net model for segmentation tasks.

(Huot et al., 2020) has considered different fire-influencing parameters such as terrain features, meteorological parameters, and remote sensing image derived indices and applied DL for predicting the fires using historical data of influencing parameters and fire data as label features. Different kinds of fire prediction tasks are performed by changing the way the input and label features are given as input to the model. Convolutional autoencoders and residual U-net architectures are utilized by considering the data from different dates as separate samples and prepared fire forecast maps. Another kind of deep learning method, Recurrent Neural Networks (RNN), which extracts information from sequences of data, is also utilized in the study since the fire-influencing parameters also have a temporal influence on fire occurrence. One of the variants of RNN, Long Short-Term Memory (LSTM), is utilized with

convolutional layers by considering the last seven days of fire-influencing parameters as a sequence input feature. Outputs from LSTM architecture provide comparable results with convolutional autoencoders, but data augmentation techniques were suggested to improve the accuracy further.

(Huot et al., 2022) have utilized the fire-influencing parameters to predict fire spread by considering the fire extent of the next day as a label feature and fire-influencing parameters of the day before the fire as input features. Convolutional autoencoder was used to predict fire spread and compared with RF and Logistic Regression as the baseline. DL predicts comparatively well than the other two models. The spatial resolution of the dataset was also changed to find the model's sensitivity to different spatial resolutions as input. It gives a positive response as accuracy metrics improved with coarser resolution data, but operational-wise, that would be less useful. Ablation studies were also carried out by adding and removing each influencing parameter to quantify its influence on the prediction. Another similar study for predicting the Wildfire burn in the Australian state of Victoria using deep learning methods (Bergado et al., 2021) considers factors such as meteorological, terrain, forest type, spectral indices depicting fuel moisture, and anthropogenic factors. The study was performed for the years 2006 to 2017. The burned area obtained from the state of Victoria's official departmental site was used as a label feature. This study integrated the availability of diversified big data into a single framework for forest fire prediction. The study also provided feature statistical importance by considering the gradient assigned by the architecture. That gave an idea of each feature's significance in different models. The study suggested the usage of data that considers the reason for ignition in an area for improving the model's efficiency and reliability of the model's output.

A wildfire danger prediction study was conducted by (Kondylatos et al., 2022) for Greece with a data cube prepared with 90 fire-influencing parameters and fire labels. That was utilized for the study of fire danger prediction. Baseline ML models such as RF and XGBoost, and DL models such as LSTM and ConvolutionalLSTM were used. The DL models outperformed the ML models. It showed that the temporal sequence can better help understand fire's nature. This study also performed an interesting aspect of AI: Explainable AI (xAI). This provides information about the influence of input features on model output. It was interpreted in the study. The variables which got higher importance have a good relationship with the temporal domain, which depicts the usefulness of LSTM-based applications in fire prediction studies. xAI will help to quantitatively improve the understanding of the various features involving fire.

A study on the sensitivity of a neural network with the various variables used for fire modelling was performed by (Vasilakos et al., 2009). A Multi-layer perceptron model with a single hidden layer was used to model three fire danger indices with meteorological, terrain, vegetation, and anthropogenic features as feature datasets. They have compared four different methods for calculating the feature importance for the model. They are Garson's algorithm, Tchaban's weight product, Logistic regression, and Partial derivative of network outputs. Through these different techniques, they were able to find the feature's importance. Though neural networks are called 'black box' models, it is possible to understand the model's outputs.

From these studies, it is evident that the deep learning models are utilized for studies that have inherent non-linear relationships between their variables to model the fire-related applications. This advantage of DL is also to be utilized in this study for fire forecasting.

2.5.2 Chosen model and Design experiments

Fire forecasting or fire danger prediction studies are performed with data from a single day (Bergado et al., 2021)(Huot et al., 2022) and with data from multiple days of fire-influencing variables (Kondylatos et al., 2022). In this study, the fire forecasting task is addressed in both ways. Models are built with data from a single day and multiple days of fire-influencing variables. In the coming sections, it will be mentioned as the study of non-sequential data (fire-influencing variables of a single day) and sequential data (fire-influencing variables of multiple days before fire).

2.5.2.1 Image segmentation with non-sequential data

U-Net is an encoder-decoder-based fully convolutional neural network initially designed to perform segmentation tasks in medical images (Ronneberger et al., 2015). The architecture can model the problem with fewer training images with better accuracy than other convolutional networks in comparatively less time. Its success in the medical field makes the researchers incorporate the model for other image-related studies.

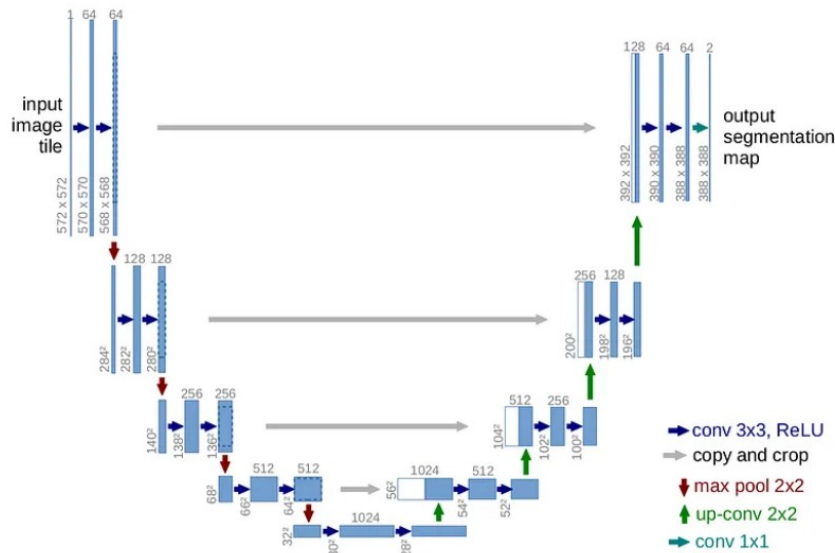


Figure 2-5: U-Net architecture

Source: (Ronneberger et al., 2015)

U-Net has three characteristic components in its architecture: encoder, decoder, and skip connections. The encoder part extracts the features from the input image while reducing the dimension of the image. The decoder resamples the image to the original resolution to localize the classified results. The skip connection connects the corresponding encoder with the decoder to pass the high spatial information from the encoder part to the decoder, thereby increasing the model's accuracy. U-Net is also used in some of the fire-related studies we discussed earlier. (de Almeida Pereira et al., 2021) has used variants of U-Net to detect active fires. The model provided good results in their study. Fire forecasting is considered as an image segmentation challenge and for this U-Net is to be utilized in this study. It will be used to segment active fires in the study area using fire-influencing variables of a single day. The model will be trained with

various network parameters and different scenarios. Their corresponding results are discussed in the following sections.

2.5.2.2 Image segmentation with sequential data

A Convolutional LSTM architecture is selected to perform image segmentation with sequential data. Since it has both convolutional layers and LSTM layers, it can learn the features spatially and temporally. It was initially proposed for precipitation nowcasting (Shi et al., 2015) and has been used in studies related to sequential images (Burge et al., 2020)(Alléon et al., 2020). In the current fire forecasting study, this architecture is to be used to analyse the efficiency of the model to learn about fire likelihood from sequential images of fire-influencing variables. A convolutional LSTM architecture is similar to an LSTM architecture, where the convolutional operations are performed in state-to-state and input-to-state transitions. Figure 2-6 shows the state-to-state and input-to-state transitions being performed through convolution operation in a convolutional LSTM architecture.

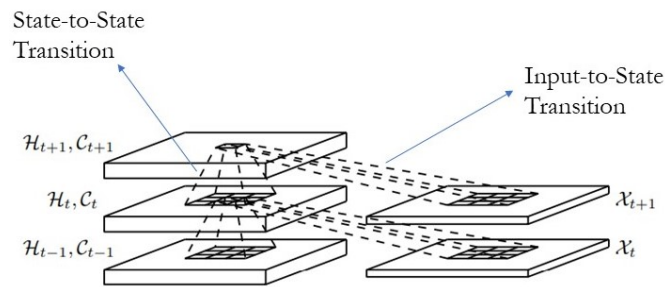


Figure 2-6: Inner structure of ConvLSTM architecture

Source: (Shi et al., 2015)

2.6 Class Imbalance problem

The challenge in fire forecasting studies is that it is an anomaly-related study. Therefore, the distribution of fire and non-fire points will vary significantly. It is defined as class imbalance, where the distribution of classes of interest will be imbalanced. The class which is high in number is called the majority class, and the other is called the minority class. In most cases, the minority class will be the focus of our study. In this scenario, the model will be able to see a lot of the majority class during learning which helps the model to focus on the majority class most of the time than the minority class, which is less in number. This will affect the model's performance. Various studies in recent days have covered this. There are two types of methods to address class imbalance. They are data-level methods and algorithm-level methods. Changing the nature of the dataset to attain balance in classes – data level; changing how neural networks or models deal with the imbalance dataset is algorithm level correction.

(Johnson & Khoshgoftaar, 2019) has given proper insights into the various methods and practices followed by different researchers for imbalance data handling. (Buda et al., 2018) has given insights into the working of different correction methods applied to class imbalance problem in CNN. (Mayaki & Riveill, 2022) has performed different methods of imbalance data correction and showed their performance on different datasets. They got comparatively better results on the data, which is uncorrected

for imbalance nature. However, some contrasting studies (van den Goorbergh et al., 2022), discuss the corrections performed to address class imbalance and the ill-effects of performing them. The study took an imbalanced dataset and performed a logistic regression model with and without data-level corrections to address the class imbalance. It concluded that the model with imbalanced dataset correction performed worse than the one without correction. (Harrell, 2017) has mentioned the usage of imbalance correction methods in different scenarios. When the task at hand has inherent randomness, it is not advised to perform correction for imbalance classes; instead, predictors that can well differentiate the classes should be chosen. Also, those results should be delivered as probabilities rather than classification results. Proper selection of validation data is also important to model the imbalanced class distribution problem. A comparison is performed for active fire detection with and without validating the model for validation data (Langford et al., 2018). This has yielded good accuracy in model classification.

The loss function concerned with the false positive rate and the false negative rate is proposed by (Wang et al., 2016), and the combination of them into a Mean False Error (MFE) loss function and Mean Squared False Error (MSFE) loss function. These loss functions show more attention to the false classifications of the positive class, giving them more loss values. This will make the model change its weights to reduce the loss values. (Lin et al., 2017) has proposed a loss function sensitive to the classification errors in minority classes, ‘focal loss’. This function gives more importance to the classification of minority classes with a modified cross-entropy loss function where two new parameters are added, alpha and gamma. The parameter gamma specifies how much the majority class samples should be down weighted, and alpha is a class weight value.

$$FL = -\alpha(1 - p_t)^\gamma \log(p_t) \quad (2.5)$$

In Equation 2.5, ‘ α ’ denotes the alpha–class weighting value, γ denotes the gamma–majority class down-weighting value, p_t denotes the predicted value for an input sample.

3 STUDY AREA AND DATASET

3.1 Study Area

Uttarakhand is a north-western state of India, lying in the Central Himalayas. The state shares international borders with Tibet in the north, Nepal in the east, and inter-state borders with Himachal Pradesh in the northwest and Uttar Pradesh in the south. The state has differing landscapes, such as greater Himalayan mountains and glaciers in the northern part and plains in the southern region. The state is divided into 13 districts for administrative purposes. The elevation in the state ranges from 300m to 7000m above mean sea level (Chauhan, 2010). The state receives a yearly average rainfall of 1631mm (*Uttarakhand at a Glance 2017-18*, 2019). Southwest monsoon winds are the major rain-bearing winds for the state which results in 1162.7mm of rainfall (70% of the yearly average) between the months of June and September (Chauhan, 2010)(Southwest Monsoon-2022 End of Season Report for Uttarakhand State, 2022).

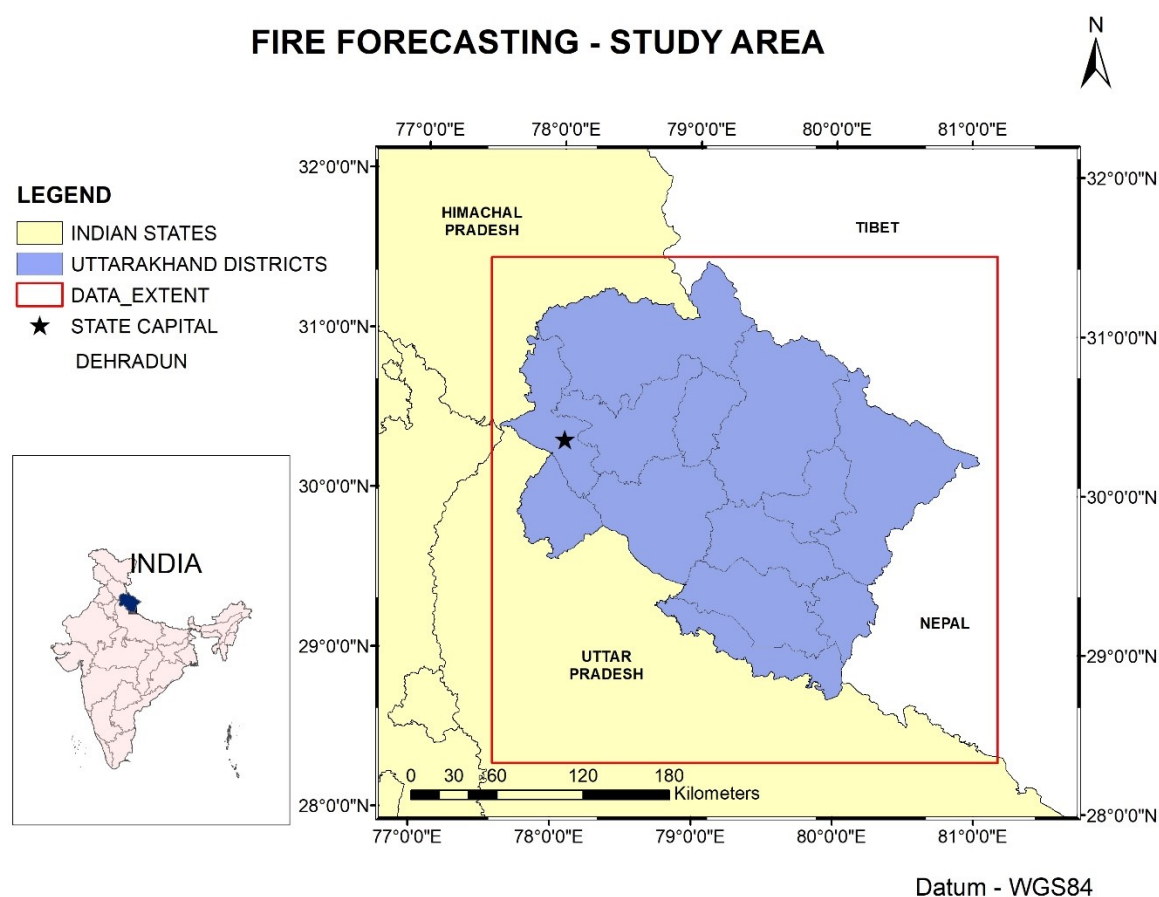


Figure 3-1: The Political map of Uttarakhand and its districts. (Inset map - Indian states)

The state has a total geographical area of 53,483 sq. km with a population of over 1.01 crores (approximately 10 million) as of the 2011 Census (The recent census officially conducted by the Government of India). 70% of the population lives in rural areas, and the main livelihood is crop and livestock mixed farming. The people also depend upon the forest products such as timber, fuel wood, fodder for livestock, and non-timber products such as honey, flowers, fruits, lichens, etc. (Chauhan, 2010). The state also has a number of temples which makes it a popular site for devotional tourism. The rich biodiversity and the snow-capped mountains also attract tourists from all over the world.

3.1.1 Topography

The state has varied landforms, such as deep valleys, high mountains, glaciers, snow-covered peaks, perennial rivers, streams, creeks, plateaus, and plains. The state also has the second-highest peak in the country, Nanda Devi (7,817 m above mean sea level). The state has different physiographic zones running parallelly from northwest to southeast. The fast-flowing rivers denote the steep slope in the region, which usually results in landslides and landslips in the rainy season (Chauhan, 2010). Figure 3-2 is the topography map of Uttarakhand showing different elevation ranges.

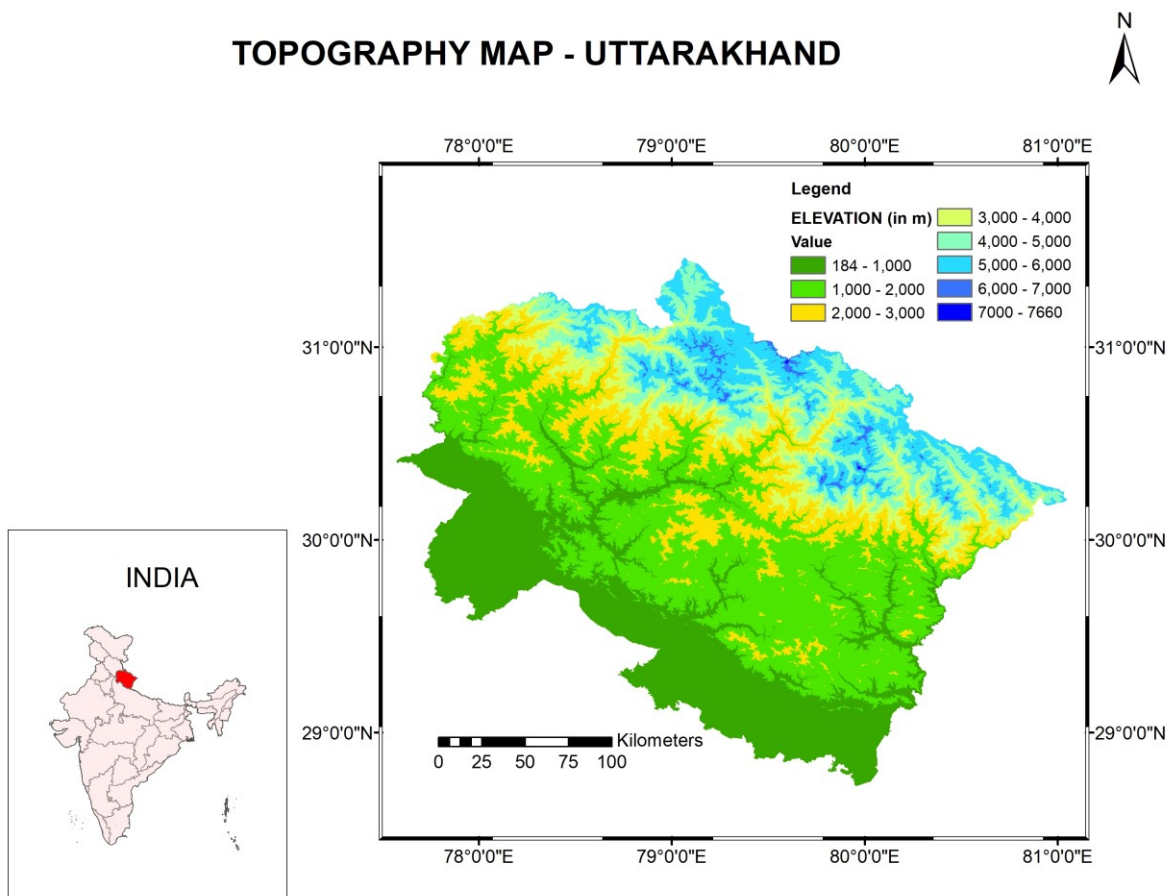


Figure 3-2: Topography map of Uttarakhand. (Inset map – Outline of India and location of Uttarakhand)

3.1.2 Climate

The different regions of the state experience varied weather and climatic conditions, and it's because of the difference in elevation, aspect, and topography. The south-facing slopes receive direct sunlight for longer periods and more rain than others while receiving less snowfall (Chauhan, 2010). The southern plains experience a tropical climate, whereas the valleys experience a sub-tropical climate. A temperate climate exists between 800m and 2400m and places above 2400m experience an alpine climate (Chauhan, 2010). There will be a huge difference in temperature within a day between different places because of varied climate zones.

3.1.3 Forests

The state is gifted with rich and diversified forest resources, which provide economic support to the people who depend on them. The distribution and diversity of varied species of flora and fauna depend upon the location's altitude. The state has 112 species of trees, and 73 and 94 species of herbs and shrubs, respectively (India State of Forest Report 2019, 2019) . The state has 38,000 sq. km. of recorded forest area, of which around 7,300 sq. km. of forests are designated as Van Panchayat. These are the forest land where the local community people manage the forest. This system began in 1921 (India State of Forest Report 2019, 2019). The presence of different floral species with respect to differing elevations is mentioned in Table 3.1.

Table 3.1: Floral species available in different climatic regions

Region	Elevation	Floral species
Tropical	Less than 300m	Sal, Shisham, Teak
Sub-tropical	300 – 1100m	Mixed tropical forests, bushes and shrubs
Temperate	1100 – 1800m	Pine forests Mixed oak forests – Banj oak, Buransh, Tilong and Kafal
Sub-alpine	1800 – 2800m	Coniferous forests – Deodar, Spruce and Fir
Alpine	2800 – 3400m	Alpine meadows, medicinal plants

Source: (Chauhan, 2010)

3.1.4 Landcover Statistics

As per the Land Use Land Cover map prepared during Natural Resource Census – Third cycle (2015-2016), Uttarakhand has most of its area covered by forests (54.52% of 53,483 sq. Km.). Agriculture class comes second after forest with 20.16%, followed by snow and glacier - 13.51% of total area. There are five subclasses in forest type (Saxena et al., 2019). The distribution of top landcover classes and their subclasses are as below.

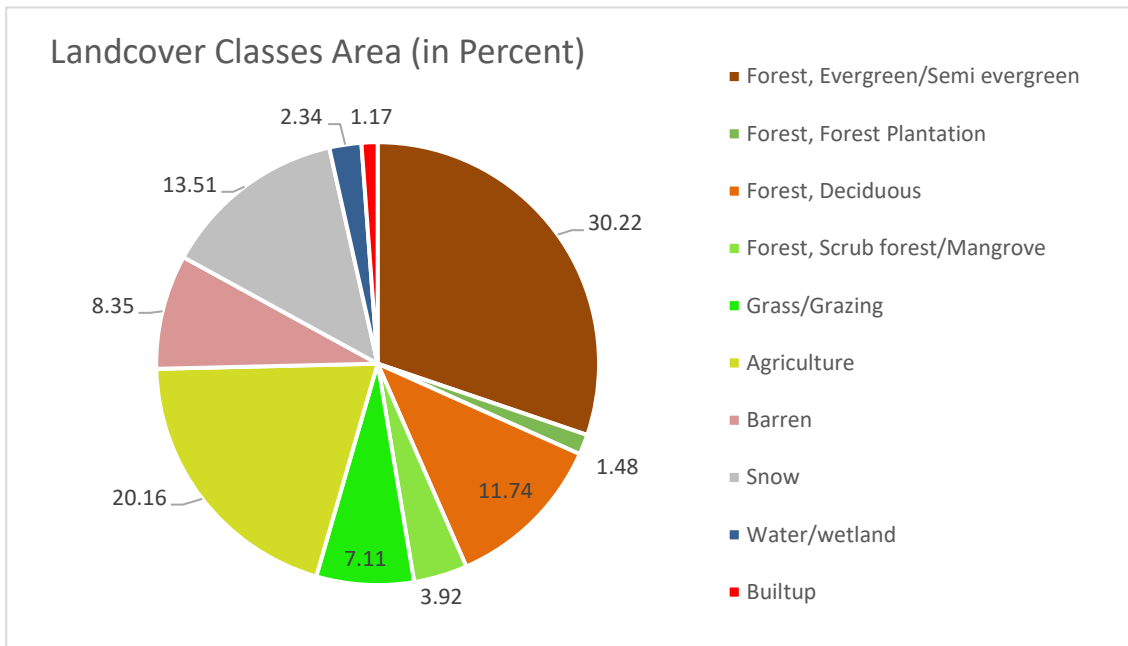


Figure 3-3: Pie-chart representing different landcover classes in Uttarakhand

Source: BHUVAN

3.2 Datasets used

For any kind of supervised deep learning study, two different types of inputs are required. The independent variables are called the features and the dependent variable is called as label data. In this study, fire-influencing variables are features and the target variable data, fire and non-fire is label data. The application of the study and deep learning architecture changes how we give the data as features and labels into the model. The datasets used for the study are mentioned in the following section. The study period is from 2016 to 2023.

3.2.1 Feature dataset

The fire-influencing variables are categorized into static and dynamic dataset, based on the nature of the dataset. As the name denotes, the variables which do not change frequently are categorized as static and the ones which change frequently are categorized as dynamic. The source dataset, derived variables and other information is mentioned in the following table.

Table 3.2: Feature Datasets used and their specifications.

	Source dataset	Derived variable	Spatial resolution	Temporal resolution	Source
Static variables	Digital Elevation Model	Elevation	30m	-	NASA SRTM DEM – Google Earth Engine (GEE)
		Aspect	-		
		Slope	-		
	Global friction surface	Land-based travel speed	~1000m		Malaria Atlas Project - GEE
	WorldPop Gridded population	Population density	~100m	1 year	WorldPop - GEE
	Landcover/use	Landcover/use classes	500m	1 year	NASA LP DAAC – GEE
Dynamic variables	Meteorological data ERA5-Land	Average Temperature 2m	0.1°	Daily	ECMWF - GEE
		Precipitation	0.1°		
		u-wind 10m	0.1°		
		v-wind 10m	0.1°		
		Maximum Temperature 2m	0.1°		
		Minimum Temperature 2m	0.1°		
		Dewpoint Temperature 2m	0.1°		
		Surface Pressure	0.1°		
	Meteorological data Station Data	Air Temperature 2m	-	15 minutes	IMD
		Maximum Temperature 2m			
		Precipitation			
		Wind Speed			
		Wind Direction			
	Relative Humidity				
	Optical imagery - VIIRS	Optical imagery and spectral indices	1km	Daily	NASA LP DAAC - GEE

0.1° is equivalent to 11Kms

ECMWF – European Centre for Medium-Range Weather Forecasts

3.2.1.1 **Global Friction Surface**

The dataset provides the time taken to travel in minutes per meter in a particular pixel. The travel time is calculated by considering various other features present in the pixel. Those features include road, railway lines, lakes, rivers or any other waterbody, the type of landcover, terrain characteristics and the national borders. Each variable is given different travel speed in accordance with different values and at the end they result in the final travel time in every pixel (Weiss et al., 2018). This dataset is prepared in collaboration between various research institutes for the Malaria Atlas Project in order to find the time taken to travel in motorized vehicle. This kind of datasets are also used to study about the influence of human on forest resources, healthcare facilities (Weiss et al., 2018). (Weiss et al., 2018) have prepared dataset to find the distance to the nearest urban centre in a global scale, which was extended to prepare the Global friction surface map. The land-based travel time for motorized transport in Uttarakhand is shown in the figure3-4. The units of the data is changed to minutes per kilometre for better understanding.

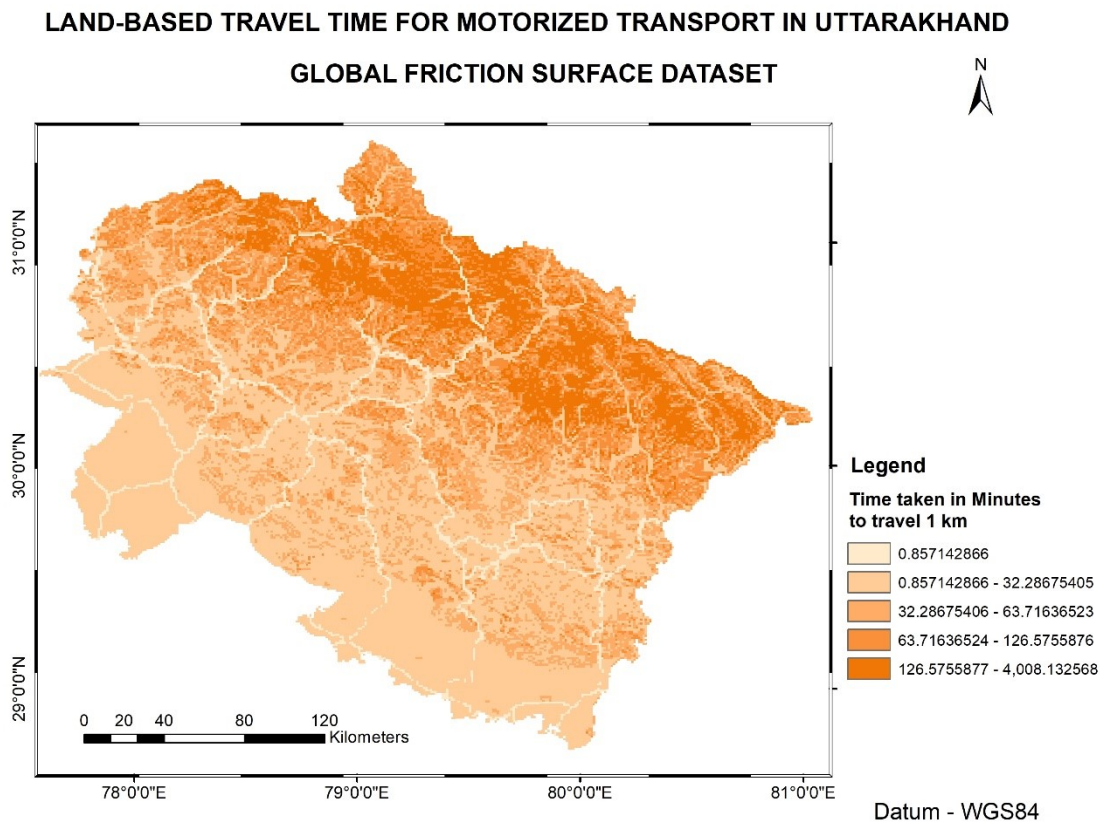


Figure 3-4: Land-based travel time for motorized transport map for the Indian state of Uttarakhand

3.2.1.2 Landcover data

Landcover data for this study is taken from MODIS yearly landcover data product. The dataset is available in GEE from 2001 till 2021. There are five landcover type maps available by considering different methods of landcover types classification. In this study, Annual Plant Functional Types classification scheme is utilized (Sulla-Menashe & Friedl, 2022). The classification scheme and the description for each class of the Plant Function Type are mentioned in Table 3.3. The land use land cover map for the year 2021 of Uttarakhand is shown in Figure 3-4. Landcover classes are aggregated for modelling purposes and the aggregated classes are mentioned in Appendix section.

Table 3.3: Landcover classes and description for Annual Plant Functional Type classification

S. No.	CLASS	DESCRIPTION
0	Water Bodies	Permanent water bodies – at least 60% area
1	Evergreen Needleleaf Trees	Evergreen conifer trees (height >2m, tree cover > 10%)
2	Evergreen Broadleaf Trees	Evergreen broadleaf trees (height >2m, tree cover > 10%)
3	Deciduous Needleleaf Trees	Deciduous needleleaf trees (height >2m, tree cover > 10%)
4	Deciduous Broadleaf Trees	Deciduous broadleaf trees (height >2m, tree cover > 10%)
5	Shrub	Shrub (1-2m height, cover>10%)
6	Grass	Herbaceous annuals (<2m)
7	Cereal croplands	Cultivated herbaceous annuals of cereal crops (<2m)
8	Broadleaf croplands	Cultivated herbaceous annuals of broadleaf crops (<2m)
9	Urban and Built-up lands	30% impervious surface area
10	Permanent Snow and Ice	Snow and ice covered by snow and ice for at least 10 months of the year
11	Barren	Less than 10% of vegetation (sand, rock, soil)

MODIS LULC UTTARAKHAND - 2021 Annual Plant Functional Types Classification

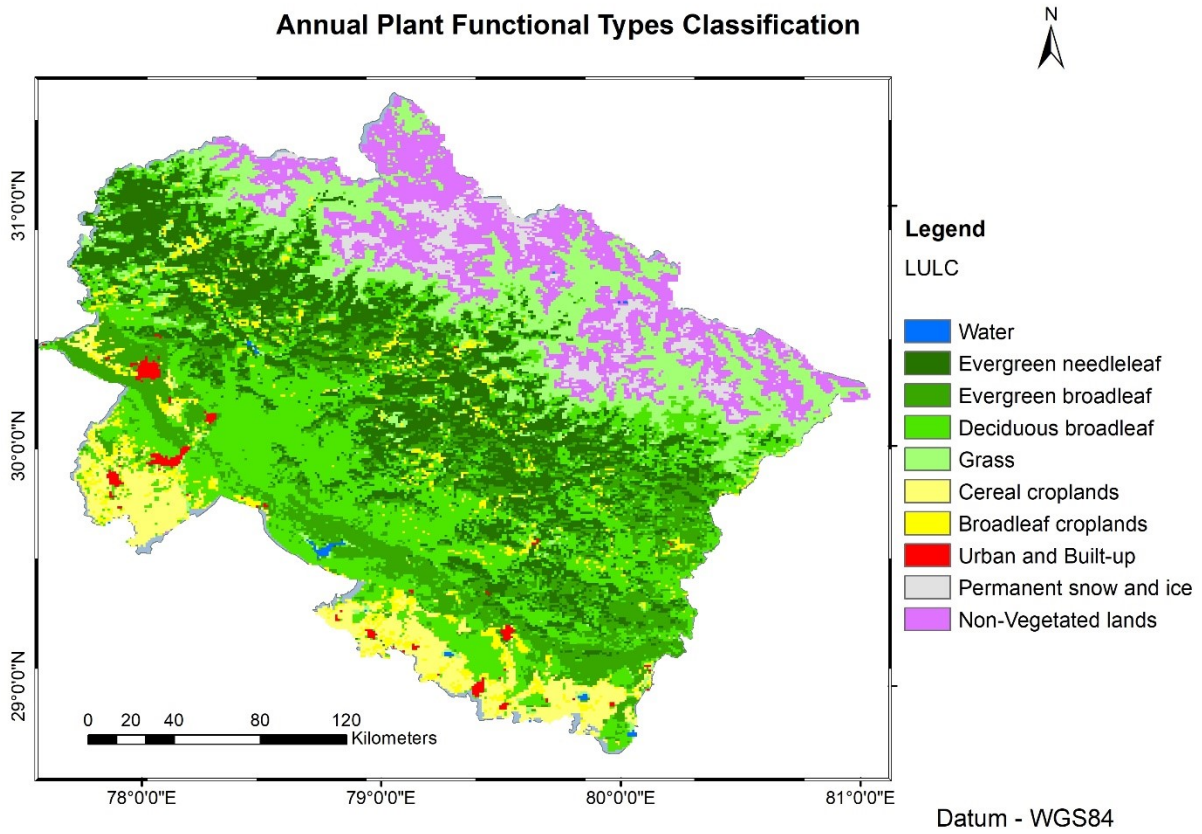


Figure 3-5: MODIS LULC classification map of 2021 for the Indian state of Uttarakhand

3.2.1.3 VIIRS Optical Imagery

VIIRS sensor onboard SNPP and NOAA-20 satellites, is launched to act as a continuation for MODIS, AVHRR (Advanced Very High-Resolution Radiometer) by providing high temporal optical and thermal imagery of the planet. It has also increased spatial resolution and improved the system to reduce the gaps in between the image strips (Smith, 2022). There are two types of systems with spatial resolution 375m and 750m in the VIIRS sensors. They are calibrated and processed and delivered as 500m and 1000m respectively to act as a continuation for MODIS data products. The moderate resolution bands of visible and infrared wavelength range in VIIRS sensor is given in the following table.

Table 3.4: VIIRS Moderate-resolution visible and infrared bands and their wavelength ranges

VIIRS BANDNAME	WAVELENGTH RANGE (μm)	BAND
M1	0.402 - 0.422	Visible/Reflective
M2	0.436 - 0.454	Visible/Reflective
M3	0.478 - 0.488	Visible/Reflective
M4	0.545 - 0.565	Visible/Reflective
M5	0.662 - 0.682	Near Infrared
M7	0.846 - 0.885	Shortwave Infrared
M8	1.230 - 1.250	Shortwave Infrared
M10	1.580 - 1.640	Shortwave Infrared
M11	2.230 - 2.280	Medium-wave Infrared

3.2.2 Label dataset

Active fire points data is the label feature in this study. The data is obtained from the thermal images collected by the sensors MODIS and VIIRS and available in NASA FIRMS (Fire Information Resource Management System) website. MODIS sensor present in satellites Aqua and Terra can provide active fire points derived from thermal anomalies on daily basis in 1 km spatial resolution (Giglio et al., 2016). VIIRS sensor in the SNPP satellite provides active fire points in 375m and 750m spatial resolution daily (Schroeder et al., 2014). The active fire product from VIIRS sensor is resampled into 1000m (750m), in order to maintain the consistency with MODIS active fire product. This dataset is available in Google Earth Engine and is used as label feature in this study. Year-wise fire pixels count for the study years in mentioned in the bar graph shown in Figure 3-6.

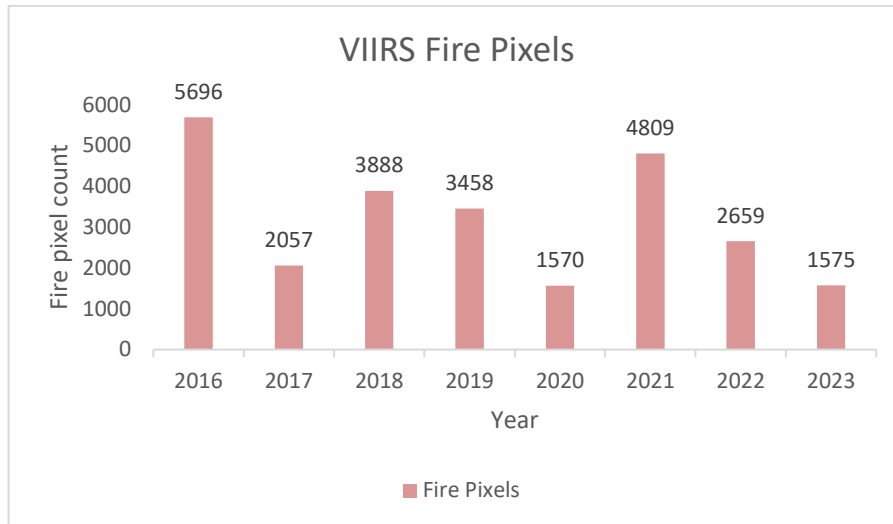


Figure 3-6: Year-wise fire pixels count for the study years.

3.3 Platforms used

Various applications and open-source libraries used for the study for different tasks are mentioned in the Table 3.5.

Table 3.5: Platforms used for the study

Task	Platform used
Data	Accessed from Google Earth Engine through 'geemap' package in Python
Processing	Jupyter Notebook
Mapping and Visualization	ArcMap 10.8 & QGIS 3.22
Graphs and charts	MS Excel
Web Application	'Greppo' package in Python

4 METHODOLOGY

The methods followed for the research can be divided into five sub-sections. They are,

1. Preliminary analysis
2. Data Preparation
3. Model Building
4. Hyperparameter tuning
5. Model Validation
6. Creating a user interface for fire forecasting

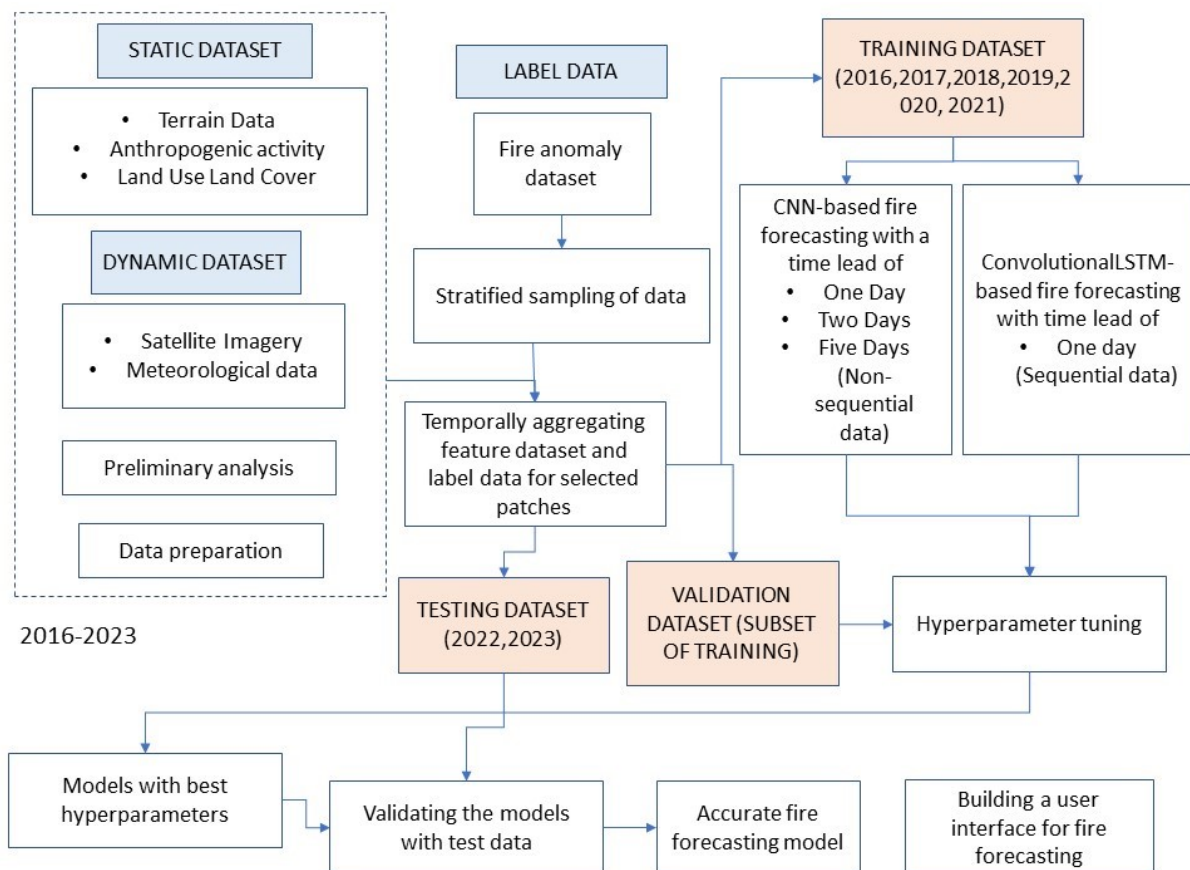


Figure 4-1: Workflow adapted for the research.

Workflow adapted for the research is shown in the Figure 4-1. The primary datasets used, and the datasets prepared for the deep learning modelling are highlighted for differentiation. The

4.1 Preliminary Analysis

A preliminary examination of the distribution of fire hotspots across various terrain features in Uttarakhand is conducted. This type of analysis demonstrates how those variables affected the fire. It also sheds light on the impact of other elements on fire, including land use and land cover and weather aspects associated with the terrain's physical characteristics. Terrain features that are analysed for the distribution of fire include elevation, aspect, and slope.

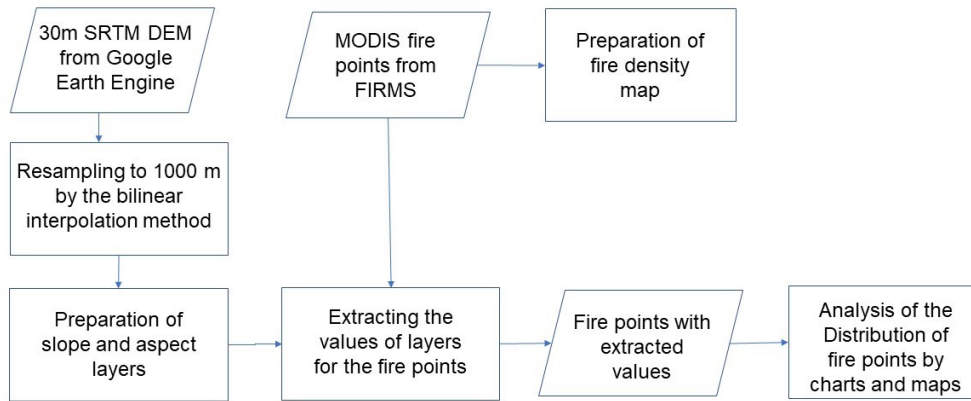


Figure 4-2: Flowchart of the preliminary analysis

4.2 Data Preparation

Data forms an integral part when dealing with study of fire where lots of variables have influence in different magnitudes and multiple ways of interactions can happen between them. Therefore, selecting appropriate dataset, which can provide accurate information appropriate to the challenge in hand for the considered spatial and temporal scales is important. Comparison of datasets based on their resolution, accuracy and consistent availability of data for the whole study period helps us to select the best suited dataset. Also, in a study which involves different datasets, the temporal and spatial scale of the datasets should match for better understanding and giving as input for the deep learning models. It also makes the implementation easier. This calls for the processes like resampling datasets to common spatial and temporal resolution, data scaling, projecting dataset to a common projection. The data is further split into training, validation, and testing for training, selecting the hyperparameters, and for validating the model performance respectively. The following subsections provide an explanation of the procedures used in the research on data-related topics.

4.2.1 Data selection

4.2.1.1 Terrain Dataset

Considering the data for terrain features, SRTM DEM from GEE is used in this study. There are other DEM datasets available such as Advanced Spaceborne Thermal Emission and Reflection Radiometer (ASTER) DEM, Cartosat DEM. All the datasets are of common spatial resolution 30m. A study by (Baral et al., 2016) has performed a comparison of all the above mentioned DEM datasets for different terrain

conditions such as plain areas, medium and extremely undulating terrain. It was observed that the SRTM DEM was able to provide values equivalent to the values from toposheet height values in all the terrain conditions. Therefore, based on this study SRTM DEM is further used.

4.2.1.2 Meteorological data comparison

The datasets commonly used for fire studies as mentioned in the section 2.2.2 can be obtained from two different sources. They are ERA5 Land reanalysis data and ground meteorological stations. ERA5 Land reanalysis data is mainly prepared for climatological studies. Their main advantage is data availability for all the regions without any gap. They are prepared with different advanced modelling techniques incorporating data from ground stations and satellite observations (*ECMWF Reanalysis v5 (ERA5)*, n.d.). Their continuous temporal and spatial availability are the prime advantage. But the spatial resolution of the dataset is 0.1° (approximately 11kms). This is the challenge to use such dataset for the event which happen in smaller scale especially in Uttarakhand (Singh et al., 2016). But proper availability of data is important for the preparation of model. Therefore, following analysis is done to compare the station data with ERA5 reanalysis dataset.

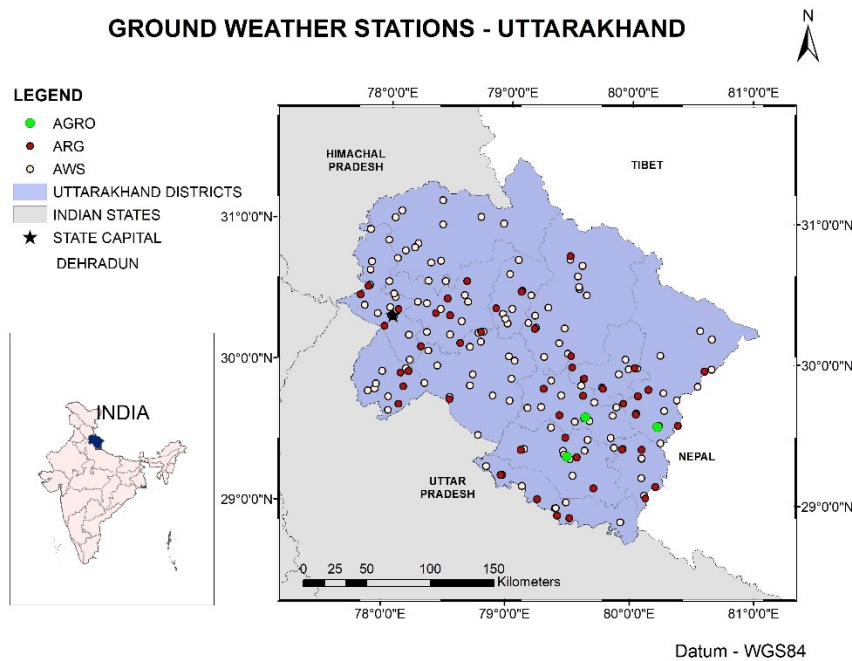


Figure 4-3: Ground Meteorological stations present in Uttarakhand (as of 31/03/2023)

In the Figure 4-2, various ground weather stations present in the state of Uttarakhand area shown. AWS refers to Automatic Weather Station, ARG stands for Automatic Rain Gauge and AGRO stations measures all the variables required for agricultural fields. In the following Table 4.1, the meteorological variables considered in the study and their units are mentioned.

Table 4.1: Meteorological variables and their units in Station data and ERA5 data.

Meteorological Variables	Station data (unit)	ERA5 Land Reanalysis data (unit)
Precipitation	millimetre	metre
Wind Speed 10m	knots	-
Wind Direction 10m	Degrees	-
Relative Humidity	%	%
Average Temperature 2m	°C	K
Maximum Temperature 2m	-	K
Minimum Temperature 2m	-	K
Dewpoint Temperature 2m	-	K
u-wind 10m	-	m/s
v-wind 10m	-	m/s
Surface Pressure	-	Pa

Table 4.2: Description of different meteorological datasets

Meteorological data source	Description
ERA5	Available from 1950 – till last fortnight (in GEE)
Ground meteorological stations	From Jan'18 – Aug'20 – 25 stations available Aug'20 – Now – 105 stations available

From the Table 4.2 it can be inferred that the data from ground station is not available in enough number for the whole time period when considering the area of the whole state. Also, there were lots of missing data and anomalous data in it. It poses a risk to use the data for the study. Therefore, a comparative analysis is performed between station data and ERA5 Land reanalysis data to check the data quality of ERA5 by considering station data as ground truth. The stations are selected where the values are present for the whole year of 2021. The comparative analysis is performed for maximum temperature (T_{max}) variable.

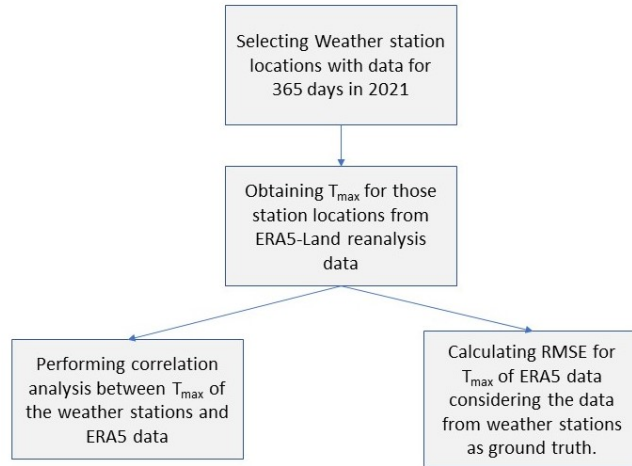


Figure 4-4: Methodology for comparing meteorological datasets

Correlation analysis is performed between T_{max} of station data and ERA5. This correlation analysis shows the trend of the maximum temperature (T_{max}) of both the datasets for the year 2021. By considering the station data as ground truth, the root means square error value of maximum temperature value between ERA5 and station data is also calculated for all the station points.

4.2.2 Deriving significant variables for fire-related study

4.2.2.1 Spectral indices

As discussed in the section 2.2.1 the following spectral indices are calculated by using the visible and infrared satellite images from VIIRS sensor. The application and importance of the following indices are mentioned in the literature review.

NDVI (Normalized Difference Vegetation Index)

$$NDVI = \frac{\rho_{M7} - \rho_{M5}}{\rho_{M7} + \rho_{M5}} \quad (4.1)$$

where ρ_{M7} and ρ_{M5} are the reflectance values of the bands M7 (NIR) and M5 (Red) in VIIRS sensor.

NBR (Normalized Burn Ratio)

$$NBR = \frac{\rho_{M7} - \rho_{M11}}{\rho_{M7} + \rho_{M11}} \quad (4.2)$$

where ρ_{M7} and ρ_{M11} are the reflectance values of the bands M7 (NIR) and M11 (SWIR) in VIIRS sensor.

PMI (Perpendicular Moisture Index)

$$PMI = -0.73[(\rho_{M7}) - 0.94(\rho_{M8}) - 0.028] \quad (4.3)$$

where ρ_{M7} and ρ_{M8} are the reflectance values of the bands M7 (NIR) and M8 (NIR) in VIIRS sensor.

MNDFI (Modified Normalized Difference Fire Index)

$$MNDFI = \frac{\rho_{M11} - \rho_{M7} - 0.05}{\rho_{M11} + \rho_{M7} - 0.05} \quad (4.4)$$

where ρ_{M11} and ρ_{M7} are the reflectance values of the bands M11 (SWIR) and M7 (NIR) in VIIRS sensor.

4.2.2.2 Meteorological Variables

Meteorological Variables wind speed, wind direction and relative humidity are not directly available in ERA5 Land Reanalysis dataset. There are other variables which are available through which they can be derived. Wind Speed and Direction are derived from u (positive for wind from west) and v (positive for wind from south) components of wind.

$$Wind\ Speed = \sqrt{u^2 + v^2} \quad (4.5)$$

$$Wind\ Direction = mod(270^\circ - atan2(v, u) * \frac{180^\circ}{\pi}, 360) \quad (4.6)$$

$$relative\ humidity = \frac{e^{\frac{(17.625*(T_d-273))}{(T_d-273)-243.04}}}{e^{\frac{(17.625*(T-273))}{(T-273)-243.04}}} * 100 \quad (4.7)$$

In the equations 4.1 and 4.2, u and v correspond to u-component and v-component of wind respectively (*Wind Direction Quick Reference*, n.d.). The unit of wind speed is metres per second (m/s) and wind direction is Degrees (0° - North, 90° - East, 180° - South and 270° - West). In the equation 4.3, T_d and T are Dewpoint temperature and Average Temperature respectively (Lawrence, 2005). The unit of relative humidity is Percentage.

4.2.3 Data pre-processing

The data used for the study is obtained from GEE. The GEE can be accessed through an API for python. Therefore, in this study the data is extracted from GEE through python. GEE provides functionalities for clipping the data to study area while selecting the dataset itself. Also, dataset is projected to a common projection system EPSG:32644 - WGS 84 / UTM zone 44N. The unit of geographic coordinates is metres. The dataset is resampled to a common resolution of 1000m to be in accordance with fire anomaly data (label dataset). Bilinear interpolation technique is used for resampling the dataset to 1000m. Population data which is in 100m spatial resolution is reduced by sum to obtain the value for 1000m. Also, for machine learning and deep learning applications, the all the data should be in common scale for the model to learn from the features. Therefore, the whole dataset is normalized with their minimum and maximum (0 to 1).

$$Normalized\ value = \frac{band\ value - minimum\ value}{maximum\ value - minimum\ value} \quad (4.8)$$

According to this equation, for a variable minimum and maximum value will be calculated and each value in the dataset is normalized with those values.

4.2.4 Data splitting for model

The major challenge of fire related study is the distribution of fire and non-fire points in the dataset and in the reality as well. It means fire is an anomalous incident which will not happen everywhere and every time. The imbalance nature of the dataset will cause serious issue in the learning process of the model as well. Therefore, there are various techniques being applied in different researches as discussed in section 2.6. Also, a place which is vulnerable to fire because of its vegetation and meteorological conditions may not burn, if there is no initiation factor. This makes the modelling part complex. This will need a powerful model to learn the information from the data. Stratified sampling is performed in study based on terrain and land use and land cover characteristics.

Total number of fire and non-fire pixels present in the study period for the complete study area is 25,712 and 338,975,632 respectively which shows that the ratio is 1:0.0000758 between non-fire and fire pixels in the total study period. This severe data imbalance will drastically affect the model's performance. Therefore, a stratified sampling strategy has been applied to select data of particular patches by considering the fire density, terrain, land cover, anthropogenic activities and fire regime in the study area. This is performed in order to reduce the imbalance nature and at the same time to sample all the important fire influencing characteristic of the study area.

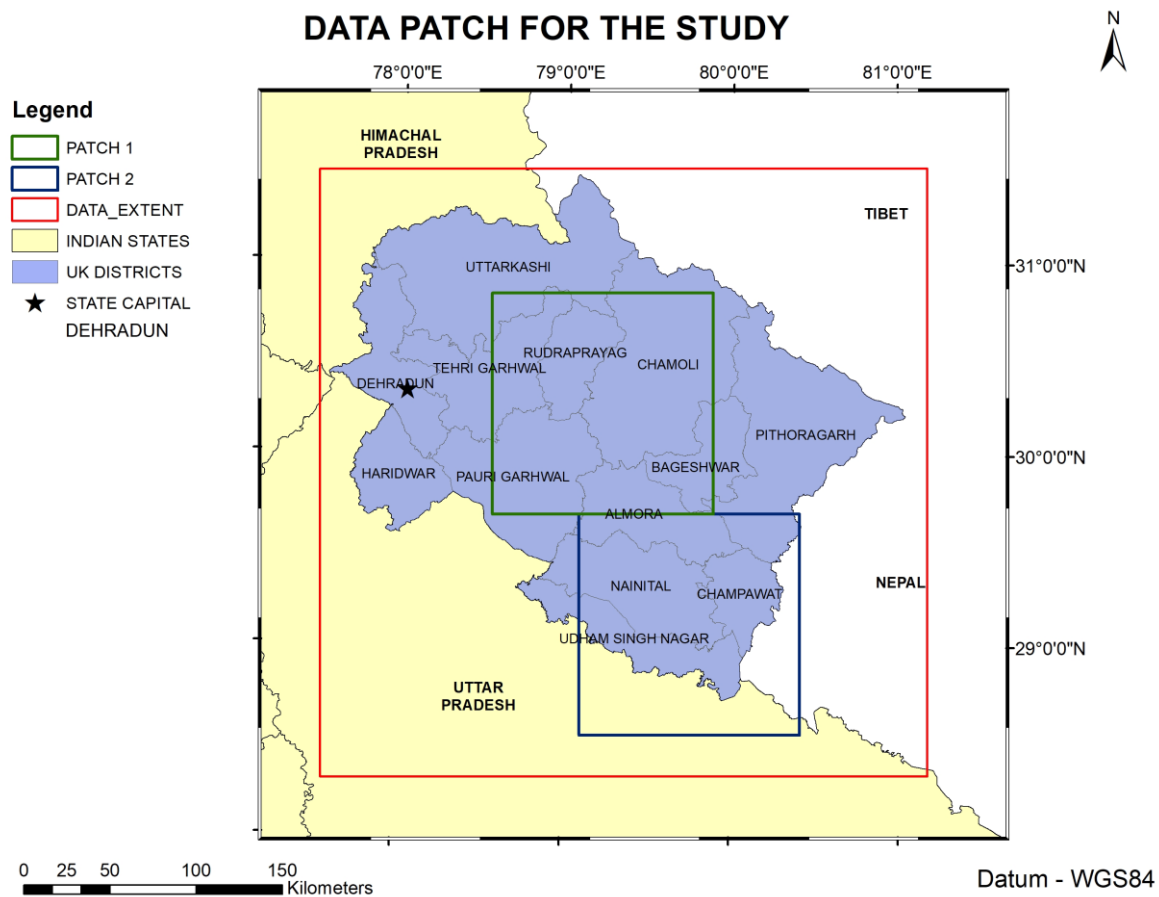


Figure 4-5: Patches selected for the study

According to (Srivastava et al., 2012), A report of Vulnerability of India’s Forests to Fires – districts of India are classified into three classes of vulnerability to fire YEAR. Less Vulnerable – a district where fire occurred in 2 to 3 years at a same area, Moderately Vulnerable – fire occurred in 4 to 6 years at the same area, Highly Vulnerable - fire occurred in all 7 years at the same area of their study. According to their classification, the selected first patch covers the districts Pauri Garhwal which is highly vulnerable, Bhageshwar, Chamoli, Almora, and Tehri Garhwal which are moderately vulnerable and Rudraprayag which is less vulnerable. The selected patch covers both mid elevated regions (where pine trees are common) to glacier peaks. Even in the patch, the data is selected for different temporal periods in order to cover all the major season of the year. The data is selected from the month February to Mid of July. From February to June it is fire season in mid elevation regions, end of winter in high elevation regions and in July the monsoon rain will start. The patch is selected in such a way that the model will be able to learn the fire characteristics from all the seasons and terrain characteristics.

While considering the second patch Nainital, Udham Singh Nagar are highly vulnerable to fire, Almora is moderately vulnerable, and Champawat is less vulnerable. The second patch is selected based on the land use patterns as well. As the terrain is plain, agricultural is common in southern region and the northern region is moderately elevated. The time period of data is from October to December and April to June. In the plains, agricultural residue burning happens from October and in the mid elevation regions, fire will occur during fire season which is February to June.

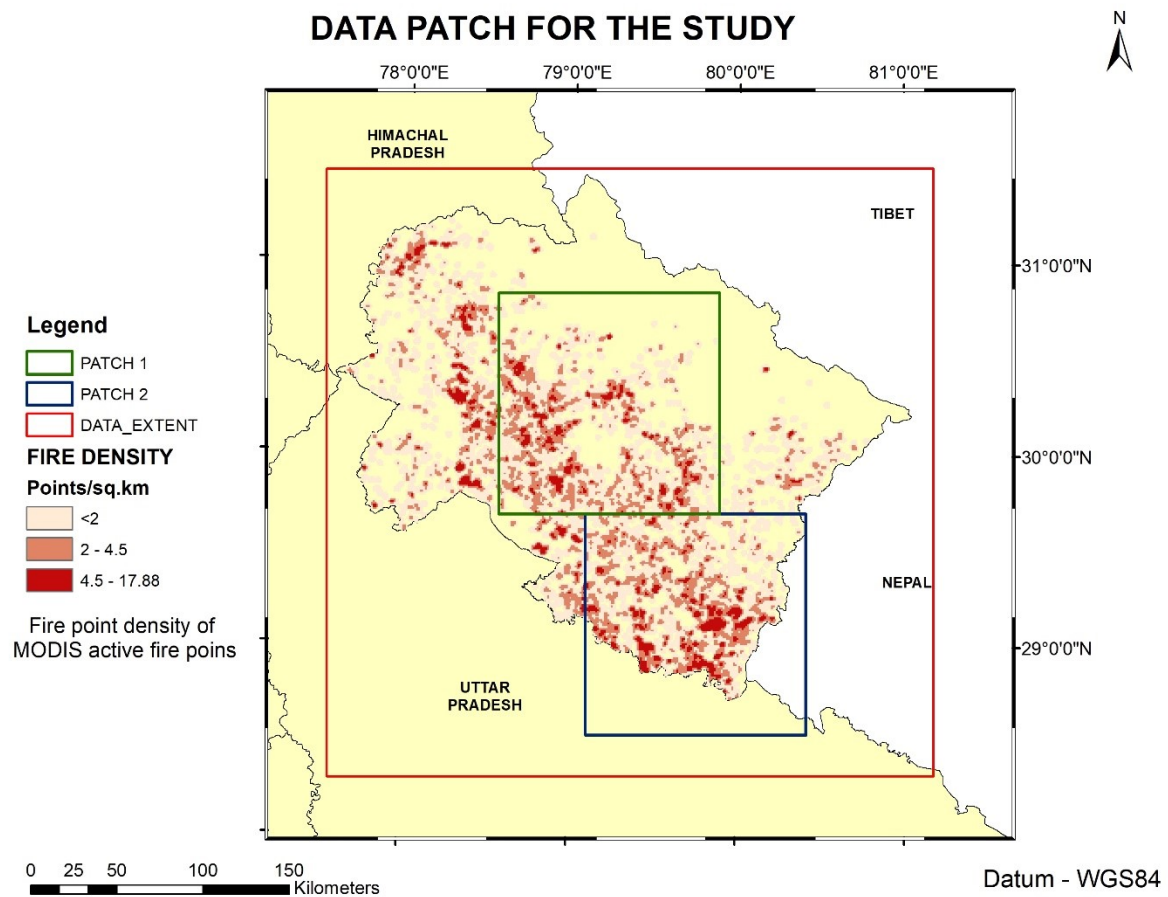


Figure 4-6: Fire density map for the state of Uttarakhand and the selected patches for the study

The map in Figure 4-5 represents the density of fire points (per sq.km.) from 2018 to 2021 over Uttarakhand. This map is prepared using the kernel density estimation function. The function takes input parameters such as the Cell size of the output raster, the search radius around the features (fire points), and the kernel to be used for density estimation. This particular map is prepared with a cell size of 1 km X 1 km raster, a search radius of 2 km for each fire point, and ‘Epanechnikov’ as kernel function (Epanechnikov, 1969). The patches are selected for the study by visually interpreting this map as well alongside the official reports.

Table 4.3: Training and testing data for the study and its significance

Data	Patch	Time Period	Significance
<ul style="list-style-type: none"> • Training and Validation set (2016 – 2021) • Testing set (2022, 2023) 	Patch 1	February – July 15th	Includes Fire season in Mid-elevation regions; Includes Higher elevation region; Includes monsoon season as well.
	Patch 2	April - June	Fire season in Mid-elevation region
		October – December	Agricultural residue burning season in plains

As mentioned in the Table 4.3, the dataset selected as two different patches are split into training and testing sets. Data of 2021 is used as validation dataset for tuning the hyperparameters of the model. The remaining data in training set is used for minimizing the loss function and for updating the weights and bias values of filters. The trained model is validated with the test dataset. The patches are created with dimension 128 x 128 to give as input to the models. Since fire is prominent during the fire season, day of the year is also used as a feature along with the geospatial dataset. Totally 32 features are prepared for fire forecasting analysis.

4.3 Deep learning models

4.3.1 Fire forecasting with non-sequential data of fire influencing variables

As discussed in the section 2.5.2, modified and shallower U-Net model architecture will be used for active fire forecasting with fire influencing variables of a single day (non-sequential) in the study.

4.3.1.1 Model architecture

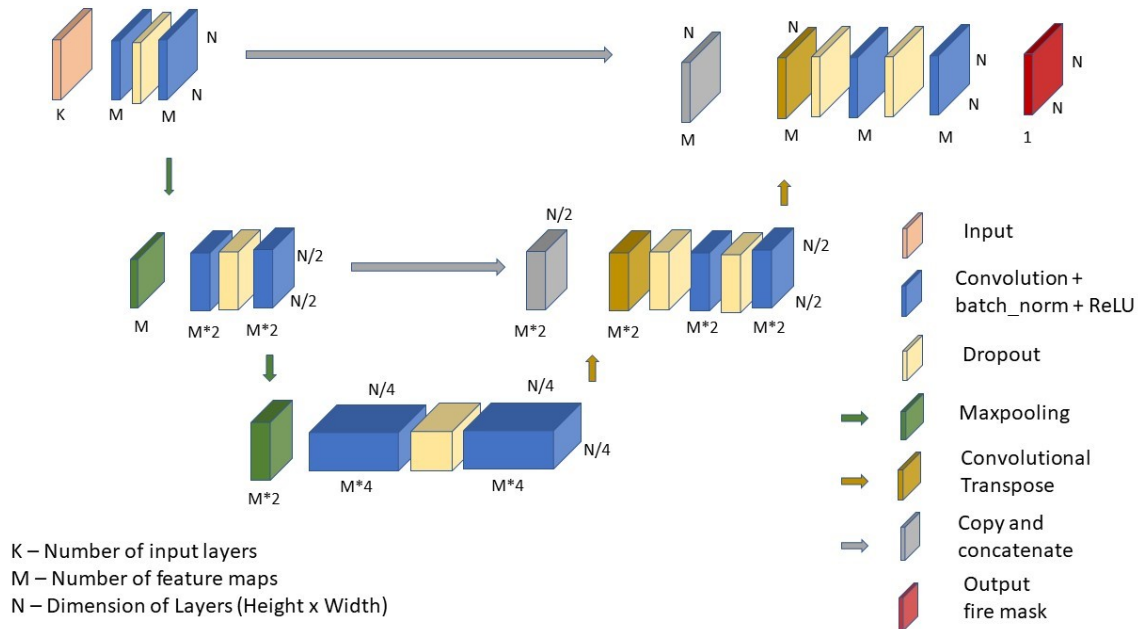


Figure 4-7: U-Net model architecture for active fire forecasting with non-sequential data

The model will take $N \times N$ dimension of input data and series of operations will be taking place in the model and finally, the output fire forecast image will be obtained as output. The operations include convolution, batch normalisation, non-linear activation, dropout, maxpooling, convolutional transpose, concatenation, skip connections. A 2D Convolutional operation is performed in this network, where a 3×3 kernel is used to move over the image to learn the features. The values of the filters are called weights and are learned through backpropagation. It is a process in which the model initially starts with a random or arbitrary weight values, through which the model will sense its response with the target label and according to the difference in values, the weight will be updated. There are some common initialization

functions to generate random numbers namely GlorotNormal, GlorotUniform, HeNormal, HeUniform, identity, etc. In this study HeNormal is used, which generates random numbers based on the number of input units in the weight tensor. The weight updation will be monitored by a function called ‘loss function’ and it calculates the difference between the target and predicted values called loss value. The weights will be updated in the filters according to the loss value. Focal loss (mentioned in the Equation 2.5) is used in this study to focus more on fire samples. An optimizer function optimizes the weight value to reduce the loss. In this study, ‘Adam’, a variant of stochastic gradient descent optimizer is used. Batch normalisation (mentioned as batch_norm in the Figure 4-7) is performed after convolutional operation. It normalises the data with mean of 0 and 1 standard deviation to keep the data in a normalised form. It increases the stability of the model and leads to faster convergence (Raparelli & Bajocco, 2019). The non-linear activation function allows only the values which has necessary information in it. In this study, Rectified Linear Unit (ReLU) is used as activation function. It acts like a filter to filter out values less than zero. Dropout layer randomly sets the value of certain number of neurons to zero for increasing the generalization capability of the model. The proportion of neurons to set zero is a hyperparameter which has to be found through experiments. Maxpooling is a 2X2 non-overlapping maximum filter over the image arrays to reduce the dimensionality of the data and also to learn the abstract spatial features from the dataset.

It is used in the encoder part of the U-Net architecture. Convolutional transpose is the opposite of convolutional layer, where deconvolution takes place to increase the spatial dimension of the image. Concatenation of data from encoder part to the corresponding decoder part is also performed to transfer the learned information from the encoder part to the decoder part. A convolutional layer with ‘Sigmoid’ activation function is used as final layer to produce fire segmentation output.

A shallower encoder-decoder network will be used for this study to reduce the receptive fields as the input data is of coarser resolution and to reduce the computational time. The fire which takes place in the study area is also not influenced by that many neighbouring cells. Therefore, shallower network will serve good. The input will be the fire influencing variables of a single day as feature dataset, and active fire dataset as feature labels. Three different scenarios are to be tried in this research with U-Net model, to find whether the fire influencing variables of a single day will be able to forecast the fire with a time lead of

- one day
- two days
- five days

These different analyses can be performed by modifying the label dataset given to the model. It is shown in the Figure 4-7. The different scenarios are selected to analyse the influence of a particular day’s dynamic variables in the future fire occurrence of a location. The different scenarios are to be performed by changing the label dataset in the model input data. Generally neural networks are used for finding the optimal weights and bias of the neurons in the network to learn the features in the label dataset (LeCun et al., 2015). By keeping that base idea for these three scenarios, the label dataset is prepared. In all the scenarios, fire influencing variables of day T_0 is taken as feature dataset. In the first scenario, active fire points of day T_1 is taken as label data. In the second scenario, the active fire points of day T_1 and T_2 is aggregated to a single image and used as the label dataset. Likewise, in the third scenario, active fire points of next five days from day T_0 is considered as label dataset. With these three scenarios, three different modified U-Net architecture model is built and analysed.

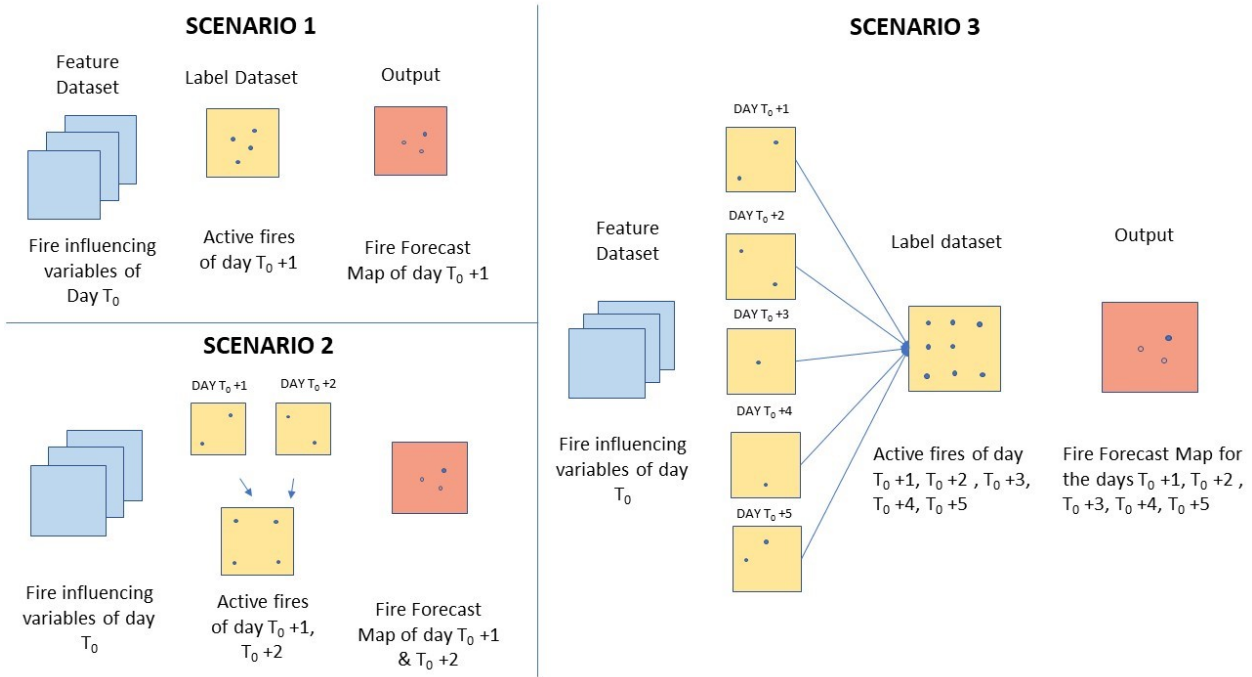


Figure 4-8: Different scenarios of fire forecasting with non-sequential data

4.3.2 Fire forecasting with sequential data of fire influencing variables

Fire forecasting with sequential data of fire influencing variables is built with series of convolutional LSTM, and convolutional layers. It is built to exploit the temporal information from the sequential data to model fire in the future. It will be analysed whether the addition of temporal features is improving the accuracy of fire forecasting. The architecture used for processing sequential data of fire influencing vari

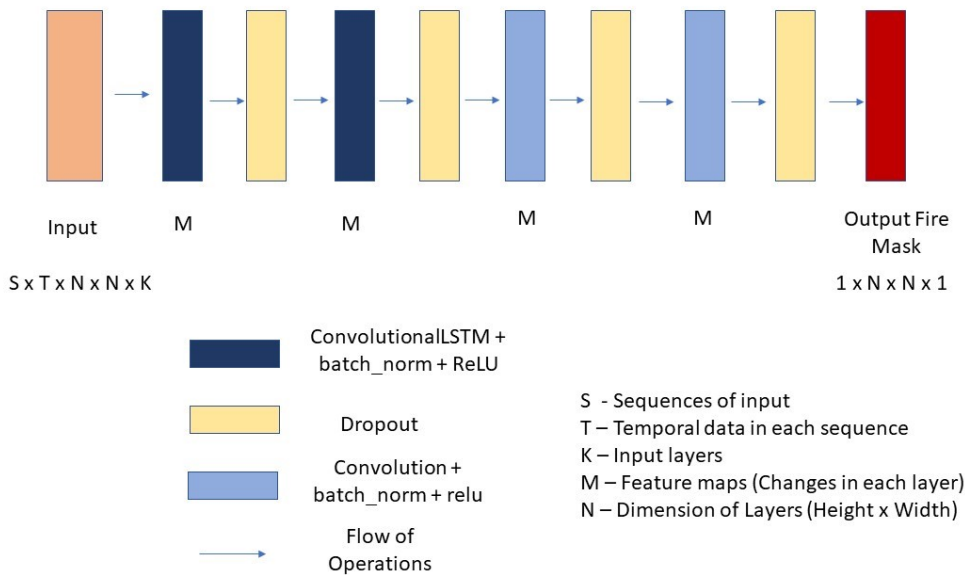


Figure 4-9: Convolutional LSTM architecture for active fire forecasting with sequential data

The architecture used for processing sequential data of fire influencing variables is shown in the Figure 4-9. As mentioned in the section 2.5.2.2 Convolutional LSTM cells have three gates in them namely forget gate, input gate and output gate. They regulate the flow of information from long and short-term memory states. The state operations are convolutional in convolution LSTM cell. Batch normalization (mentioned as `batch_norm` in the Figure 4-9) and non-linear activation function is applied then. A dropout layer is added to reduce overfitting of the model. Another series of layers of Convolutional LSTM, batch normalisation, non-linear activation and dropout is followed by a pair of convolutional 2D layers, batch normalisation, non-linear activation, and dropout layer. Finally, a convolution 2D layer with ‘sigmoid’ activation function is used to obtain the fire forecasting segmentation output. ‘Sigmoid’ function scales the input value to 0 to 1. ‘Adam’ is used as optimizer to optimise the loss function. Focal loss mentioned in the Equation 2-5 is used as loss function for this architecture.

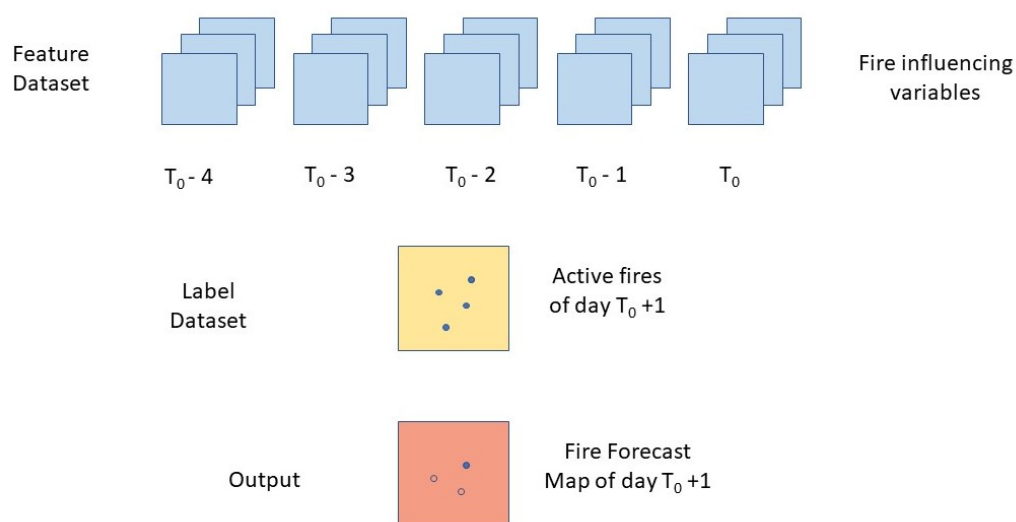


Figure 4-10: Fire forecasting scenario with data of sequential fire-influencing variables

The scenario followed to forecasting fire with sequential data of fire-influencing variables is shown in the Figure 4-10. The fire-influencing variables of the past five days is taken as feature dataset and the active fire in the next day is taken as label dataset. This scenario maps the evolution of historical data to find the relationship between them and the fire in the future.

4.4 Hyperparameter Tuning

Deep learning models and their basic structure, neurons generally fit a function between the input features and the corresponding label features. It can be represented with the following function.

$$f(x) = mx + c \quad (4.9)$$

In the above equation, x is the input variable and $f(x)$ is the corresponding output for the variable. ‘ m ’ and ‘ c ’ are called as weight and bias respectively. These values are learned in a process known as backpropagation. When lots of neurons get interconnected, it forms a neural network and each neuron learns these values. There are various operations performed to learn these values based on the task in hand

like convolution, maxpooling, dropout, etc. These operations have certain parameters which govern this learning process and there is no fixed value for those parameters. They are called as hyperparameters. These values are unique for each application and dataset. The function fits well when the hyperparameters are tuned for the task in hand. It has to be done carefully, by considering our dataset and objectives. Some of the hyperparameters considered in this study are mentioned in the Table 4.4. The model is trained with training data and ran with validation dataset to evaluate the hyperparameters. Hyperparameters with minimal loss value in validation data and maximum accuracy metrics is selected.

Table 4.4: Hyperparameters considered in the study and their description

Hyperparameter	Description
Learning rate	It is a constant value which determines the rate at which the weight value changes in between every epoch.
Number of feature maps in U-Net	Number of feature maps present in the encoder and decoder part of the U-Net which determines how well the contextual features can be learnt from the dataset.
Number of features in Convolution LSTM and Convolutional layer	Number of feature maps present in each convolutional LSTM and convolutional layer of the deep learning architecture which is built to deal with sequential data of fire influencing variables.
Batch size	Batch size determines how many input image patches are seen by the model in each step of the learning procedure to update the weight values. An increased batch size allows the model to learn from many features at a time also it will reduce the processing time but that requires huge computational power. A batch size of 1 will take one input image patch at a time and updates weight after processing it.
Gamma (Focal loss)	The gamma parameter is a non-negative integer in the focal loss function which determines how much the majority class samples are to be downweighted during loss value calculation. This will help the model to focus more on minority class.
Alpha (Focal loss)	Alpha value is a non-negative integer in the focal loss function which specifies the class-wise weight value.

4.5 Validating the model

The trained models with the selected hyperparameters are validated with the testing dataset. All the scenario tested are separate models and evaluated with the following metrics. These metrics are calculated to quantify the efficiency of the model to forecast fire. Overall accuracy normally used for image classification cannot be used in this case, since the distribution of non-fire and fire classes is highly imbalanced. The results will be biased towards negative (non-fire samples) if explained with overall accuracy. Therefore, some common metrics used in the case of imbalance dataset classification are used in this study for validating the model performance. Table 4.5 shows the confusion matrix for a binary classification. In the confusion matrix all the samples are classified under four groups based on their reference value and predicted value. A sample referenced as positive, if gets classified as positive class then it is called a True Positive (TP) sample. Otherwise, it is a False Negative (FN) sample. At the same time, a referenced negative sample if classified as negative class then it is True Negative (TN). Otherwise, it is a False Positive (FP) sample. In this study, all the models' output will be a continuous value from 0 to 1 and

it can be treated as probability of the event to occur. In this study, probability of fire to occur. A value greater than 0.5 is considered as positive.

Table 4.5: Confusion matrix for binary classification

Predicted value	Reference value		
		1	0
1		True Positive (TP)	False Positive (FP)
0		False Negative (FN)	True Negative (TN)

$$Sensitivity = \frac{TP}{TP + FN} \quad (4.10)$$

$$Specificity = \frac{TN}{TN + FP} \quad (4.11)$$

Sensitivity is the ratio of the true positives to the number of positive samples (sum of true positives and false negatives) given as reference. Sensitivity is also referred as recall. Specificity is the ratio of the true negatives to the number of negative samples (sum of true negatives and false positives) given as reference. These both metrics quantifies the ability of the model to classify the positive and negative samples given as reference. In other words, sensitivity and specificity can be referred as recall of Positive and negative classes respectively. Recall is given importance as it quantifies the proportion of samples classified correctly out of the given samples.

$$G - mean = \sqrt{Sensitivity * Specificity} \quad (4.12)$$

Equation 4.12 is the formula for calculating G-mean. It is also known as Kubat G-mean (Kubat & Matwin, 1997). This metric calculates the geometric mean of Sensitivity (True positive rate) and Specificity (True negative rate). G-mean value of less than 0.5 denotes the model's inability to classify any one of the class accurately. G-mean scores is a good representation for taking minority class into consideration while validating the model (Johnson & Khoshgoftaar, 2019)(Hu et al., 2015).

$$Class\ Balance\ Accuracy^+ (CBA^+) = \frac{TP}{\max(TP + FP, TP + FN)} \quad (4.13)$$

$$Class\ Balance\ Accuracy^- (CBA^-) = \frac{TN}{\max(TN + FN, TN + FP)} \quad (4.14)$$

$$Class\ Balance\ Accuracy = 0.5 (CBA^+ + CBA^-) \quad (4.15)$$

Class balanced accuracy is a combined metric calculated for both majority and minority class separately. This shows the overall assessment of the model's predictive power. The denominator in each class takes

either of the maximum sum, therefore acting as a conservative metric for accuracy calculation (Mosley, 2013). All metrics have a range of values between 0 and 1. Values closer to 0 indicate low accuracy, while values closer to 1 indicate high accuracy.

4.6 Building user interface for fire forecasting

Final stakeholder for this fire related analysis in the state of Uttarakhand is the Forest department officials. It will be helpful if pre-fire alerts are provided on time to them. It will guide them to allocate resources properly. A proper dissemination of fire forecasting has to be done to meet the requirements in time. There are various web frameworks and applications are available. In this study, Greppo, a python package for publishing web application is used (Krishnan & Tangirala, n.d.). It is a web application framework built with JavaScript and other python libraries. The speciality of this application is that the user interface can be designed using simple python functions itself. It is especially designed for disseminating data analysis studies performed in Python. The steps to be followed to create a web application in local system is shown in Figure 4-11. The application can also be hosted in a web server which has necessary python packages.

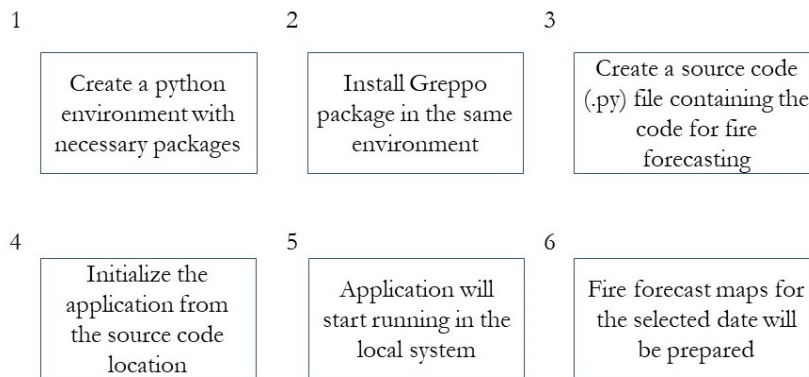


Figure 4-11: Steps to create fire forecast maps in the web application

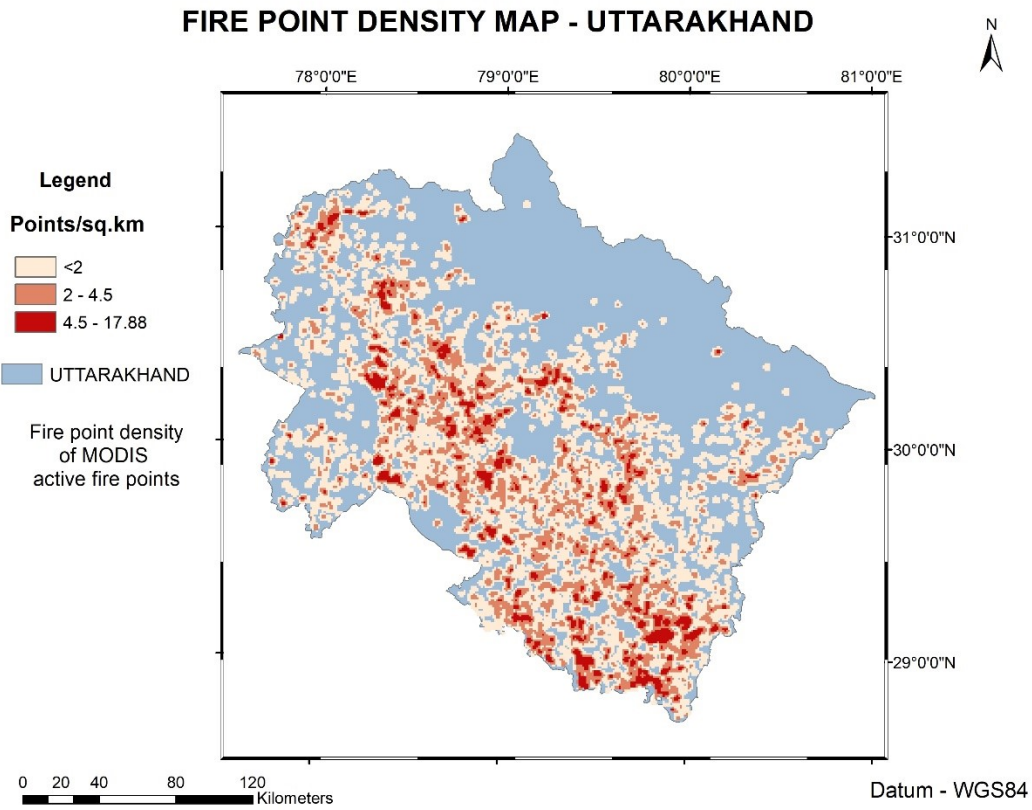


Figure 5-2: Fire point density map of Uttarakhand

The map in Figure 5-2 is a fire point density map of Uttarakhand state prepared from the fire points of 2016 to 2021. It accurately describes how frequently fires occur in various parts of the state. From this density map, it can be inferred that the fire point analysis is inevitable in the hotspot locations as it affects the flora and fauna present there. This is a critical input for forest management officials as this map guides them in performing surveillance activities, clearing dry vegetation, and management of their resources.

5.1.2 Fire point distribution in different Terrain features

5.1.2.1 Elevation

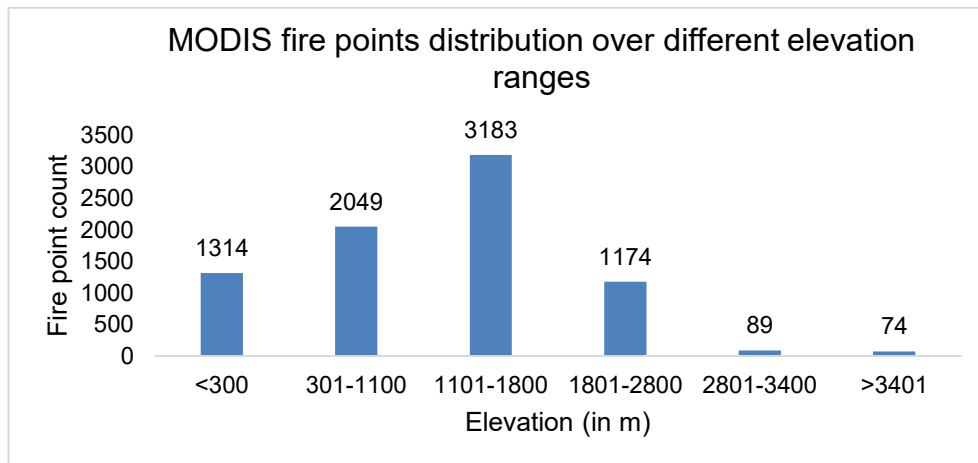


Figure 5-3: MODIS Fire points distribution over different elevation ranges

The distribution of fire points over different elevation ranges is shown as a bar graph in Figure 5-3. MODIS active fire points from 2016 to 2021 are used to prepare this graph. This graph shows that the fire points count increases as the elevation range increases, and beyond 1800m elevation, the fire points count decreases. This can be linked with the fire point distribution map shown in Figure 5-2. Also, the distribution of fire points in the lower elevation is interlinked with the land use and land cover characteristics present in those elevation ranges. The Land use and land cover map of Uttarakhand in Figure 3-5 and the topography map of Uttarakhand in Figure 3-2 show the relationship between the land use land cover features and the elevation. Agriculture and deciduous broadleaf classes are common in the lower elevation <300m and 300 – 1100m. This shows the fire activities in agricultural fields and forests. In the elevation range of 1100 – 1800m, broadleaf, and needleleaf forest classes are common, showing the presence of vegetation for fire to occur. Dry needles of pine trees are highly flammable in nature and the trees are common in the elevation range of 1100 – 1800m (Chauhan, 2010). This shows the increased fire activity in that elevation range.

5.1.2.2 Slope

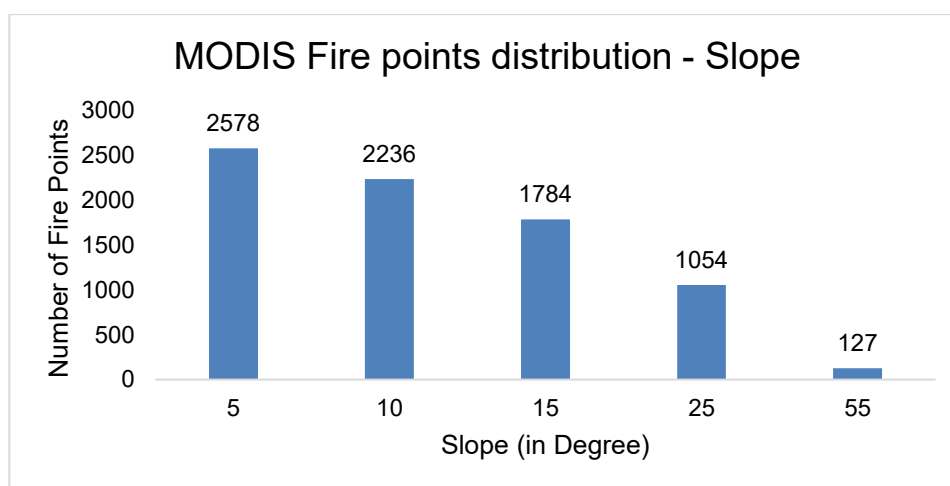


Figure 5-4: MODIS Fire point distribution in different slope conditions

The number of fire points distributed over different slope conditions is depicted in the bar graph shown in Figure 5-4. A slope of 0° denotes flat terrain and the steepness increases towards 90° denoting a vertical structure. It can be inferred that the trend of fire count decreases gradually as the slope increases. Slope can act as a proxy to understand the anthropogenic cause of fire initiation. Human activities, such as farming, camping, and cattle grazing is more common in plain areas or areas with little slope. Hence, slope layer when used in fire related studies give information about the human influence on fire.

5.1.2.3 **Aspect**

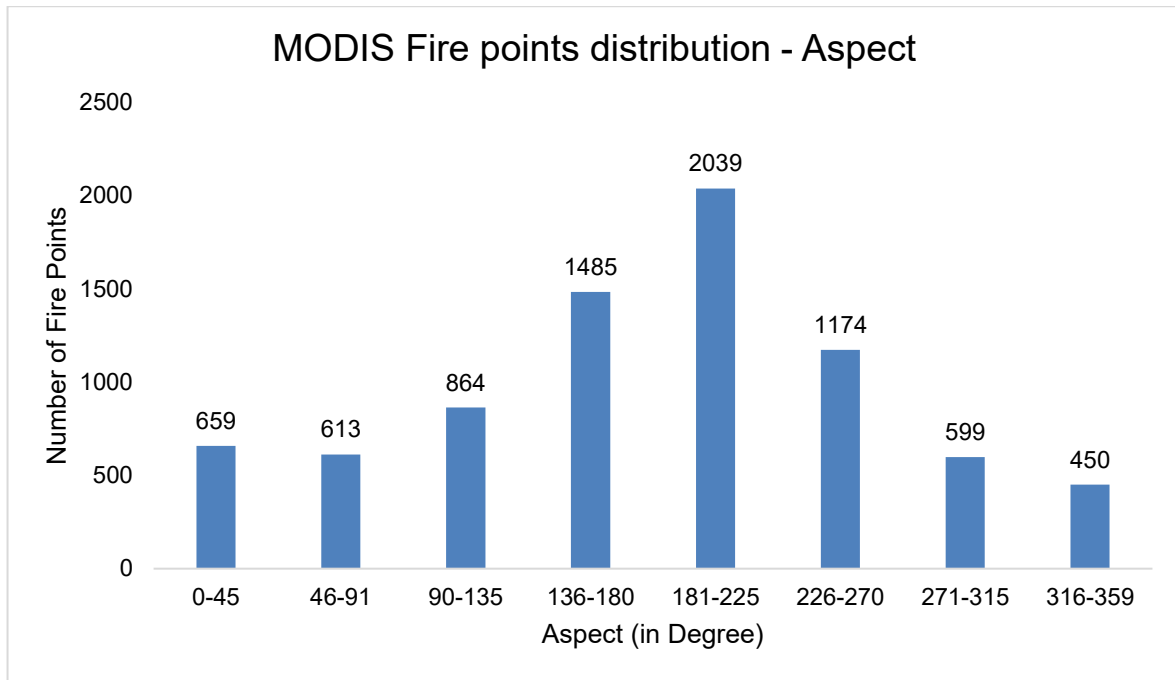


Figure 5-5: MODIS fire points distribution on different aspect (slope directions)

The bar chart in Figure 5-5 depicts the distribution of MODIS fire points on different aspect ranges (slope direction). The aspect is denoted in degrees where 0° is towards North, 90° is East, 180° is South and 270° West. This is shown in Figure 2-2. It can be inferred from the graph that the fire point distribution is high between 136° to 270° range. These values denote the slope direction of South East to South West and West in ground. This increased fire activity in the southern slope of Uttarakhand can be attributed to the increased solar radiation on these regions. During summer, southern side of the mountain receives more sunlight than the northern slope. Therefore, the temperature is high and the vegetation in southern slope gets dried quicker when compared to the northern slope. This shows the importance of aspect in the state of Uttarakhand for fire analysis.

These analysis on fire point distribution shows that the fire regime in the state of Uttarakhand is strongly influenced by the terrain features and the accompanying land use and land cover features.

5.2 Meteorological data comparison

Two sources of meteorological data are available for the study area. Ground meteorological station and ERA5 Reanalysis data from ECMWF available in GEE. But the continuous availability of data for the whole study area and for the whole study time is necessary for utilizing them in the analysis effectively. Ground station points are not available for all the years in the study. The ground station data for meteorological variables is available from 2018 for Uttarakhand. Till 2018, approximately only 20 stations were present the whole state. This poses a serious risk. A data analysis is done to check the reliability of the station data with those 20 stations. Maximum temperature variable of a day (07/04/2018) is selected for all the stations and interpolated for the whole state using ‘Kriging’ method. Figure 1-6 shows the maximum temperature map for the state of Uttarakhand overlaid by the station points.

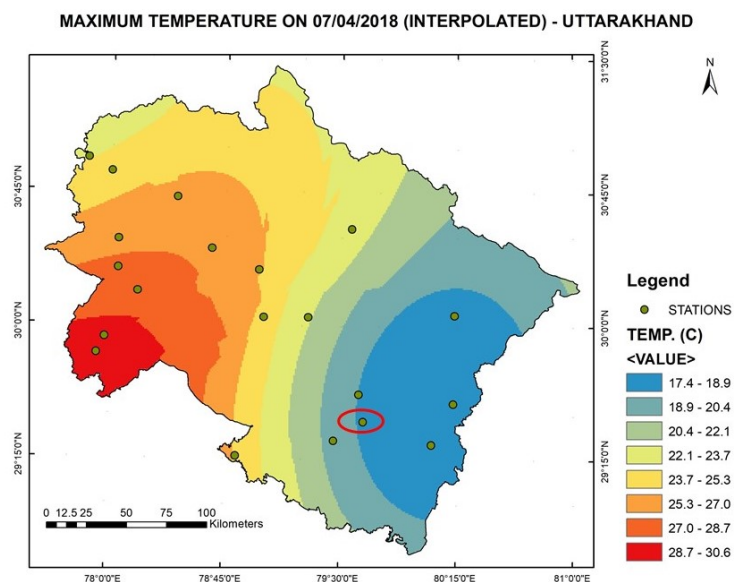


Figure 5-6: Interpolated maximum temperature on 07/04/2018 from ground station data

The station point which is marked with red circle in the Figure 5-6 is Mukteshwar ground observation station located in the district Nainital, Uttarakhand. The actual ground-based observation of maximum temperature for that day is 5.7 °C but the interpolated value is in the range 17.4 – 18.9 °C. This demonstrates the amount of error between the ground observed value and the interpolated value. At the same time from mid-September of 2020, ground station data from approximately 105 stations are available for each day. But this doesn't match with the study time period. Interpolated maximum temperature on 07/04/2022 for the state of Uttarakhand from ground station data is prepared using 'Kriging' method and shown as map in the Figure 1-7. From this figure it can be noted that the temperature values are changing in accordance with the elevation change. This is the ground nature which is not the same for the maximum temperature map of 07/04/18. Therefore, interpolated maps from 2018 cannot be used for further analysis.

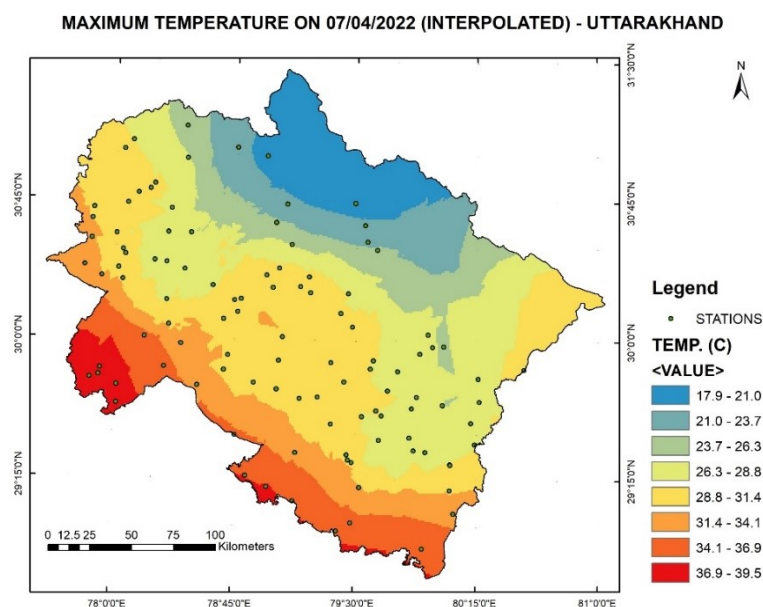


Figure 5-7: Interpolated maximum temperature on 07/04/2022 from ground station data

5.2.1 Correlation analysis

In order to find the relationship between the ground station observations and ERA5 reanalysis data for the state of Uttarakhand, correlation analysis is performed for the year 2021 with station having data for all the 365 days. Pearson correlation coefficient (r) is calculated for the two datasets. It ranges between -1 to 1 which denotes the direction and magnitude of linear relationship between the two variables (Mistry et al., 2022). A positive value towards 1 denotes a positive relationship between the variables and value near to -1 denotes a strong negative relationship. A value of 0 denotes no relationship between the variables.

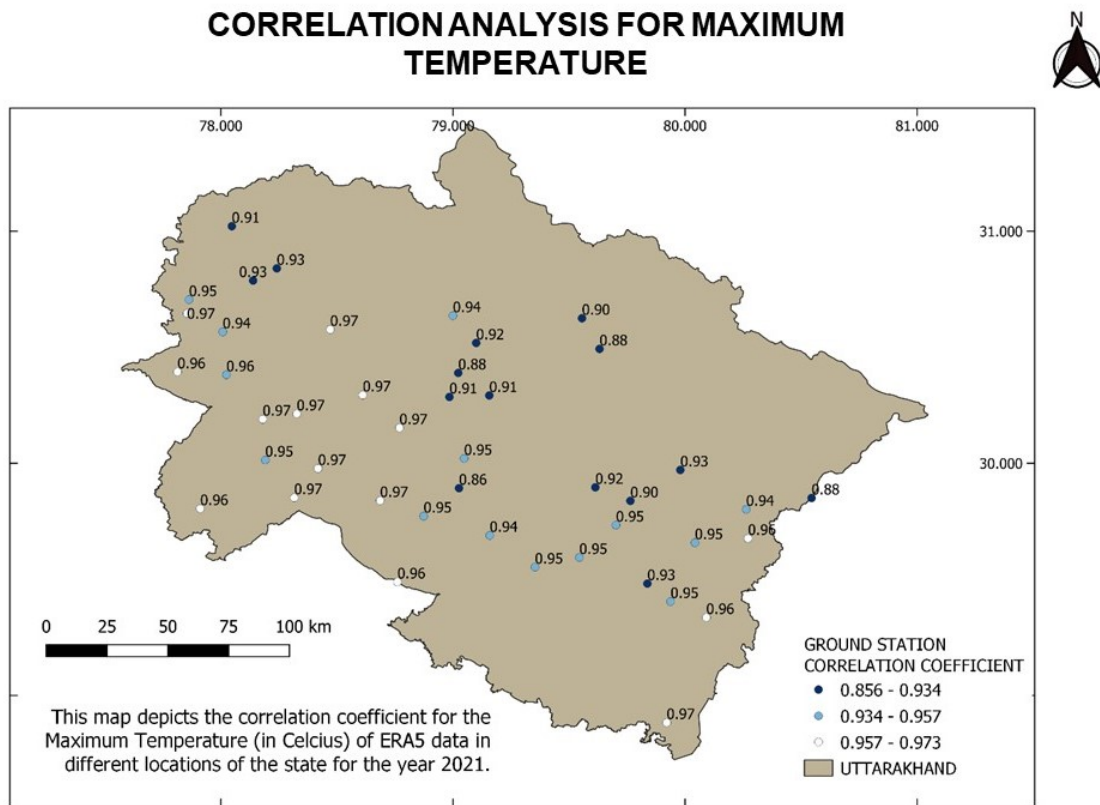


Figure 5-8: Correlation analysis between ERA5 and ground station data for Maximum temperature for 2021

From the legend of the map shown in Figure 1-8, it can be inferred that the minimum value of the correlation coefficient is 0.856. This shows that all the stations' values are strongly correlated with their ground station counterparts. The high correlation coefficient value signifies that the trend of maximum temperature value in ERA5 reanalysis data is matching with the data monitored from ground stations.

5.2.2 RMSE Analysis

Root Mean Square Error (RMSE) value is commonly used measure to find the change in value of a predicted value and the actual value. In this analysis, ground station data is considered as actual value and the ERA5 value is compared against it. The analysis is performed for 2021 maximum temperature variable. From the map shown in the Figure 1-9, it can be inferred that the RMSE value ranges between 1.2 – 10.5 °C. Maximum of the stations in lower elevation range has smaller RMSE values. The stations in higher elevation are having high RMSE values. This high RMSE is possible because there are fewer stations in

higher elevation regions. It is because the ERA5 Reanalysis data is also prepared with the combination of various models' output, satellite data and ground observation data. However, the RMSE value is relatively low in the lower elevation region, where the study of fire is more concentrated. Therefore, ERA5 data can be used as an alternative instead of ground station data for studies involving meteorological data.

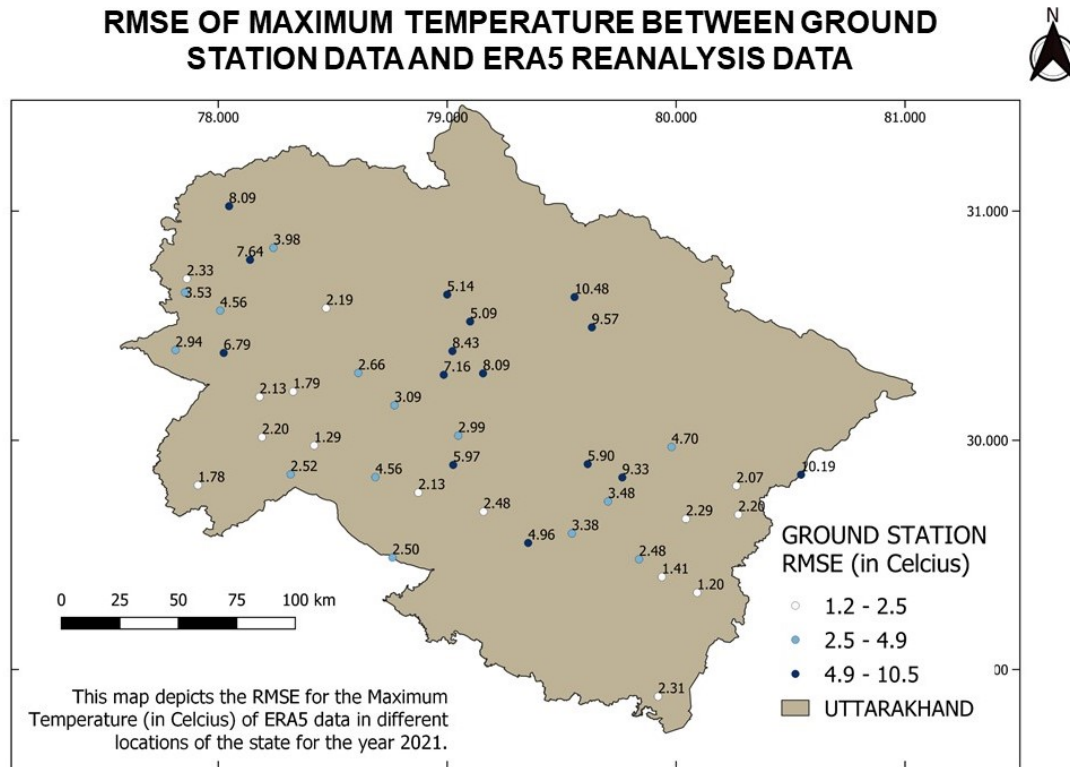


Figure 5-9: RMSE value of Maximum temperature between ground station data and ERA5 reanalysis data

5.3 Fire forecasting models

Fire forecasting models built with non-sequential and sequential data of fire influencing variables are discussed in this section. Model training, hyperparameter tuning, quantitative and qualitative analysis of the results are discussed in the following sections.

5.3.1 Model for fire forecasting with single day fire influencing variables

Fire forecasting with non-sequential data is performed with fire influencing variables of single day for three different scenarios. Each scenario is formulated to analyse the influence of a single day fire-influencing variables for fire in the future. The basic structure of the model is taken from U-Net and altered to match the need for the study's objective. Stratified sampling technique is performed to select training and testing dataset as two different patches in the study area.

5.3.1.1 Training and hyperparameter tuning

In all the three scenarios of fire forecasting, fire influencing variables' data is taken for the years 2016 to 2020 for training and the data of 2021 is used for hyperparameter tuning. The patches for the modelling are of size 128 X 128 and the total number of input features are 32.

5.3.1.1.1 Fire forecasting for next day

Table 5.1: Patch count and number of fire and non-fire pixels in training and validation set for forecasting fire of next day

	Patch count	Fire pixel count	Non-fire pixel count
Training set	1,747	6,541	2,86,16,307
Validation set	349	1,730	57,16,286

The information about the patch count, fire and non-fire pixel distribution in training and validation set is mentioned in the Table 5-1. It can be evident from the above table that even after the stratified sampling of patches, the fire and non-fire pixels are highly imbalance. The ratio of fire and non-fire pixels in training and validation set are 1: 0.0002 and 1: 0.0003 respectively. The hyperparameters mentioned in the Table 4.4 are experimented for different values to prepare the model.

Table 5.2: Hyperparameters and the experiment values

Hyperparameter	Values
Learning rate	0.0001, 0.00001
Feature Maps	[32,64,128], [64,128,256], [16,32,64,128]
Batch size	32, 64
Gamma	2, 10, 50, 100
Alpha	0.25, 0.9, 1000, 1500

Hyperparameters are experimented in a trial and error method and the best hyperparameter is selected based on the model's performance on the validation dataset. The performance of the model is evaluated by using the accuracy metrics and also visual comparison of outputs. The trial and error methods are followed by considering the dataset resolution, the extent of influence of fire in the study area and the imbalance nature in the fire and non-fire classes. Three strategies are framed for selecting best hyperparameter for forecasting fire of next day.

Strategy 1 - Addressing imbalance in dataset

Since the dataset is of highly imbalance in nature, binary focal loss function is selected as the loss function. The binary focal loss function itself has two hyperparameters, which denotes the majority class downweighting parameter and minority class upweighting parameter. First these parameters are given importance for learning. The other parameters' values are selected based on results from other studies. Learning rate of 'Adam' optimizer is initialized with 0.0001 (Huot et al., 2022), batch size of 32, and number of filters in encoder part of U-Net is selected as [64, 128, 256]. The corresponding decoders are also provided the symmetrical number of filters. Activation function in convolutional layers are 'ReLU' and in the final segmentation layer it is 'Sigmoid'. Dropout layers are added after each convolution layer. The percentage of dropout is proportional to the filter size. In the encoder part of the U-Net architecture, the order of dropout values assigned for each block is 0.05, 0.1, 0.15. These values represent the percentage of neurons which will be turned off randomly to reduce overfitting in the model. The models with these hyperparameter values are run for 100 epochs with early stopping parameter monitoring the validation loss with patience value of 10 epochs. Whenever there is no improvement in validation loss value continuously for the 10 epochs, the model will stop the learning process.

Table 5.3: Hyperparameter search for focal loss function

Alpha	Gamma	TP	FN	FP	Recall	CBA	Inference
0.25	2	17	1,713	20	0.01	0.505	Predicting most of the pixels as non-fire.
0.25	10	15	1,715	43	0.009	.504	Predicting most of the pixels as non-fire
0.9	2	23	1,707	465	0.013	.506	Not able to differentiate fire and non-fire pixels
0.9	10	18	1,712	890	0.01	.505	Predicting all the pixels as non-fire
0.9	50	87	1,643	1,215	0.05	.525	Predicting all the pixels as non-fire

From the observations in Table 5.3, it is observed that when the alpha value is changed between 0.25, and 0.9 and gamma values between 2, 10, and 50, the model is not able to identify fire pixels. All the pixels are predicted as non-fire because of the severe imbalance characteristic. Therefore, the strategy has to be changed to tune the batch size and filter count of U-Net encoders as well along with change in alpha and gamma values. The accuracy metrics mentioned in the Table 5.3 are the values obtained for the validation set.

Strategy 2 – Changing the network architecture

In this step, filters in the U-Net encoder are changed along with the change in alpha and gamma values. The filter count selected for this strategy is [16,32,64,128]. Batch size is also experimented with 32 and 64 in this strategy.

Table 5.4: Observations of hyperparameter tuning while changing the network architecture

Batch size	Alpha	Gamma	TP	FN	FP	Recall	CBA	Inference
32	0.25	100	600	1,130	4,15,455	0.347	0.464	Recall is best out of all the experiments. But, more false positives.
64	1000	0	428	1,302	2,85,689	0.247	0.476	False positives are comparatively less, and recall is 0.27.

From the observations in the Table 5.4, it is evident that either the change in batch size, alpha, gamma in focal loss function, or the filter count in U-Net encoder has its impact on the increase in recall value and the smaller number of False positives.

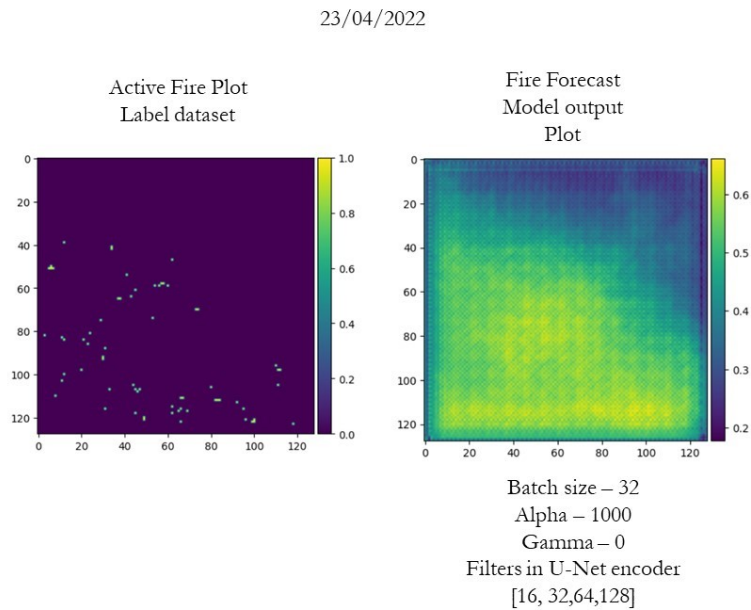


Figure 5-10: The Active fire plot and the corresponding day's forecast plot for 23/04/2022

The model is able to predict the locations of fire by assigning higher probability values to those locations, as seen in Figure 5-10. Additionally, it can be noticed that the prediction plot contains grid-like structures, which need to be smoothened.

Strategy 3 – Changing U-Net network architecture and alpha value of focal loss function.

As per the equation 2.5, when the gamma value in equation is set 0, the equation will be transformed into a weighted binary cross entropy loss function. This function can also be used for training models with imbalanced label distribution. Therefore, in this strategy alpha value is kept constant as 1000, gamma is assigned as 0 and tested. Filters in U-Net architecture is set in the order [32, 64, 128]. These network parameters are changed to observe the difference in accuracy metrics.

Table 5.5: Hyperparameter tuning observations while changing alpha value and the U-Net network architecture

Batch size	Alpha	Gamma	TP	FN	FP	Recall	CBA	Inference
32	1000	0	624	1,106	2,11,052	0.361	0.483	Recall and CBA are best out of all the experiments.

23/04/2022

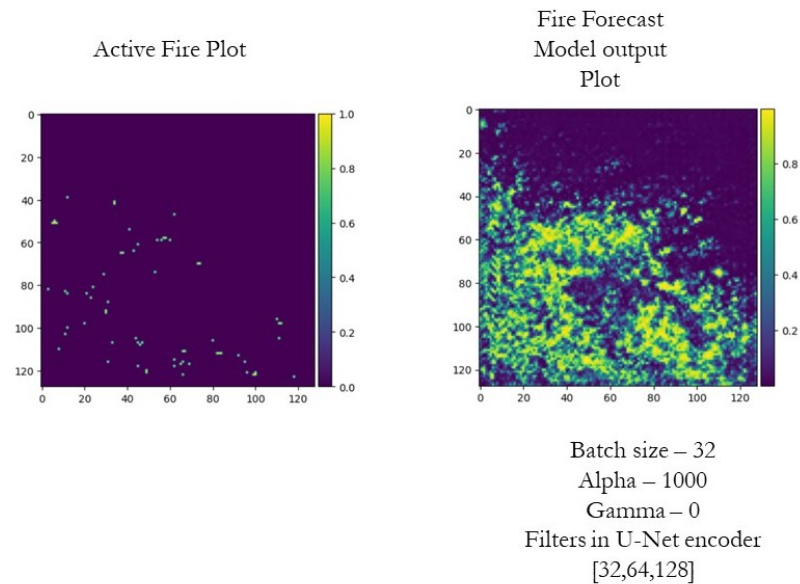


Figure 5-11: The active fire plot and fire prediction plots with tuned alpha and neural network architecture

Fire forecast plots for the next day with updated alpha value for the binary focal loss function and the U-Net network architecture is shown in Figure 5-11. When compared with the Figure 5-10, it can be inferred that the fire forecast plots with updated hyperparameters are good in approximating the fire locations. The accuracy metrics of the model with updated hyperparameters are also improved than the previous ones. Learning rate of 0.00001 is tried with this model, which shows the model’s inability to learn features. Therefore, 0.0001 is selected as learning rate parameter. This updated U-Net encoder has [32, 64, 128] number of filters in each block of encoder and corresponding decoder blocks. Two encoder and two decoder blocks with a single bridge block will be suitable for the study as the resolution of the data is less and the problem in hand doesn’t require higher receptive fields. Higher number of encoder and decoder blocks yield higher receptive fields. Batch size is fixed to 32, alpha as 1000, and gamma as 0. These hyperparameters are selected for forecasting fire for next day.

5.3.1.1.2 Fire forecasting for next two days

For the two days and five days fire forecasting, label data is aggregated accordingly and matched with the corresponding feature dataset. The number of patches, fire and non-fire pixels in training and validation dataset for forecasting fire of next two days are mentioned in the Table 5.6.

Table 5.6: Patch count and number of fire and non-fire pixels in training and validation set for forecasting fire of next two days

	Patch count	Fire pixel count	Non-fire pixel count
Training set	1,742	12,419	2,85,28,509
Validation set	348	3,251	56,98,381

It is evident from the hyperparameter tuning performed for scenario 1 that, the model is able to learn the fire forecasting problem, even though there is huge class imbalance. The focal loss function used in the model, helps to learn the problem effectively. In the fire forecasting scenario of next two days and next

five days, the hyperparameters selected for scenario 1 are used except the class weighting parameter in focal loss function ‘ α ’. ‘ α ’ will be tuned to find the sensitivity of the model for that parameter.

Table 5.7: Sensitivity of two days fire forecasting model for different alpha values and accuracy metrics

Alpha	TP	FN	FP	Recall	CBA
1500	1,341	1,910	7,55,434	.41	0.4350
1000	1,233	2,018	6,97,778	0.38	0.44
500	1,593	1,658	3,52,647	.49	0.471
100	63	3,188	22,734	0.02	0.49

From the Table 5.6, it can be inferred that with decrease in alpha value, there is increase in True positive and also decrease in false positive. For value less than $\alpha = 500$, True Positives are drastically reducing. Also, $\alpha = 500$, yields the highest recall value and second highest CBA score.

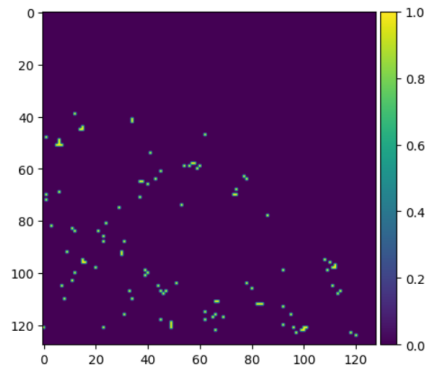


Figure 5-12: Aggregated active fire plot of 23/04/2022 and 24/04/2022

The plot in Figure 5-13, is the aggregated active fire points for the Patch 1 of study area. This particular day is selected to show the sensitivity of the model prediction on a day in fire season for different ‘ α ’ values.

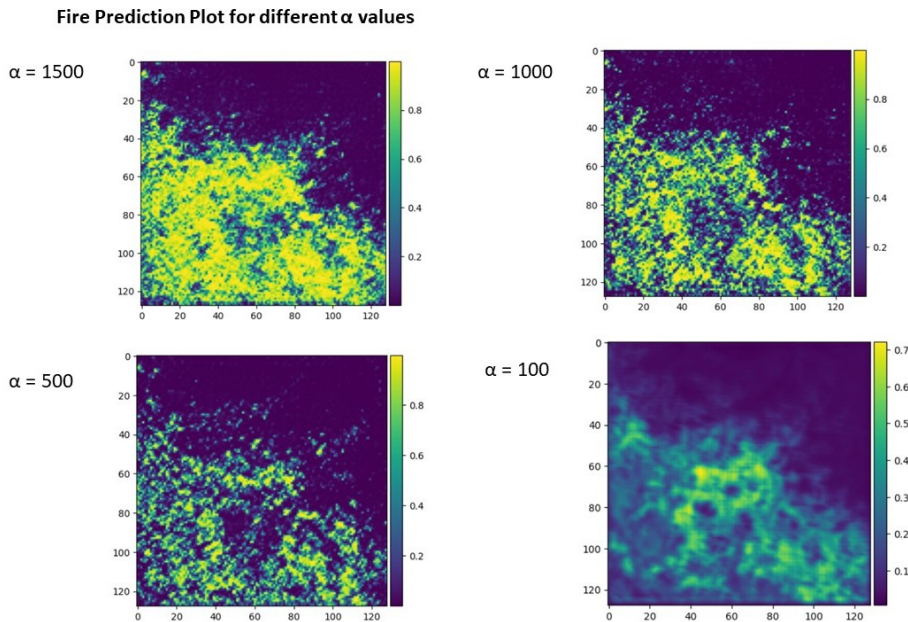


Figure 5-13: Fire prediction plots for the dates 23/04/2022 and 24/04/2022 for different alpha values

The plots in Figure 5-14 shows the estimation of fire probability with respect to change in ‘ α ’ in the focal loss function. As it is observed quantitatively from the Table 5.6, it can be visually seen in these plots that the overestimation of fires is evident in larger ‘ α ’ values. Comparatively, ‘ α ’ = 500 gives visually good results. Even though the model with ‘ α ’ = 100 has highest CBA score, the predictions are having less probability values for the entire patch compared to the other plots. This shows the model with ‘ α ’ > 100 will give higher accuracy in this scenario. Therefore, ‘ α ’ is fixed to 500 for this scenario. The other network parameters are same as the ones used for building the model for forecasting next day’s fire (scenario 1).

5.3.1.1.3 Fire forecasting for next five days

As mentioned in Scenario 3, the fire pixels of the next five days are aggregated and used as segmentation mask in this scenario. Number of patches used for this study, fire and non-pixels in those patches are mentioned in Table 5.8.

Table 5.8: Patch count, number of fire and non-fire pixels in five day forecast training and validation label dataset

	Patch count	Fire pixel count	Non-fire pixel count
Training set	1,727	31,467	2,82,63,701
Validation set	345	8,091	56,44,389

In this scenario also, only the ‘ α ’ is to be analysed to find the sensitivity of the model and all the other hyperparameters are same as used for the other two models. It can be inferred from Fire pixels count of Table 5.8 that it is approximately five times higher than the number of fire pixels in fire forecasting for next day scenario. This shows a reduction in imbalance nature of label dataset. Therefore, reducing ‘ α ’ will yield optimal results.

Table 5.9: Sensitivity of five days fire forecasting model and accuracy metrics

Alpha	TP	FN	FP	Recall	CBA
1000	7,067	1,024	18,08,539	.87	0.342
500	5,776	2,315	11,70,005	.71	0.4
250	4,151	10,361	6,32,434	.48	0.447

The sensitivity of the model for different ‘ α ’ values in focal loss function along with the corresponding accuracy metrics is shown in Table 5.9. Even though the model has high recall values in higher ‘ α ’ values, False Positives is very high. This can be evident from the CBA score. Therefore, the model with higher CBA value is selected.

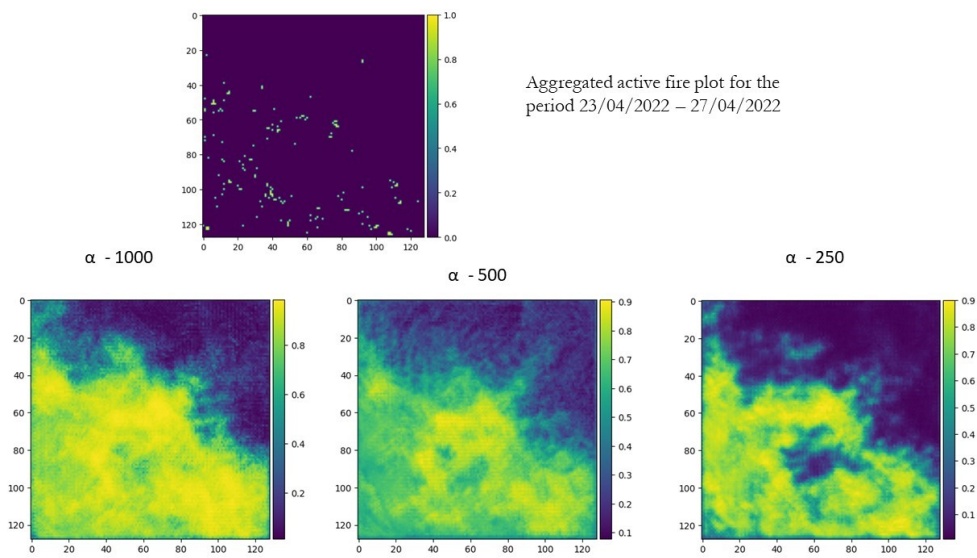


Figure 5-14: Fire forecasting plots for the next five days with different alpha values in focal loss function

Fire forecasting plots for the next five days along with the fire mask is shown in Figure 5-14. All the models are able to find the locations of fire but, overestimation is very high when ‘ α ’ is equal to 1000, which will not be suitable for operational fire forecasting management activities. Comparison of the accuracy metrics and fire forecast plots shows that, ‘ α ’ = 250 is the optimal value for this model.

5.3.1.2 Quantitative analysis

Models with best hyperparameters for fire forecasting are selected and evaluated and their results are discussed in this section. The models’ efficiency to forecast fires is compared using the validation metrics mentioned in Section 4.5. Patches prepared from the years 2022 and 2023 are used for testing the model accuracy. Number of patches, fire and non-fire pixels in testing dataset for all three scenarios of fire forecasting models are mentioned in Table 5.10.

Table 5.10: Number of patches, fire and non-fire pixels in testing dataset

Scenario	Patch count	Fire pixel count	Non-fire pixel count
One day forecast	602	1,639	98,61,529
Two days forecast	600	3,251	98,27,149
Five days forecast	594	8,042	97,24,054

From Table 5.10, it can be inferred that the fire pixel count gradually increases from scenario 1 to scenario 3. Aggregation of fire pixels has resulted in it. This will have an impact on the model feature learning process as well. This can be attributed to the decrease in imbalance between fire and non-fire pixels due to aggregation of fire pixels. Estimated predictive model accuracy for three different fire forecasting scenarios with single day fire-influencing variables is shown in the following tables.

Table 5.11: Estimated predictive model accuracy based on sample counts for all the scenarios of fire forecasting models

Scenario	True Positive	False Negative	False Positive	True Negative
One day forecast	478	1,161	3,12,225	95,49,304
Two days forecast	1,147	2,104	4,21,234	94,05,915
Five days forecast	3,869	4,173	8,54,807	88,69,247

In Table 5.11, model accuracy is shown with the sample counts of true positives, true negatives, false positives, and false negatives. Since, each model has different number fire-pixels in it, the models cannot be compared with their TP and FN counts. The accuracy metrics in Table 5.12 shows the difference in the model accuracy through recall, specificity, G-mean, and CBA scores. As they are calculated as the ratio of the TP, FP, FN, and TN counts, they are compared.

Table 5.12: Estimated predictive model accuracy based on recall, specificity, G-mean, CBA for all the scenarios of fire forecasting models

Scenario	Recall	Specificity	G-mean	CBA
One day forecast	0.29	0.97	0.53	0.485
Two days forecast	0.35	0.96	0.58	0.48
Five days forecast	0.48	0.91	0.66	0.46

From the metrics it can be inferred that, recall values increase as the time lead to forecast fire increases. This shows that the model built for two- and five-days fire forecast can accurately predict the fire points than the model built for next day fire forecast. This can be attributed to the smaller number of fire pixels in training set in the model for scenario 1. Even though the focal loss function was applied to increase the weight of fire class, the model's ability to correctly predict the fire points is less. At the same time, specificity of the model decreases with increase in time lead. This shows that the true negatives are correctly classified in the model which predicts next day's fire than the next two- and five- days forecast ones. Also, it can be inferred from Table 5.11 that, False Positives increases with increase in time lead of fire forecast. This shows that the model has given more weightage to fire pixels and given more importance to the classification of fire pixels which leads to a higher number of false positives. G-mean behaves the same as recall, that with increase in time lead for fire forecast, G-mean also increases. Since, G-mean is the square root of the product of recall and specificity. Though there is a decrease in specificity value in the models, the magnitude of change in recall is more. Therefore, G-mean increases with the increase in time lead of fire forecasting.

$$Precision = \frac{TP}{TP + FP} \quad (5.1)$$

CBA⁺ is calculated based on the formula given in Equation 4.13. This takes either the sum of TP and FN or TP and FP whichever is maximum. CBA⁻ is also calculated by following a similar approach. This particular design of formula always increases the denominator thereby acting as a hard prediction accuracy metric. From our models' accuracy metrics, it can be observed that the count of false positives is high. A model having lower number of false positives will have a good CBA score. Therefore, this metric will provide a good understanding about a model's performance to assess the accuracy of both fire and non-fire pixel classification. From Table 5.12, it can be observed that the model to forecast fire of next day ranks first in CBA score.

5.3.1.3 **Qualitative analysis**

Fire forecasting is carried out with the selected models for all the three scenarios and the corresponding output are discussed in this section. The dates for analysis are selected based on the terrain, and land use and land cover characteristics for the particular patch. In patch 1 as shown in Figure 4-5, the dates are selected as end of January and Mid-April. End of January is the offset time of Winter and Mid-April is the forest fire season in the state. The dates are selected from testing dataset. The models are used to forecast fire for those patches and the results are visualized along with Elevation plot and LULC of the patches.

5.3.1.3.1 **Next day fire forecasting model output plots**

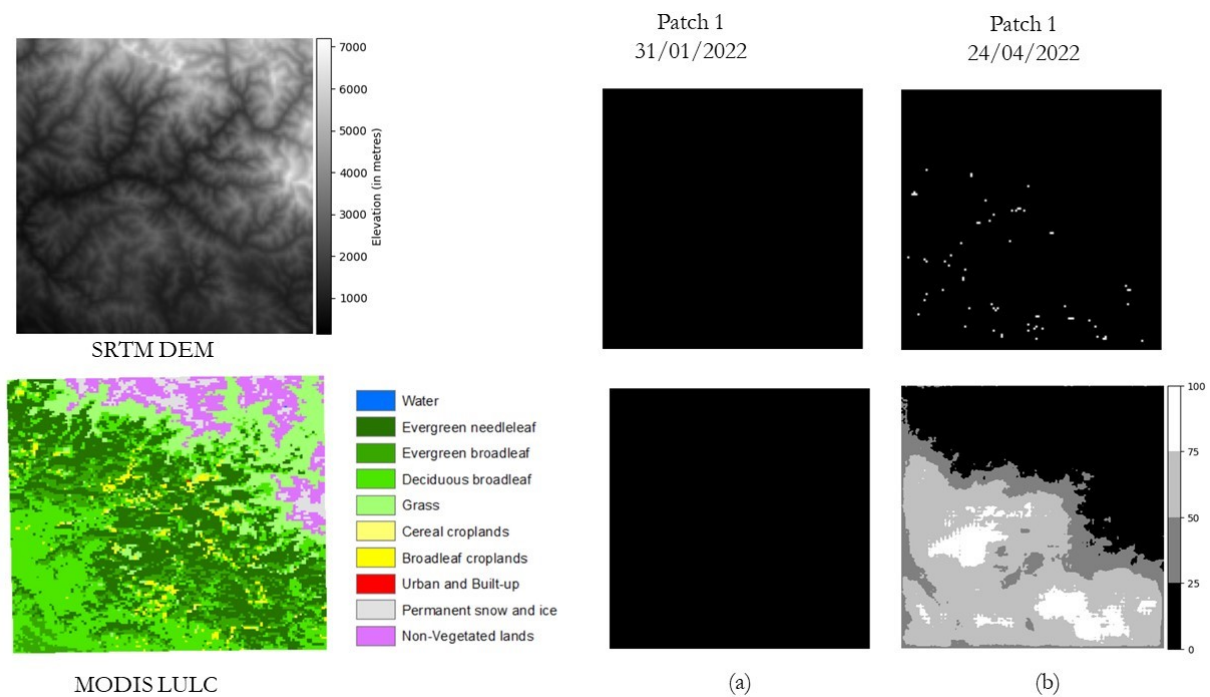


Figure 5-15: Next day fire forecasting scenario's active fire reference plots and model output plots. Terrain and Land use land cover plots of patch 1. (a) End of Winter, (b) Forest Fire season

In Figure 5-15, (a) and (b) are the fire patches where model forecasts are performed. The plots in top row are the active fire plots for corresponding dates. The plots in the second row are the fire forecast outputs. The forecast plots are plotted with values ranging from 0 to 100. The output of model was from 0 to 1, as the final activation function in the models are 'sigmoid' which scales the value to 0 and 1. The final output score from sigmoid activation function is scaled to 0 and 100 for interpreting that as percentage of probability. Value of 100 denoting high probability of fire and 0 denoting no-fire. The output of fire forecasting models is categorized into four different classes from 0 to 100. This has been performed to understand the scores provided by the model. A threshold applied at any particular value, will not give a complete understanding of the model. From the plot (a), it can be inferred that the model performed well for that day, predicting 0 – 25% for all the pixels. Since, that was a winter day, there was no actual fires as well. From the plot (b), it can be seen that the model is able to give high scores for actual fire locations. At the same time, there are a greater number of pixels with model prediction score greater that 50%. From this output plot, it is evident that the models are predicting higher than actual number of fire pixels,

leading to increased false positives. This can also be attributed the fact that, the pixels which are actually not burnt, may also be having dry inflammable materials except the fire initiation agents. From the plot (b) it can be seen that the fire prediction is high for areas in southern parts. These regions are having higher proportion of deciduous and evergreen broadleaf, and evergreen needleleaf trees. This shows that the model has identified all the regions where fire can be possible and given high score to certain locations.

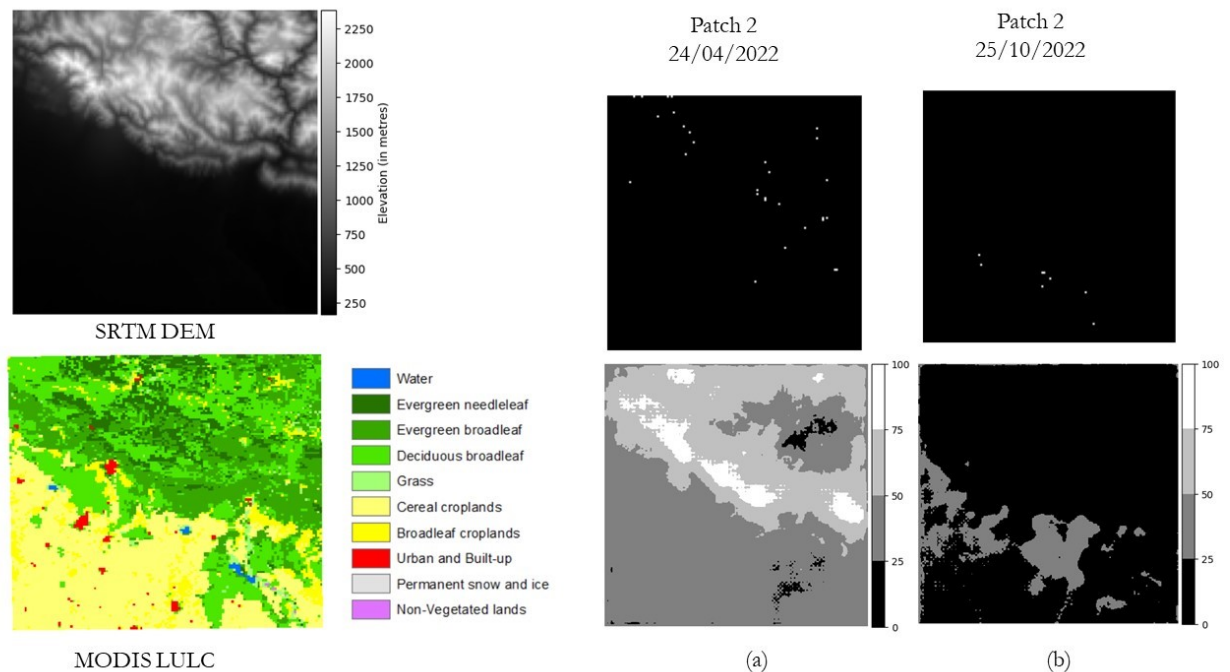


Figure 5-16: : Next day fire forecasting scenario's active fire reference plots and model output plots; Terrain and Land use land cover plots of patch 2. (a) Forest Fire season (b) Agriculture residue burning season

Elevation, MODIS LULC, actual active fire plots and fire forecast output plots for patch 2 of the study are shown in Figure 5-16. In the plot (a), the model has given higher scores for the forest cover and predicted most of the active fire pixels as well. Almost all the pixels in the plot are having fire values greater than 25%. This can be due to the dry weather conditions on the season. In the plot (b), fire predictions with value in the range of 25 – 35 is evident. The southern region in patch 2, is dominated with agricultural land. From this it can be inferred that the model has learned about the agricultural fires also from the dataset.

5.3.1.3.2 Next two days fire forecasting model output plots

In this section, the fire forecasting outputs for next two days are shown for the two study patches along with elevation, LULC, and reference plots. The plots in top row of (a) and (b) of Figure 5-17 are active fire points aggregated for those two dates and plots in bottom row are the fire forecast plots for those days. From the fire forecast plot of (a), it can be observed that there are some pixels with score between 25-50. Since, the time period is end of winter (31st January and 1st February), there is less chance of fire in the region. Fire forecast plots of (b), gives higher scores for most of the active fires and lesser scores for other regions. When compared with the corresponding plot in Figure 5-15, it can be inferred that, both the models predict score greater than 25 for similar regions. The locations with score greater than 75 is high in the model for forecasting next two days of fire. As the labels are aggregated, the model has given higher scores to those locations as well resulting in an output with more area having higher score for fire.

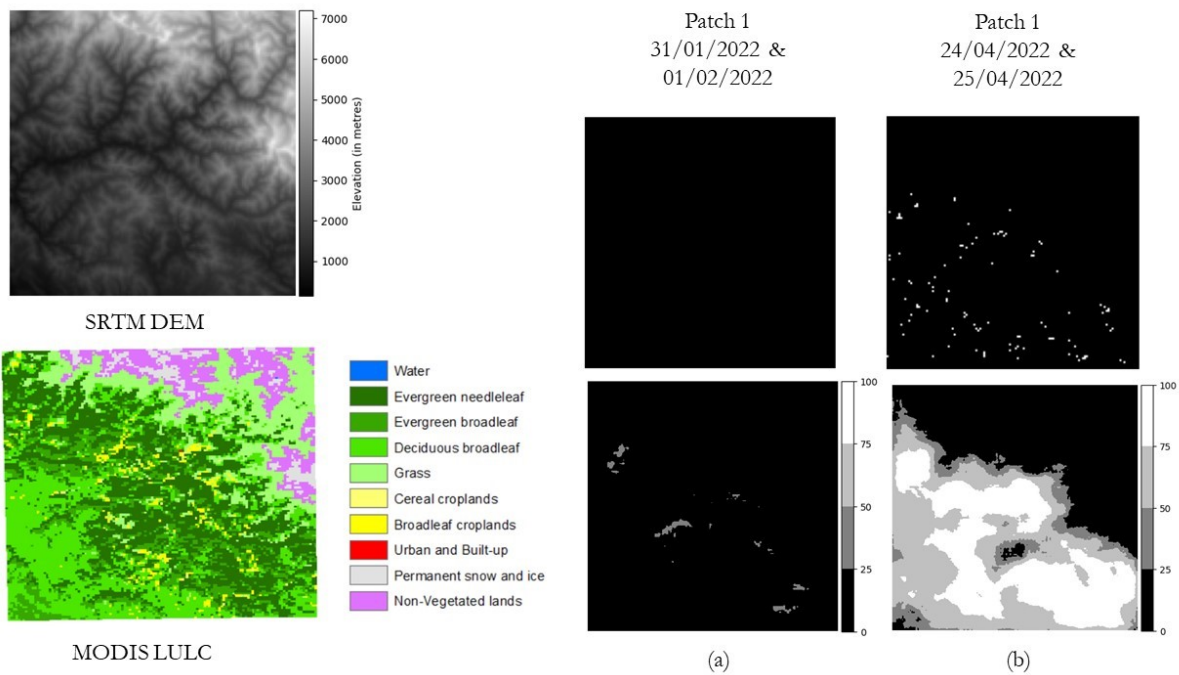


Figure 5-17: Next two days fire forecasting scenario's active fire reference plots and model output plots; Terrain and Land use land cover plots of patch 1. (a) End of Winter (b) Forest Fire season

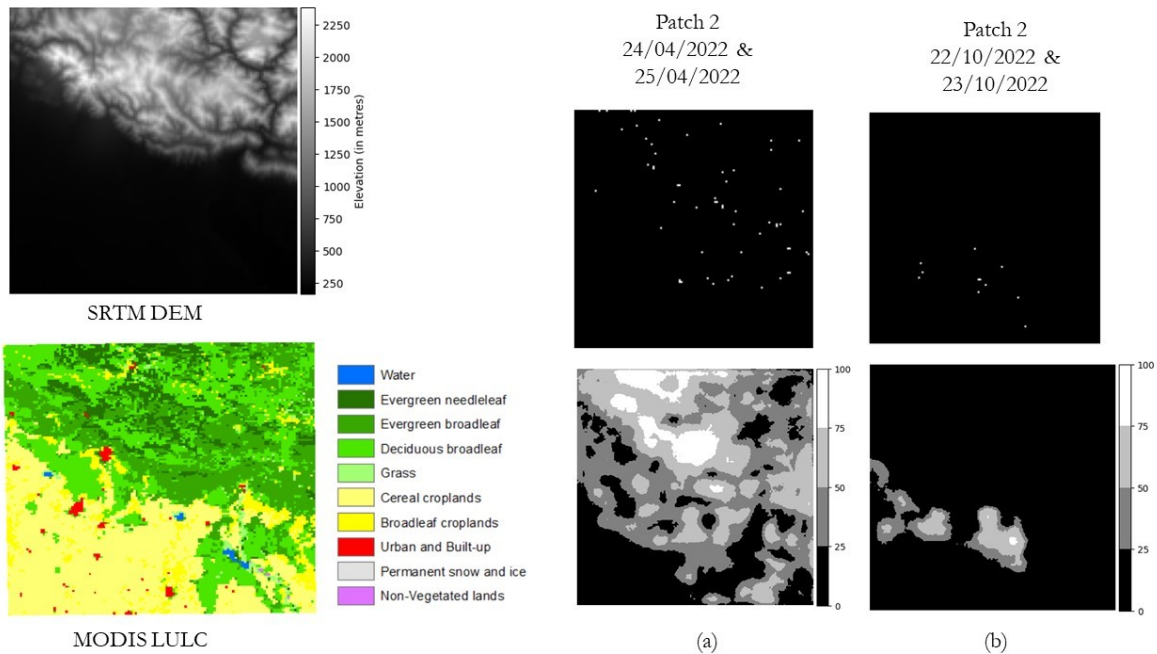


Figure 5-18: Next two days fire forecasting scenario's active fire reference plots and model output plots; Terrain and Land use land cover plots of patch 2. (a) Forest Fire season (b) Agriculture residue burning season

Next two days fire forecasting plots of two different dates along with the elevation and LULC plots are shown in Figure 5-18. The plots in (a) shows the aggregated active fire points of the dates 24/04/2022 and 25/04/2022 and the model fire forecast outputs for those days. The model has given higher score for actual fire locations. From this plot (a), it can be inferred that model as given higher fire forecast scores for the locations with vegetation. In the fire forecast plot of (b), the active fire points are correctly classified with scores ranging from 50 – 100. This has shown higher predictive accuracy of the model for

these locations in the particular time period of the year. It is evident from the fire forecast outputs of two days fire forecast model and next day fire forecast model, the former one's prediction score is higher for the actual fire locations than the other locations even if those regions are vulnerable to fire.

5.3.1.3.3 Next five days fire forecasting model output plots

The fire forecasting for next five days with the fire-influencing variables of a single day is performed for the two study patches. The model outputs for the testing dataset is shown for both the patches in different time periods.

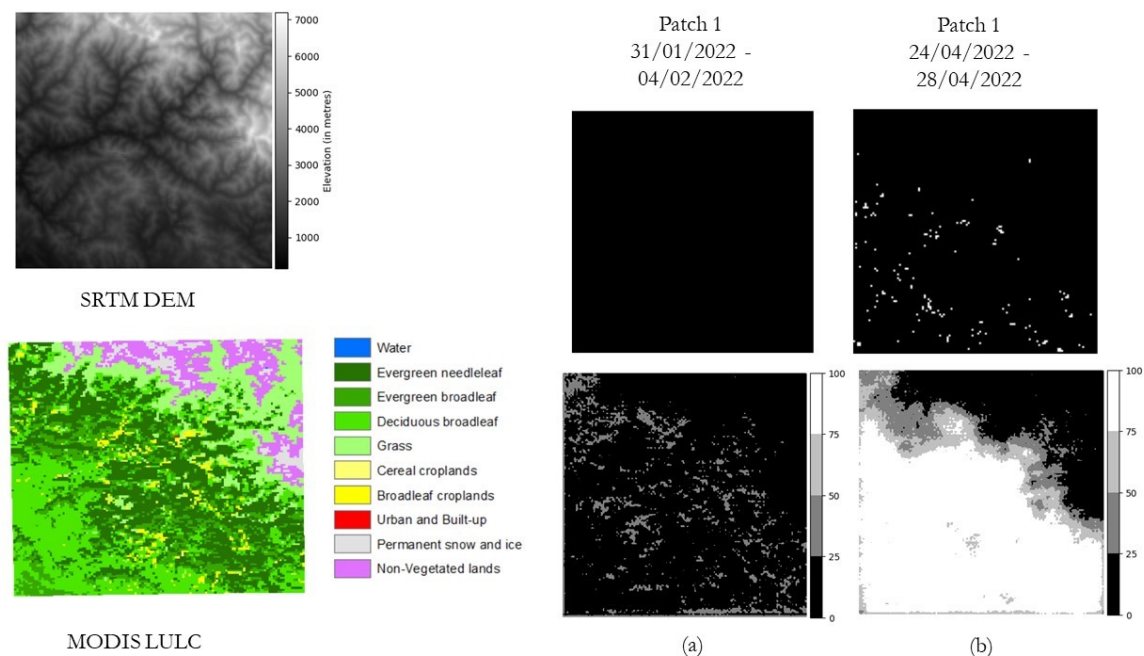


Figure 5-19: Next five days fire forecasting scenario's active fire reference plots and model output plots; Terrain and Land use land cover plots of patch 1. (a) End of Winter (b) Forest Fire season

The fire forecast plot prepared for the days 31/01/2022 to 04/02/2022, has given scores from 25 to 50, to the vegetation. At the same time, the fire forecast plot for the days 24/04/2022 to 28/04/2022 shows higher scores for most of the mid elevation ranges, vegetation parts. It is a sign of overestimating fires in the location. When compared with the fire forecast plots of other two models in the corresponding dates, the scores for this particular scenario is highest. This can be attributed to the number of fire pixels used in the training dataset. The higher number of fire pixels and the corresponding alpha value in the focal loss function might have influenced the model's learning.

The fire forecasting output plots shown in Figure of two different time period in patch 2 also shows higher number of pixels with high scores. The fire forecast for the time period 24/04/2022 to 28/04/2022 shows that the most pixels are given maximum score. It is evident from the plot that, most of the actual fire pixel falls under the model score ranging from 75 to 100. Operationally this kind of plots will be difficult for usage as it gives higher score to almost all the locations. But the model is able to correctly predict the scores based on the terrain, land use and land cover, weather characteristic of the patches. In the fire forecast plot (b) of Figure 5-20 shows less forecast scores for most of the pixels of

north eastern parts. In those parts, that time period is the onset of winter and end of monsoon. So, the possibility of the fires will be less generally.

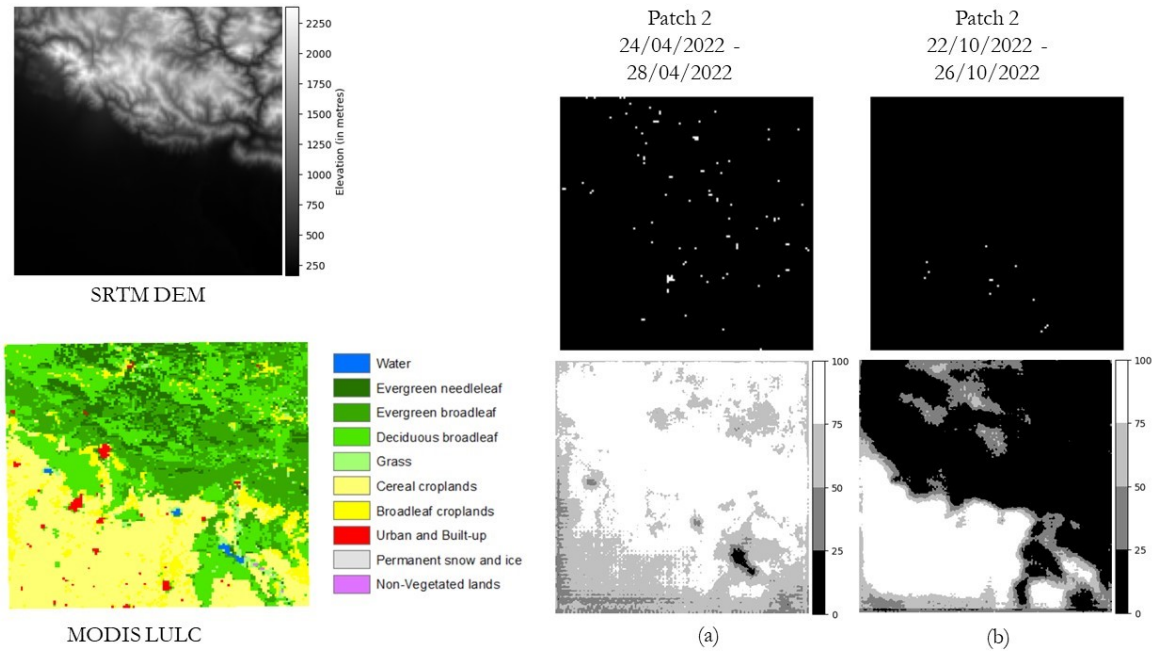


Figure 5-20: Next five days fire forecasting scenario's active fire reference plots and model output plots; Terrain and Land use land cover plots of patch 2. (a) Forest Fire season (b) Agriculture residue burning season

5.3.2 Model for fire forecasting with sequential data of fire influencing variables

A fire forecasting model is built with temporal data of fire-influencing variables to forecast fire of the next day. The methods followed for the model training and hyperparameter tuning are discussed in this section. The temporal data of past five days is considered in this study to find the relationship between the weather, spectral indices, and other stationary data with the next day's fire.

5.3.2.1 Training and hyperparameter tuning

Training, validation and testing data used for this model is taken from two different patches as mentioned in Section 4.2.4. The data is temporally stacked to make pairs of past five days of fire-influencing variables' data with the next day's active fire points. Active fire points act as label data whereas the temporally stacked fire-influencing variables data is feature dataset. In order to efficiently use the available hardware, dataset of first four years of study period is used for this model. Training set is taken from the patches of years 2016 and 2017, validation set from 2018 and testing set from 2019. The conceptual diagram for representing feature dataset and label dataset is shown in Figure 4-10.

Table 5.13: Fire and non-fire pixel count for different datasets used for fire forecasting with temporal fire influencing variables' data

	Fire pixel count	Non-fire pixel count
Training set	2,865	11,42,416
Validation set	1,688	57,16,328
Testing set	1,555	57,16,461

Three different parameters are considered as hyperparameters in this modelling process. They are, alpha value (or class weighting value) in the focal loss function, number of layers of Convolution LSTM and Convolutional layers and their filters, addition of max-pooling and convolutional 2D transpose layers.

STRATEGY 1

Two strategies were followed, initially focal loss and number of convolutional LSTM and convolutional layers are experimented.

Table 5.14: Hyperparameter tuning and validation set accuracy metrics for fire forecasting with temporal fire influencing data

Experiment	Alpha	Dropout	TP	FN	FP	Recall	CBA
1	1000	-	759	766	798456	0.498	0.428
2	500	0.1	405	1275	74410	0.24	0.496

In the experiment 1 mentioned in Table 5.14, the network architecture was two consecutive layers Convolutional LSTM layers with 64 filters each followed by a convolutional 2D layer of 32 filters. Batch Normalization was performed after each convolution layer. Dropout layer was not added in first experiment. In the experiment 2, the network architecture used was two consecutive Convolutional LSTM layers with 32 filters each followed by a convolution 2D layer with 32 filters and another convolutional 2D layer with 16 filters. ‘ReLU’ was used as activation function in all the convolutional layers. The last convolutional 2D layer is provided with ‘Sigmoid’ activation function to obtain the output in the range of 0 to 1. Activation functions are same in both the experiments. Batch size of 4 was used for all the experiments. From the above two experiments, the parameters of second one was selected for further experimentation as it resulted in higher CBA value. And for alpha value, the values between 1000 and 500 will be experimented.

STRATEGY 2

In this strategy, network architecture was two convolutional LSTM layers with 32 filters each, a 3D maxpooling layer in between them. This was followed by two convolutional 2D layers with filters 32 and 16 respectively. A Convolutional 2D transpose layer was used to perform deconvolution to get back the image dimensions to the original size. These layers were added to utilize the advantages of maxpooling layer in convolution operations. A final convolution layer with ‘Sigmoid’ activation function was used in the output layer. Dropout of 0.1 was used after every convolution layer in order to reduce overfitting.

Table 5.15: Hyperparameter tuning experiments performed for different alpha values

Experiment	Alpha	TP	FN	FP	Recall	CBA
1	500	512	1,168	1,48,976	0.3048	0.488
2	650	779	901	3,50,557	0.46	0.469
3	800	1,064	616	5,42,569	0.63	0.4518

From the table 5.15, it can be inferred that with increase in alpha value, CBA decreases. This can be attributed to the loss function which gives more importance to positive samples, thereby resulting in

higher false positives. Therefore, CBA score decreases with increase in alpha value. An inverse reaction happened for recall value as it gets increased with increase in alpha. As recall is related with TP and FN, whose count increase and decrease respectively with increase in alpha value. A model with higher CBA will provide both higher TP and lesser FP. Another experiment with the same architecture, except the filter count in second Convolutional LSTM layer. It is changed to 64 from 32 and alpha to 550. The experiment resulted in recall of 0.4839 and CBA of 0.463.

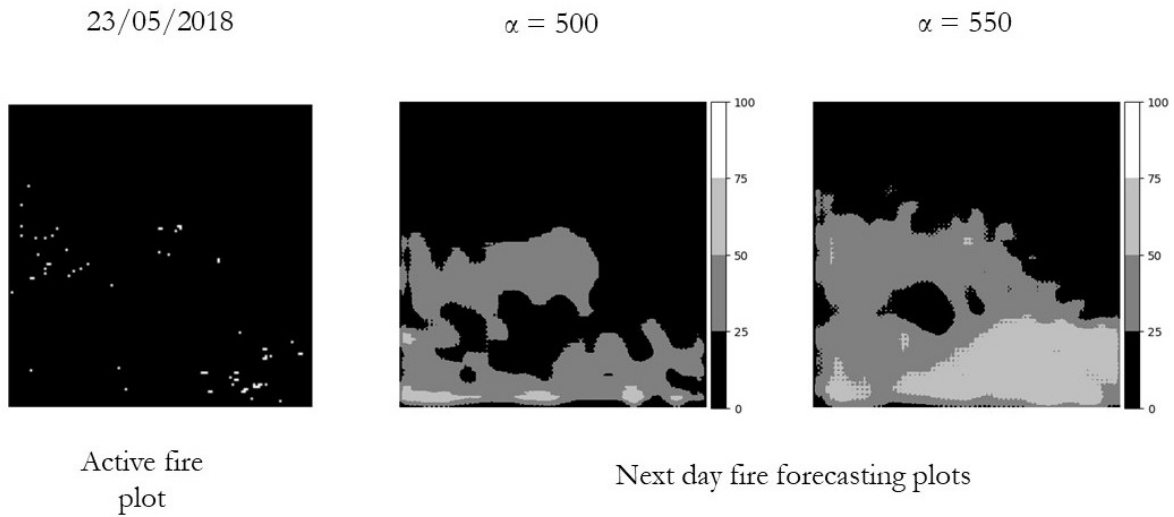


Figure 5-21: Reference active fire plot for 23/05/2018 in patch 1 and the corresponding fire forecast plots with different alpha values

Sensitivity of fire forecasting with different alpha values and network architectures are evident from the fire forecasting plots in Figure 5-21. The model with alpha value 500 is selected for further implementation as it has the best CBA score. The final architecture selected for building the model with sequential data is shown in Figure 5-22.

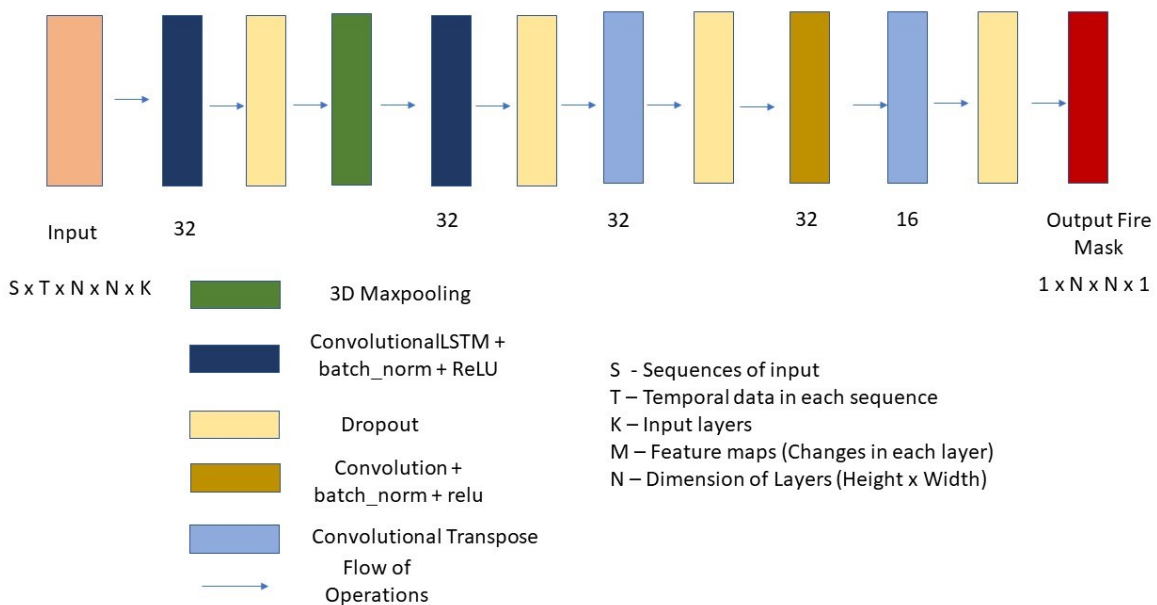


Figure 5-22: The convolutional LSTM architecture used for fire forecasting

5.3.2.2 Quantitative analysis

With the selected network hyperparameters, the model is built, and prediction accuracy is found for the testing dataset.

Table 5.16: Evaluation metrics of next day fire forecasting model with temporal features in testing dataset

True Positives	351	Recall	0.23
False Negatives	1,174	Specificity	0.976
True Negatives	54,17,435	G-mean	0.476
False Positives	1,18,832	CBA	0.491

From the evaluation metrics of the model, CBA score obtained is 0.491 which is the highest even compared with the model evaluation metrics of the fire forecasting with non-temporal datasets. This shows that this model is best in order to correctly predict both the fire and non-fire pixels. A model with high score of CBA produces less false positives at the same time accurately predict fire pixels. That kind of models are required for field level deployment. But the model, should be designed to increase its efficiency to predict fire pixels accurately. A recall value of 0.23 depicts the model performs poor in classifying the fire pixels.

5.3.2.3 Qualitative analysis

Fire forecasting using temporal data of fire-influencing variables is performed with the Convolution LSTM network architecture and the model outputs for the selected patches are shown and discussed in this section.

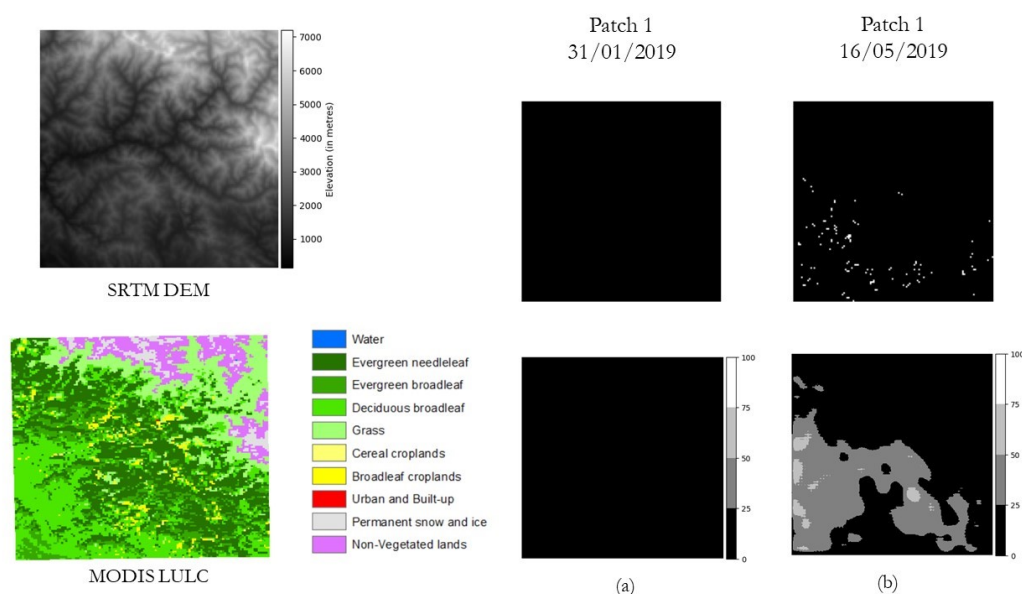


Figure 5-23: Terrain and Land use land cover plots of patch 1; Active fire reference plots; Fire forecasting output plots. (a) End of Winter, (b) Forest Fire season

Fire forecast plots for selected patches and the reference active fire points along with the elevation and LULC plots are shown in Figure 5-22. The plot (a) corresponds to the date 31/01/2019 and there were no

actual fire points. The model’s accuracy is good, it didn’t predict any false positive for that day. This can be evident from the Specificity of the model. Specificity of the selected model is high, and it correctly classifies non-fire pixels. From the plot (b), it can be inferred that the model produces score of 25 – 50 to maximum pixels. This shows the inability of the model to predict actual fire points.

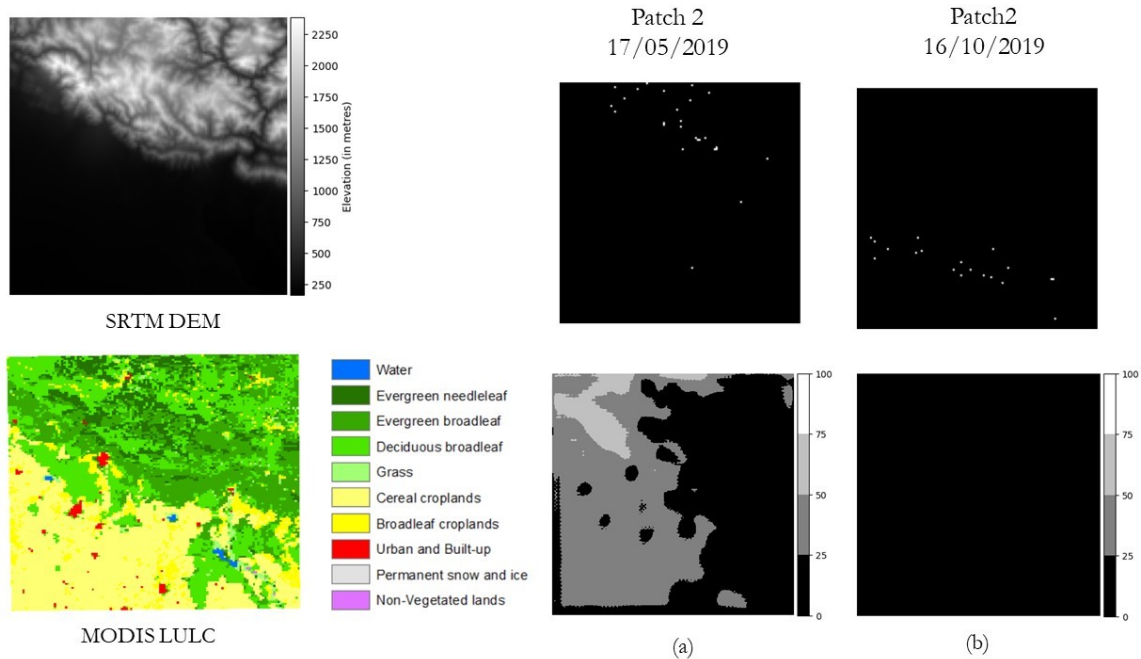


Figure 5-24: Terrain and Land use land cover plots of patch 2; Active fire reference plots; Fire forecasting output plots. (a) Forest Fire season, (b) Agricultural residue burning season

From Figure 5-23, it can be inferred that most of the fires during fire season, occur over the mid elevation region in this patch. In the fire forecast plot of (a), the prediction score of 25 – 50 is given for areas where fire will not usually occur in that time period. At the same time, model was not able to give high scores to actual fire points. From the plot (b), it can be inferred that the model was not able to forecast agricultural fires. The model has given very less prediction score of 0 – 25. This shows that the model has not learned to forecast fires from the given features.

5.4 User interface for fire forecasting

The user interface can be created by following the steps mentioned in the Section 4.6. The model which has good predictive accuracy for both the classes will be selected for deploying in the application. Tables 5.11 and 5.16 provides the prediction accuracy metrics for the models. Quantitatively a model with high CBA score has good prediction accuracy of both the classes. But in this study, it was not that evident from the analysis that has been done. For instance, the model built with temporal data of fire influencing variable had highest CBA value, but it’s prediction accuracy for fires is very less. Therefore, visual analysis of the model prediction plots will also be used along with accuracy metrics to select an accurate model. The model accuracy of scenario 2 in fire forecasting for next days using non-temporal fire-influencing variables is good in all the metrics. It has second highest value of recall and G-mean (0.35 and 0.53 respectively) out of all the four models. It scores third in specificity and CBA metrics. But the values are

very close to the second model architecture. Also, from Figure 5-17, it can be inferred that the model has good forecast ability for non-fire days. The model also has given higher scores to active fire point forecast locations. From Figure 5-18, plot (a) it can be visualized that the model has good accuracy in predicting negative classes as well. At the same time, the model has given higher prediction score for agricultural fires. This shows that the model has ability to forecast agricultural residue burning as well. This model is selected for deploying in the web application. The prediction map is displayed in the browser and is shown in Figure 5-25. The prediction is plotted with gradient of red colour. Dark red denotes higher chance of fire. It matches with the LULC of the state which experience in that time period.

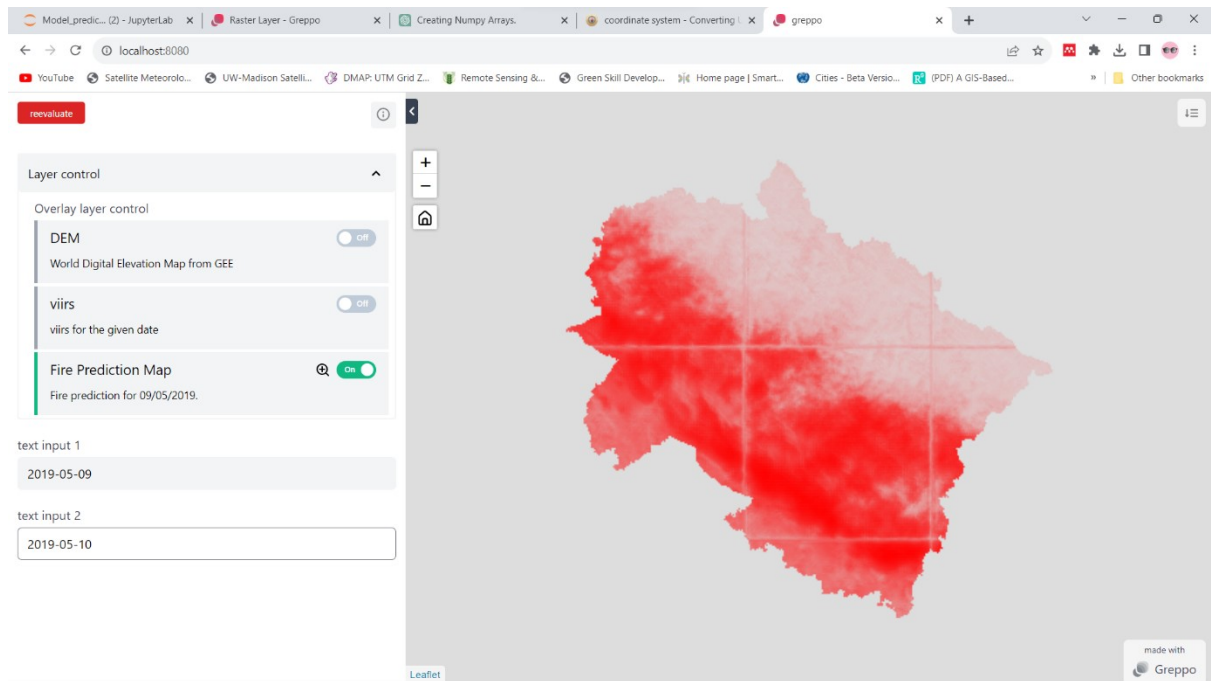


Figure 5-25: Fire prediction application hosted in local server and the prediction map of 09/05/2019

6 CONCLUSION AND RECOMMENDATIONS

6.1 Conclusion

From the study it has been shown that, deep learning models can be built and utilized for fire forecasting tasks which includes various influencing factors having interrelationships between them. The models have given higher prediction scores to fires happening in forest areas and even the agricultural residue burning fires which is completely anthropogenic in nature. Fires during different dates has also been correctly forecasted by the model. Model is able to differentiate between fire and non-fire season, and able to give predictions accordingly. This has shown that the model has learnt to discriminate and to delineate the areas which are more probable to fire in different time periods from the dataset used.

Broadly the modelling process in this study involved fire forecasting by using data of fire-influencing variables of a single day and using data of fire-influencing variables of five continuous days before fire. The modelling part is extended from next day fire forecasting to next two days and next five days using fire-influencing variables of single day. But with the increase in time lead, the model resulted large number of false positives which is not welcoming for using this model outputs for operational fire management. But with the time lead of two days, the model is able to give high prediction scores to fire locations. This is evident from the recall and CBA score of the model. Considering the model built with temporal sequential data for fire-influencing variables, it was not able to forecast fire as its counterpart. This has to be viewed in two different perspectives. The LSTM model is particularly built for problems involving high temporal dependency. But the temporal dependency used should match with the problem in hand. Five days of fire influencing parameters is used in this study. Further experiments can be performed with the different date combinations. The other part is the network architecture. It should be designed to extract the temporal features accordingly.

As discussed in the earlier sections, all the three elements of fire triangle should be present in order for a fire to occur. This nature of fire has created different scenarios, where the vegetation will be dry enough to burn, but the absence of the initiation factor makes the problem complex from a modelling perspective. The location would be vulnerable to fire and it might show all the characteristics of a burnt location which had before igniting. But the absence of igniting factor will make it to fall under non-fire region. This shows the complex nature of the challenge. The model built in this study also has suffered by this problem. Precision is a metric to measure the ability of the model to accurately forecast fire locations. Higher precision value denotes lesser false positives. The precision value was too less for all the models in this study. It shows that all the models had large number of false positives in their outputs. In order to overcome this challenge, it is necessary to integrate the datasets which provide information about the fire ignition as well. This will improve the understanding of the phenomenon and the modelling process as well.

This section also answers the research questions formulated in Chapter 1.

1. What are the influencing factors to be considered for fire in Uttarakhand?

As per the preliminary analysis performed, the terrain features of the state have huge influence on fire. The slope direction is having major influence, as the south facing portion of the hilly terrain in the state receives more sunlight during summer. This reduces the moisture in the vegetation and thereby increasing the vulnerability of locations to fire. With different terrain features, the land use and land cover pattern are also changing in the state, thereby indirectly depicting the influence of terrain of the state for fire. Dry pine needles are highly flammable in nature and the trees are found majorly in mid-elevation regions. Agricultural residue burning is common in the plain areas. These activities show the change in nature of fire, with respect to the change in elevation.

2. Will multi-temporal data increase the accuracy of fire forecasting?

This has been analysed by building deep learning models with two different architectures and data structures. The results of the model with temporal data is not good as the one without temporal data. Most of the fires happening in the state are surface fires, which is primarily ignited by human activities. The fires are used to collect forest products, to improve the growth of mushrooms from burnt trees, negligence, etc. These fires will not burn continuously in most cases. In worst case scenario, these fires will burn huge patches of forest when left uncontrolled. As most of the fires in the study area did not have temporal dependency in it, it can be a reason for the model's inefficiency to forecast fires. At the same time, different model architectures have to be trained with different alpha and gamma values in focal loss function or other loss functions useful for data imbalance problems can be used.

3. For how many days in the future fire can be forecasted accurately?

Different scenarios of fire forecasting with different time leads are performed. Each scenario had its own applicability. The fire forecast predictions for the time lead of one day had less accuracy in predicting actual fires and at the same time, it had less false positives. This is because of the smaller number of fire pixels available for training the model in this scenario. The model built for forecasting fire for next five days had high number of accurate predictions which comes with the cost of high false positives. This particular model with time lead of five days can be used to predict the fire danger conditions but not the exact fire locations. The model built to forecast fire of next two days had good accuracy in giving prediction scores to both fire and non-fire locations, thereby having an increased predictive accuracy for both the classes. This model only had both higher recall value and specificity value. Therefore, according to the fire situation in the study area, the model built to forecast fires with time lead of two days can give reliable results.

4. How to integrate the various datasets and the prepared deep learning model for fire forecasting application?

The various kind of datasets available in Google Earth Engine has opened up the applications for performing environmental studies. This study also has utilized the data catalogue of GEE for model training and testing. The ability to access the data of GEE through python is an added advantage where python has many open-source libraries for Deep learning and GEE had variety of datasets. The python package, Greppo, built for creating web applications from

python code was useful to integrate the prepared deep learning model for fire forecasting with the user interface.

6.2 Recommendations

The following recommendations are suggested for future development in studies related to fire modelling using deep learning techniques.

- Higher resolution dataset can be used. Because 1 km prediction is too less in operational perspective. This is a challenge of a study requiring data of high temporal frequency whereas it is difficult to obtain data of both high spatial and temporal resolution. But with the launch of ‘cubesat’ satellites it can be possible to acquire dataset with much higher spatial resolution dataset.
- Data imbalance and the inherent nature of fire is a challenge involved in this study. The proper understanding of the variables involved in the phenomena and the model’s output can improve the reliability of the deep learning model outputs for the problem. Explaining the predictions of the model using the Explainable AI tools available can be tried to interpret the model predictions.
- ERA5 is a global reanalysis dataset. Whereas an Indian reanalysis dataset – NCMRWF (National Center for Medium Range Weather Forecast) dataset is also available. It can be utilized as this dataset is prepared with the data from ground station observations. A comparative study between the ERA5 and NCMRWF can improve the understanding of the error estimates of meteorological variables between ground observation and reanalysis data observation.
- In this study, historical data of past five days has been used to model the fire with convolutional LSTM model. Different time periods can be experimented. Different model architectures of Convolutional LSTM can also to be tried.
- The generalization ability of the model can be tested in other areas with similar terrain and land use land over characteristics.

REFERENCES

- Abd El-Hady, A. E.-N., Aggag, A., Abdelaty, E., & Bahnassy, M. (2015). GIS-Forecasted Surface Hydrology for Reducing Risks of Food Production (Northern West Coast, Egypt). *Journal of the Advances in Agricultural Researches*, 20(1), 138–157. <https://doi.org/10.21608/jalexu.2015.161386>
- Alléon, A., Jauvion, G., Quennehen, B., & Lissmyr, D. (2020). *PlumeNet: Large-Scale Air Quality Forecasting Using A Convolutional LSTM Network*.
- Amaral, L., & Matsumoto, Marcelo Munroe, T. (2019). *Brazil's Fire Ban Correlates a Reduction in Amazon Wildfires. The Ban Lifts Today*. Global Forest Watch. <https://www.globalforestwatch.org/blog/fires/brazils-fire-ban-correlates-a-reduction-in-amazon-wildfires-the-ban-lifts-today/>
- Andrews, P. L. (2018). *The Rothermel surface fire spread model and associated developments: A comprehensive explanation*. <https://doi.org/10.2737/RMRS-GTR-371>
- Ashutosh, S., Kumar, S., Chaudhary, A., Biswas, T., & Ghosh, S. (2019). *Technical Information Series*.
- Bar, S., Parida, B. R., & Pandey, A. C. (2020). Landsat-8 and Sentinel-2 based Forest fire burn area mapping using machine learning algorithms on GEE cloud platform over Uttarakhand, Western Himalaya. *Remote Sensing Applications: Society and Environment*, 18. <https://doi.org/10.1016/j.rsase.2020.100324>
- Baral, S. S., Das, J., Saraf, A., Borgohain, S., & Singh, G. (2016). Comparison of Cartosat, ASTER and SRTM DEMs of different terrains. *Asian Journal of Geoinformatics*.
- Bergado, J. R., Persello, C., Reinke, K., & Stein, A. (2021). Predicting wildfire burns from big geodata using deep learning. *Safety Science*, 140, 105276. <https://doi.org/10.1016/j.ssci.2021.105276>
- Bergado, J. R., Persello, C., & Stein, A. (2018). Recurrent Multiresolution Convolutional Networks for VHR Image Classification. *IEEE Transactions on Geoscience and Remote Sensing*, 56(11), 6361–6374. <https://doi.org/10.1109/TGRS.2018.2837357>
- Bonta, M., Gosford, R., Eussen, D., Ferguson, N., Loveless, E., & Witwer, M. (2017). Intentional Fire-Spreading by “Firehawk” Raptors in Northern Australia. *Journal of Ethnobiology*, 37(4), 700–718. <https://doi.org/10.2993/0278-0771-37.4.700>
- Bramhe, V. S., Ghosh, S. K., & Garg, P. K. (2018). Extraction of built-up areas using convolutional neural networks and transfer learning from sentinel-2 satellite images. *The International Archives of the Photogrammetry, Remote Sensing and Spatial Information Sciences*, XLII-3, 79–85. <https://doi.org/10.5194/isprs-archives-XLII-3-79-2018>
- Brandt, C. S. (1966). Agricultural Burning. *Journal of the Air Pollution Control Association*, 16(2), 85–86. <https://doi.org/10.1080/00022470.1966.10468447>
- Buda, M., Maki, A., & Mazurowski, M. A. (2018). A systematic study of the class imbalance problem in convolutional neural networks. *Neural Networks*, 106, 249–259. <https://doi.org/10.1016/j.neunet.2018.07.011>
- Burge, J., Bonanni, M., Ihme, M., & Hu, L. (2020). *Convolutional LSTM Neural Networks for Modeling Wildland Fire Dynamics*.
- C.S., H., & Sastry, A. K. (2023, March 9). More forest fires this year owing to heavy rain followed by rise in temperature. *THE HINDU*.
- Cano-Crespo, A., Oliveira, P. J. C., Boit, A., Cardoso, M., & Thonicke, K. (2015). Forest edge burning in the Brazilian Amazon promoted by escaping fires from managed pastures. *Journal of Geophysical Research: Biogeosciences*, 120(10), 2095–2107. <https://doi.org/10.1002/2015JG002914>
- Chauhan, M. (2010). A Perspective on Watershed Development in the Central Himalayan State of Uttarakhand, India. *International Journal of Ecology and Environmental Sciences* © NATIONAL INSTITUTE OF ECOLOGY, 36, 253–269.
- Chowdhury, E. H., & Hassan, Q. K. (2015). Operational perspective of remote sensing-based forest fire

- danger forecasting systems. *ISPRS Journal of Photogrammetry and Remote Sensing*, 104, 224–236. <https://doi.org/10.1016/j.isprsjprs.2014.03.011>
- Christin, S., Hervet, É., & Lecomte, N. (2019). Applications for deep learning in ecology. *Methods in Ecology and Evolution*, 10(10), 1632–1644. <https://doi.org/10.1111/2041-210X.13256>
- Chuvieco, E., Lizundia-Loiola, J., Pettinari, M. L., Ramo, R., Padilla, M., Tansey, K., Mouillot, F., Laurent, P., Storm, T., Heil, A., & Plummer, S. (2018). Generation and analysis of a new global burned area product based on MODIS 250 m reflectance bands and thermal anomalies. *Earth System Science Data*, 10(4), 2015–2031. <https://doi.org/10.5194/essd-10-2015-2018>
- Coskuner, K. (2022). Assessing the performance of MODIS and VIIRS active fire products in the monitoring of wildfires: a case study in Turkey. *IForest - Biogeosciences and Forestry*, 15(2), 85–94. <https://doi.org/10.3832/ifor3754-015>
- de Almeida Pereira, G. H., Fusioka, A. M., Nassu, B. T., & Minetto, R. (2021). Active fire detection in Landsat-8 imagery: A large-scale dataset and a deep-learning study. *ISPRS Journal of Photogrammetry and Remote Sensing*, 178, 171–186. <https://doi.org/10.1016/j.isprsjprs.2021.06.002>
- Dobriyal, M. J., & Bijalwan, A. (2017). Forest fire in western Himalayas of India: A Review. *New York Science Journal*, 10(6), 39–46.
- Dutta, A., Patra, A., Hazra, K. K., Nath, C. P., Kumar, N., & Rakshit, A. (2022). A state of the art review in crop residue burning in India: Previous knowledge, present circumstances and future strategies. *Environmental Challenges*, 8, 100581. <https://doi.org/10.1016/j.envc.2022.100581>
- ECMWF Reanalysis v5 (ERA5). (n.d.). ECMWF. Retrieved August 7, 2023, from <https://www.ecmwf.int/en/forecasts/dataset/ecmwf-reanalysis-v5>
- Epanechnikov, V. A. (1969). Non-Parametric Estimation of a Multivariate Probability Density. *Theory of Probability & Its Applications*, 14(1), 153–158. <https://doi.org/10.1137/1114019>
- Forest fires in India*. (2018).
- García, M. J. L., & Caselles, V. (1991). Mapping burns and natural reforestation using thematic Mapper data. *Geocarto International*, 6(1), 31–37. <https://doi.org/10.1080/10106049109354290>
- Giglio, L., Boschetti, L., Roy, D. P., Humber, M. L., & Justice, C. O. (2018). The Collection 6 MODIS burned area mapping algorithm and product. *Remote Sensing of Environment*, 217, 72–85. <https://doi.org/10.1016/j.rse.2018.08.005>
- Giglio, L., Schroeder, W., & Justice, C. O. (2016). The collection 6 MODIS active fire detection algorithm and fire products. *Remote Sensing of Environment*, 178, 31–41. <https://doi.org/10.1016/j.rse.2016.02.054>
- Graves, A., Mohamed, A., & Hinton, G. (2013). Speech recognition with deep recurrent neural networks. *2013 IEEE International Conference on Acoustics, Speech and Signal Processing*, 6645–6649. <https://doi.org/10.1109/ICASSP.2013.6638947>
- Gray, M. E., Zachmann, L. J., & Dickson, B. G. (2018). A weekly, continually updated dataset of the probability of large wildfires across western US forests and woodlands. *Earth System Science Data*, 10(3), 1715–1727. <https://doi.org/10.5194/essd-10-1715-2018>
- Harrell, F. (2017). *Classification vs. Prediction*. Statistical Thinking. <https://www.fharrell.com/post/classification/>
- He, K., Zhang, X., Ren, S., & Sun, J. (2016). Deep Residual Learning for Image Recognition. *2016 IEEE Conference on Computer Vision and Pattern Recognition (CVPR)*, 770–778. <https://doi.org/10.1109/CVPR.2016.90>
- Hochreiter, S., & Schmidhuber, J. (1997). Long Short-Term Memory. *Neural Computation*, 9(8), 1735–1780. <https://doi.org/10.1162/neco.1997.9.8.1735>
- How slope works?* (n.d.). ESRI. Retrieved July 25, 2023, from <https://pro.arcgis.com/en/pro-app/latest/tool-reference/spatial-analyst/how-slope-works.htm>
- Hu, Y., Guo, D., Fan, Z., Dong, C., Huang, Q., Xie, S., Liu, G., Tan, J., Li, B., & Xie, Q. (2015). An Improved Algorithm for Imbalanced Data and Small Sample Size Classification. *Journal of Data Analysis and Information Processing*, 03(03), 27–33. <https://doi.org/10.4236/jdaip.2015.33004>
- Huot, F., Hu, R. L., Goyal, N., Sankar, T., Ihme, M., & Chen, Y.-F. (2022). Next Day Wildfire Spread: A Machine Learning Dataset to Predict Wildfire Spreading From Remote-Sensing Data. *IEEE Transactions on Geoscience and Remote Sensing*, 60, 1–13. <https://doi.org/10.1109/TGRS.2022.3192974>
- Huot, F., Hu, R. L., Ihme, M., Wang, Q., Burge, J., Lu, T., Hickey, J., Chen, Y.-F., & Anderson, J. (2020). *Deep Learning Models for Predicting Wildfires from Historical Remote-Sensing Data*. ArXiv.

- India State of Forest Report 2019*. (2019).
- India State of Forest Report 2021*. (2021).
- Ismail Fawaz, H., Forestier, G., Weber, J., Idoumghar, L., & Muller, P.-A. (2019). Deep learning for time series classification: a review. *Data Mining and Knowledge Discovery*, 33(4), 917–963. <https://doi.org/10.1007/s10618-019-00619-1>
- Jain, P., Coogan, S. C. P., Subramanian, S. G., Crowley, M., Taylor, S., & Flannigan, M. D. (2020). A review of machine learning applications in wildfire science and management. *Environmental Reviews*, 28(4), 478–505. <https://doi.org/10.1139/er-2020-0019>
- Jaspreet. (2016). *A concise history of neural networks*. TowardsDataScience. <https://towardsdatascience.com/a-concise-history-of-neural-networks-2070655d3fec>
- Jha, C. S., GOPALAKRISHNAN, R., THUMATY, K. C., SINGHAL, J., REDDY, C. S., SINGH, J., PASHA, S. V., MIDDINTI, S., PRAVEEN, M., MURUGAVEL, A. R., REDDY, S. Y., VEDANTAM, M. K., YADAV, A., RAO, G. S., PARSI, U. D., & DADHWAL, V. K. (2016). Monitoring of forest fires from space – ISRO’s initiative for near real-time monitoring of the recent forest fires in Uttarakhand, India. *Current Science*, 110(10).
- Johnson, J. M., & Khoshgoftaar, T. M. (2019). Survey on deep learning with class imbalance. *Journal of Big Data*, 6(1), 27. <https://doi.org/10.1186/s40537-019-0192-5>
- Kondylatos, S., Prapas, I., Ronco, M., Papoutsis, I., Camps-Valls, G., Piles, M., Fernández-Torres, M., & Carvalhais, N. (2022). Wildfire Danger Prediction and Understanding With Deep Learning. *Geophysical Research Letters*, 49(17). <https://doi.org/10.1029/2022GL099368>
- Krishnan, A., & Tangirala, S. (n.d.). *Welcome to Greppo’s documentation*. Greppo. Retrieved July 7, 2023, from <https://docs.greppo.io/#>
- Kubat, M., & Matwin, S. (1997). Addressing the Curse of Imbalanced Training Sets: One-Sided Selection. *Proceedings of the 14th International Conference on Machine Learning*, 179–186.
- Kumar, S., & Kumar, A. (2022). Hotspot and trend analysis of forest fires and its relation to climatic factors in the western Himalayas. *Natural Hazards*, 114(3), 3529–3544. <https://doi.org/10.1007/s11069-022-05530-5>
- Lafon, C. W., & Quiring, S. M. (2012). Relationships of Fire and Precipitation Regimes in Temperate Forests of the Eastern United States. *Earth Interactions*, 16(11), 1–15. <https://doi.org/10.1175/2012EI000442.1>
- Lamat, R., Kumar, M., Kundu, A., & Lal, D. (2021). Forest fire risk mapping using analytical hierarchy process (AHP) and earth observation datasets: a case study in the mountainous terrain of Northeast India. *SN Applied Sciences*, 3(4), 425. <https://doi.org/10.1007/s42452-021-04391-0>
- Langford, Z., Kumar, J., & Hoffman, F. (2018). Wildfire Mapping in Interior Alaska Using Deep Neural Networks on Imbalanced Datasets. *2018 IEEE International Conference on Data Mining Workshops (ICDMW)*, 770–778. <https://doi.org/10.1109/ICDMW.2018.00116>
- Lawrence, M. G. (2005). The Relationship between Relative Humidity and the Dewpoint Temperature in Moist Air: A Simple Conversion and Applications. *Bulletin of the American Meteorological Society*, 86(2), 225–234. <https://doi.org/10.1175/BAMS-86-2-225>
- LeCun, Y., Bengio, Y., & Hinton, G. (2015). Deep learning. *Nature*, 521(7553), 436–444. <https://doi.org/10.1038/nature14539>
- Levin, K., Fransen, T., Schumer, C., Davis, C., & Boehm, S. (2023). *What Does “Net-Zero Emissions” Mean?* World Resources Institute. [https://www.wri.org/insights/net-zero-ghg-emissions-questions-answered#:~:text=Net-zero emissions%2C or “process known as carbon removal.](https://www.wri.org/insights/net-zero-ghg-emissions-questions-answered#:~:text=Net-zero%20emissions%2C%20or%20a%20process%20known%20as%20carbon%20removal.)
- Lillesand, T. M., Kiefer, R. W., & Chipman, J. W. (2015). NOAA POES SATELLITES. In *Remote sensing and Image interpretation* (Seventh, pp. 360–363).
- Lin, T.-Y., Goyal, P., Girshick, R., He, K., & Dollár, P. (2017). Focal Loss for Dense Object Detection. *IEEE International Conference on Computer Vision*.
- Liu, B. (2012). Sentiment Analysis and Opinion Mining. *Synthesis Lectures on Human Language Technologies*, 5(1), 1–167. <https://doi.org/10.2200/S00416ED1V01Y201204HLT016>
- Maeda, E. E., Formaggio, A. R., Shimabukuro, Y. E., Arcoverde, G. F. B., & Hansen, M. C. (2009). Predicting forest fire in the Brazilian Amazon using MODIS imagery and artificial neural networks. *International Journal of Applied Earth Observation and Geoinformation*, 11(4), 265–272. <https://doi.org/10.1016/j.jag.2009.03.003>
- Maffei, C., & Menenti, M. (2019). Predicting forest fires burned area and rate of spread from pre-fire

- multispectral satellite measurements. *ISPRS Journal of Photogrammetry and Remote Sensing*, 158, 263–278. <https://doi.org/10.1016/j.isprsjprs.2019.10.013>
- Mayaki, M. Z. A., & Riveill, M. (2022). Multiple Inputs Neural Networks for Fraud Detection. 2022 *International Conference on Machine Learning, Control, and Robotics (MLCR)*, 8–13. <https://doi.org/10.1109/MLCR57210.2022.00011>
- McArthur, A. . (1967). *Fire behaviour in eucalypt forest*.
- Mistry, M. N., Schneider, R., Masselot, P., Royé, D., Armstrong, B., Kysely, J., Orru, H., Sera, F., Tong, S., Lavigne, É., Urban, A., Madureira, J., García-León, D., Ibarreta, D., Ciscar, J.-C., Feyen, L., de Schrijver, E., de Sousa Zanotti Stagliorio Coelho, M., Pascal, M., ... Gasparrini, A. (2022). Comparison of weather station and climate reanalysis data for modelling temperature-related mortality. *Scientific Reports*, 12(1), 5178. <https://doi.org/10.1038/s41598-022-09049-4>
- Mosley, L. (2013). *A balanced approach to the multi-class imbalance problem* [Iowa State University, Digital Repository]. <https://doi.org/10.31274/etd-180810-3375>
- Negi. (2019). Forest Fire in Uttarakhand: Causes, Consequences and Remedial Measures. *International Journal of Ecology and Environmental Sciences*, 45(1), 31–37.
- Normalized burn ratio (NBR). (n.d.). Office for Outer Space Affairs UN-SPIDER Knowledge Portal. Retrieved July 22, 2023, from <https://un-spider.org/advisory-support/recommended-practices/recommended-practice-burn-severity/in-detail/normalized-burn-ratio>
- Olah, C. (2015). *Understanding LSTM Networks*. Colah's Blog. <https://colah.github.io/posts/2015-08-Understanding-LSTMs/>
- Outcalt, K. W. (2008). Lightning, fire and longleaf pine: Using natural disturbance to guide management. *Forest Ecology and Management*, 255(8–9), 3351–3359. <https://doi.org/10.1016/j.foreco.2008.02.016>
- Pandey, K., Karnatak, H. C., Gairola, A. R., Bhandari, R., & Roy, A. (2022). An automated and optimized geo-computation approach for spatial fire risk modelling using geo-web service orchestration. *Geocarto International*, 37(25), 7843–7854. <https://doi.org/10.1080/10106049.2021.1986577>
- Pascanu, R. R. R. (2013). On the difficulty of training recurrent neural networks. *30th International Conference on Machine Learning*.
- Persello, C., & Stein, A. (2017). Deep Fully Convolutional Networks for the Detection of Informal Settlements in VHR Images. *IEEE Geoscience and Remote Sensing Letters*, 14(12), 2325–2329. <https://doi.org/10.1109/LGRS.2017.2763738>
- Raparelli, E., & Bajocco, S. (2019). A bibliometric analysis on the use of unmanned aerial vehicles in agricultural and forestry studies. *International Journal of Remote Sensing*, 40(24), 9070–9083. <https://doi.org/10.1080/01431161.2019.1569793>
- Rawat, G. S., & Nautiyal, S. (1999). *Forest fire and its control measures*. Oriental enterprises.
- Ronneberger, O., Fischer, P., & Brox, T. (2015). U-Net: Convolutional Networks for Biomedical Image Segmentation. In Munich (Ed.), *Medical Image Computing and Computer-Assisted Intervention* (pp. 234–241). Springer. https://doi.org/10.1007/978-3-319-24574-4_28
- Roteta, E., Bastarrika, A., Padilla, M., Storm, T., & Chuvieco, E. (2019). Development of a Sentinel-2 burned area algorithm: Generation of a small fire database for sub-Saharan Africa. *Remote Sensing of Environment*, 222, 1–17. <https://doi.org/10.1016/j.rse.2018.12.011>
- Rouse, J. W., Jr., Haas, R. H., Schell, J. A., & Deering, D. W. (1974). Monitoring vegetation systems in the Great Plains with ERTS. *NASA. Goddard Space Flight Center 3d ERTS-1 Symp.*
- Rundel, P. W. (1981). Fire as an Ecological Factor. In *Physiological Plant Ecology I* (pp. 501–538). Springer Berlin Heidelberg. https://doi.org/10.1007/978-3-642-68090-8_17
- Sandel, B., & Svenning, J.-C. (2013). Human impacts drive a global topographic signature in tree cover. *Nature Communications*, 4(1), 2474. <https://doi.org/10.1038/ncomms3474>
- Saxena, M. R., Kumar, R., Mohan, C., Vijayan, D., Modi, M., Behera, D. K., Ganguly, K., Bhardwaj, R., Sahithi, V. S., Harshitha, P., & Begum, I. (2019). *Land Use / Land Cover Analysis- Third Cycle*.
- Schroeder, W., Oliva, P., Giglio, L., & Csiszar, I. A. (2014). The New VIIRS 375 m active fire detection data product: Algorithm description and initial assessment. *Remote Sensing of Environment*, 143, 85–96. <https://doi.org/10.1016/j.rse.2013.12.008>
- Shi, X., Chen, Z., Wang, H., Yeung, D.-Y., Wong, W., & Woo, W. (2015). Convolutional LSTM Network: A Machine Learning Approach for Precipitation Nowcasting. *Arxiv*.
- Singh, R. D., Gumber, S., Tewari, P., & Singh, S. P. (2016). Nature of Forest Fires in Uttarakhand: Frequency, Size and Seasonal Patterns in Relation to Pre-Monsoonal Environment.

- Current Science*, 111(2), 398. <https://doi.org/10.18520/cs/v111/i2/398-403>
- Smith, J. M. (2022). *VIIRS Instruments Become More Essential As Terra and Aqua Drift from their Traditional Orbits*. Earth Data. <https://www.earthdata.nasa.gov/learn/articles/modis-to-viirs-transition>
- Southwest Monsoon-2022 End of season report for Uttarakhand state*. (2022).
- Srivastava, M. L., Chandra, S., Kaur, T., & Singh, A. (2012). *Vulnerability of India's Forests to Fire*.
- Srivastava, K. (2020). *Most forest fires in India on account of human activity*. Mongabay. <https://india.mongabay.com/2020/01/most-forest-fires-in-india-on-account-of-human-activity/#:~:text=Around 95 percent of the,fire management is in focus.>
- Sulla-Menashe, D., & Friedl, M. A. (2022). *User Guide to Collection 6 MODIS Land Cover (MCD12Q1 and MCD12C1) Product*.
- Thakur, P. K., Ranjan, R., Singh, S., Dhote, P. R., Sharma, V., Srivastav, V., Dhasmana, M., Aggarwal, S. P., Chauhan, P., Nikam, B. R., Garg, V., & Chouksey, A. (2020). SYNERGISTIC USE OF REMOTE SENSING, GIS AND HYDROLOGICAL MODELS FOR STUDY OF AUGUST 2018 KERALA FLOODS. *The International Archives of the Photogrammetry, Remote Sensing and Spatial Information Sciences*, XLIII-B3-2, 1263–1270. <https://doi.org/10.5194/isprs-archives-XLIII-B3-2020-1263-2020>
- The evidence is clear: the time for action is now. We can halve emissions by 2030*. (2022, April 4). IPCC. <https://www.ipcc.ch/2022/04/04/ipcc-ar6-wgiii-pressrelease/>
- The State of World's Forest 2020*. (2020). Food and Agriculture Organization of the United Nations. <https://www.fao.org/state-of-forests/en/#:~:text=Forest ecosystems are a critical,of the global land area.>
- Tiwari, A., Shoab, M., & Dixit, A. (2021). GIS-based forest fire susceptibility modeling in Pauri Garhwal, India: a comparative assessment of frequency ratio, analytic hierarchy process and fuzzy modeling techniques. *Natural Hazards*, 105(2), 1189–1230. <https://doi.org/10.1007/s11069-020-04351-8>
- Urbanski, S. (2014). Wildland fire emissions, carbon, and climate: Emission factors. *Forest Ecology and Management*. 317: 51-60., 317, 51–60. <https://doi.org/10.1016/J.FORECO.2013.05.045>
- Uttarakhand at a glance 2017-18*. (2019).
- van den Goorbergh, R., van Smeden, M., Timmerman, D., & Van Calster, B. (2022). The harm of class imbalance corrections for risk prediction models: illustration and simulation using logistic regression. *Journal of the American Medical Informatics Association*, 29(9), 1525–1534. <https://doi.org/10.1093/jamia/ocac093>
- Van Wagner, C. E., & Pickett, T. L. (1985). *Equations and FORTRAN program for the Canadian Forest Fire Weather Index System*.
- Vasilakos, C., Kalabokidis, K., Hatzopoulos, J., & Matsinos, I. (2009). Identifying wildland fire ignition factors through sensitivity analysis of a neural network. *Natural Hazards*, 50(1), 125–143. <https://doi.org/10.1007/s11069-008-9326-3>
- Vatsa, D. (2022). *Colonial History of Uttarakhand Wildfires*. <https://www.talkdhartitome.com/post/uttarakhand-s-wildfires-a-colonial-offshoot>
- Venkataraman, C., Habib, G., Kadamba, D., Shrivastava, M., Leon, J.-F., Crouzille, B., Boucher, O., & Streets, D. G. (2006). Emissions from open biomass burning in India: Integrating the inventory approach with high-resolution Moderate Resolution Imaging Spectroradiometer (MODIS) active-fire and land cover data. *Global Biogeochemical Cycles*, 20(2). <https://doi.org/10.1029/2005GB002547>
- Voelkert, J. C. (2015). *FIRE AND FIRE EXTINGUISHMENT*.
- Wahab, S. (2014). Modeling the Suitability Analysis to Establish New Fire Stations in Erbil City Using the Analytic Hierarchy Process and Geographic Information Systems. *The 3rd International Geoscience and Geomatics Conference Turkey*.
- Wang, S., Liu, W., Wu, J., Cao, L., Meng, Q., & Kennedy, P. J. (2016). Training deep neural networks on imbalanced data sets. *2016 International Joint Conference on Neural Networks (IJCNN)*, 4368–4374. <https://doi.org/10.1109/IJCNN.2016.7727770>
- Weiss, D. J., Nelson, A., Gibson, H. S., Temperley, W., Peedell, S., Lieber, A., Hancher, M., Poyart, E., Belchior, S., Fullman, N., Mappin, B., Dalrymple, U., Rozier, J., Lucas, T. C. D., Howes, R. E., Tusting, L. S., Kang, S. Y., Cameron, E., Bisanzio, D., ... Gething, P. W. (2018). A global map of travel time to cities to assess inequalities in accessibility in 2015. *Nature*, 553(7688), 333–336. <https://doi.org/10.1038/nature25181>
- Wind Direction Quick Reference*. (n.d.). NCAR Earth Observing Laboratory. Retrieved August 7, 2023, from

- <https://www.eol.ucar.edu/content/wind-direction-quick-reference>
- Wright, H. E., & Heinselman, M. L. (2014). The Ecological Role of Fire in Natural Conifer Forests of Western and Northern North America—Introduction. *Fire Ecology*, 10(3), 4–13.
<https://doi.org/10.1007/BF03400628>
- Yamashita, R., Nishio, M., Do, R. K. G., & Togashi, K. (2018). Convolutional neural networks: an overview and application in radiology. *Insights into Imaging*, 9(4), 611–629.
<https://doi.org/10.1007/s13244-018-0639-9>
- Yu, Y., Si, X., Hu, C., & Zhang, J. (2019). A Review of Recurrent Neural Networks: LSTM Cells and Network Architectures. *Neural Computation*, 31(7), 1235–1270.
https://doi.org/10.1162/neco_a_01199
- Zhang, A., Lipton, Z. C., Li, M., & Smola, A. J. (2021). *Dive into Deep Learning*.
- Zhang, G., Wang, M., & Liu, K. (2019). Forest Fire Susceptibility Modeling Using a Convolutional Neural Network for Yunnan Province of China. *International Journal of Disaster Risk Science*, 10(3), 386–403.
<https://doi.org/10.1007/s13753-019-00233-1>
- Zhang, G., Wang, M., & Liu, K. (2021). Deep neural networks for global wildfire susceptibility modelling. *Ecological Indicators*, 127, 107735. <https://doi.org/10.1016/j.ecolind.2021.107735>
- Zheng, Z., Huang, W., Li, S., & Zeng, Y. (2017). Forest fire spread simulating model using cellular automaton with extreme learning machine. *Ecological Modelling*, 348, 33–43.
<https://doi.org/10.1016/j.ecolmodel.2016.12.022>

APPENDIX

There are 32 features layers prepared for the modelling purposes. They are

- 1) VIIRS M3 band
- 2) VIIRS M4 band
- 3) VIIRS M5 band
- 4) VIIRS M7 band
- 5) VIIRS M8 band
- 6) VIIRS M11 band
- 7) NDVI
- 8) NBR
- 9) PMI
- 10) MNDFI
- 11) Temperature_2m_min
- 12) Temperature_2m_max
- 13) Windspeed
- 14) Wind direction
- 15) Total precipitation sum
- 16) Relative humidity
- 17) Dewpoint temperature
- 18) Surface pressure
- 19) Population data
- 20) Water (class 0)
- 21) Needleleaf (classes 1 and 3)
- 22) Broadleaf (classes 2 and 4)
- 23) Shrub (class 5)
- 24) Grass (class 6)
- 25) Cropland (classes 7 and 8)
- 26) Non-vegetated land (class 11)
- 27) Snow and ice (class 10)
- 28) Elevation
- 29) Slope
- 30) Aspect
- 31) Global Friction surface
- 32) Day of Year
